Levy Nuclear Plant Units 1 and 2
Response to NRC Request for Additional Information Letter No. 101 Related to SRP Section 2.4.6 for the Combined License Application, dated February 28, 2011

NRC RAI #	Progress Energy RAI #	Progress Energy Response
02.04.06-17	L-0902	Response enclosed – see following pages

NRC Letter No.: LNP-RAI-LTR-101

NRC Letter Date: February 28, 2011

NRC Review of Final Safety Analysis Report

NRC RAI NUMBER: 02.04.06-17

Text of NRC RAI:

In order to satisfy the requirements of 10 CFR Part 50, Appendix A, General Design Criterion (GDC) 2, 10 CFR 52.79(a)(1)(iii), and 10 CFR 100.23(d), the applicant must provide the comprehensive geohydrological design basis which ensures that any potential hazards to the structures, systems, and components important to safety due to the effects of probable maximum tsunami (PMT) are considered in the plant design. The NRC staff reviews the PMT that may pose hazards to the site, including reviews of tsunamigenic source mechanisms, source parameters, propagation models, and near-shore inundation models.

In its review of tsunami wave propagation models, the NRC staff examines model parameters used to simulate the tsunami wave propagation from the source towards the site and input data, including bathymetry and topography data. The NRC staff's analysis of the PMT event considers the technique and conservatism used by a site and region specific model approach and its applicability to tsunami waves for calculating tsunami water levels at or near the site. Appropriate models avoid approximations of source geometry, bathymetry between the source and offshore of site, and topography near the site. Examples of shallow water wave equation models include COMCOT, ComMIT, and Delft3D, which are appropriate for earthquake-generated tsunamis. Examples of Boussinesq-type models are Coulwave, Funwave, Geowave, which are appropriate for earthquake/landslide/impact generated tsunamis.

If the applicant chooses to use a numerical model, the applicant is requested to clearly present all equations used, discuss all assumptions and associated conservatism inherent in the equations, and to present the procedure used to calculate the water-level values. Further, the applicant is requested to provide all input data sources, calculation packages, and any associated modeling input files.

If the applicant chooses to use an approach which relies on the Ward, et al. publication, the applicant is requested to provide a complete presentation of the theoretical assumptions that are relevant to propagation equations for a landslide-generated wave and runup/inundation. In addition, the applicant is requested to provide site-specific justification as to why the Ward equations are applicable and conservative for the proposed Levy County site. This discussion should include a presentation of the theoretical assumptions behind the generation, attenuation, shoaling, and runup equations, and a justification of why these assumptions are valid and conservative with respect to site-specific conditions.

Regarding tsunami generation, the applicant is requested to:

(1) Provide the reference for wave amplitude Equation 2.4.6-3, along with relevant assumptions used to develop that equation.

(2) Provide references for the expressions of slide velocity and a clear indication as to which expressions were used to calculation the slide velocities listed in Table 2.4.6-206.

(3) Provide the rationale and justification for using Equation 2.4.6-8 derived for impact tsunami sources to model landslide tsunamis, particularly with regard to difference in wave characteristics between landslide and impact tsunamis.

(4) Explain how diameter listed for each source in Table 2.4.6-206 relates to landslide parameters.

Regarding tsunami propagation, the applicant is requested to:

(1) Explain how the "measurement point" is chosen to determine R, the distance of measurement point from the source.

(2) Justify the use of Equation 2.4.6-11. Because the "measurement point" is a nearshore location, justify the use of Equation 2.4.6-11 that is derived for constant water depth, considering the broad continental shelf offshore western Florida.

(3) Provide an expression for propagation across the continental shelf. If in a revised procedure, the applicant applies the propagation and shoaling terms at the edge of the continental shelf, the applicant is requested to provide an expression for propagation across the continental shelf.

(4) Provide additional information related to the equation for the attenuation curves (2.4.6-8). The applicant must provide the correct reference, domain of applicability of these fitted curves, and assumptions used to derive these curves.

Regarding tsunami runup, the applicant is requested to:

(1) Clarify the definition of h in Equation 2.4.15. This appears to be inconsistent with the definition indicated in FSAR References 2.4.6-228 and 2.4.6-237, from which this equation was taken. In the revised FSAR, the applicant indicates that h represents "shoreline wave height" whereas it is intended to represent runup as described in the aforementioned FSAR References.

(2) Provide the theoretical assumptions behind the equation 2.4.15, and justify why these assumptions are valid and conservative with respect to site-specific conditions.

(3) Clarify revised FSAR section 2.4.6.6.3.5. If revised Equation 2.4.15 is used to calculate runup, the applicant should confirm that revised section 2.4.6.6.3.5 is not necessary.

(4) Provide the geographic location (lat, long) and water depth where the shoaled amplitude A(R) in Table 2.4.6-207 is calculated.

(5) Provide location information for revised figure 2.4.6-230 "Landward Topographic Profile," for example, in a map figure.

PGN RAI ID #: L-0902

PGN Response to NRC RAI:

To respond to this RAI, the PMT analysis was performed for the Levy Nuclear Plant (LNP) site based on numerical simulations of tsunami generation, propagation and runup, and inundation using a Boussinesq-type model. The model used for propagation, runup and inundation is the Boussinesq model FUNWAVE-TVD developed at the University of Delaware, implemented in spherical-polar coordinates. This model is used to evolve an initial source description up to and past the time of maximum shoreline inundation and runup at the LNP site. The sources used are either static (as represented by a surface displacement field) or dynamic (as represented by a surface displacement field and horizontal velocity field) at the time of model initiation, as discussed below.

As requested in the RAI, the following information is provided:

1. A description of the numerical model, including relevant equations
2. The input data sources
3. All assumptions and associated conservatisms employed for the model simulation
4. Initial water level consistent with the long-term sea level rise valid for the life of the plant together with the 10 percent exceedance high tide
5. The estimated maximum water level near the LNP site
6. Updates to FSAR Subsection 2.4.6
7. Verification and Validation document (Appendix 1)
8. Model electronic input and output files (DVD)

Probable Maximum Tsunami Analysis

Three different tsunami sources are considered for the PMT analysis: one seismic source and two landslide sources.

- Venezuela Seismic Source
- Mississippi Canyon Landslide Source
- Florida Escarpment Landslide Source

For the seismic source, the initial condition consists of a static surface displacement and a stationary water body. The initial static displacement is derived from earthquake source parameters using the method described by Okada (Reference 2.4.6-17-12).

For the two landslide sources, two approaches are considered. The first approach uses a static source based on the geometry of the initial and final positions of the slide mass. The second approach employs a dynamic source, which specifies both surface displacement and depth averaged horizontal velocity fields. This source is computed from the slide geometry using the model NHWAVE (Non-Hydrostatic Wave), Version 1.0, which is described in Reference 2.4.6-17-4. The computation of the initial source requires a value for slide velocity. This is computed using a methodology described by Enet and Grilli (Reference 2.4.6-17-2). For each of the landslides, a slide geometry equivalent to that in Reference 2.4.6-17-2 is employed with an adjustment to slide aspect ratio (width/length) to best fit the model slide to the measured shape of the excavated source region for the measured slide. This choice allows the use of the same geometric relationships between slide volume, area, thickness, length and width as utilized in Reference 2.4.6-17-2. The geometry of the slides is described below.

Parameters defining tsunami sources were obtained from ten Brink et al (Reference 2.4.6-17-11); a listing of parameters is provided in Table 2.4.6-17-1 and Table 2.4.6-17-2. The simulated tsunamis that are generated using source parameters for the different scenarios described herein are severe enough to be considered equivalent to the PMT for the LNP site.

The flood level near the LNP site due to PMT is estimated using the numerical wave model FUNWAVE-TVD (Fully Nonlinear Wave – Total Variation Diminishing Scheme), Version 1.0, described in References 2.4.6-17-3, 2.4.6-17-7, and 2.4.6-17-8. Benchmark testing of FUNWAVE-TVD is described in Reference 2.4.6-17-10. Inputs to FUNWAVE-TVD include depth grids, whose development is described herein, and information about the configuration of a tsunami source, used as the initial condition for the model run. Program documentation and users' manual for FUNWAVE-TVD is available in Reference 2.4.6-17-8.

Outputs generated by FUNWAVE-TVD include gridded surface displacement and horizontal velocities as a function of time during the model simulation. The model results are presented as snapshots of evolving surface displacement during each simulated case. The model accumulates information on the maximum runup water level occurring at each grid location during the simulation, and provides estimates of maximum inundation and runup values near the LNP site based on these accumulated values. The results are used to estimate the maximum water level due to the PMT near the LNP site, and to determine if LNP Units 1 and 2 will be affected by the PMT maximum water level.

The verification and validation of the FUNWAVE-TVD and NHWAVE computer programs are described in the Verification and Validation document (Appendix 1). Computation grids are generated using Fortran programs and MATLAB scripts, for which detailed operation procedures and verification are also described in Appendix 1.

FUNWAVE-TVD Model Description

The propagation, shoreline runup and inundation caused by tsunamis are calculated using the Boussinesq wave model FUNWAVE-TVD. In the present application, FUNWAVE-TVD solves the spherical-polar form of the weakly-nonlinear, weakly-dispersive Boussinesq equations described by Kirby et al (Reference 2.4.6-17-3). Shi et al (Reference 2.4.6-17-8) describes the operation of both Cartesian and spherical-polar versions of the code. The model incorporates bottom friction and turbulent mixing effects. The model is available to the public as open source software.

The Cartesian coordinate version of FUNWAVE-TVD, described in Shi et al (Reference 2.4.6-17-7 and Reference 2.4.6-17-8), has been benchmarked for tsunami application using the PMEL-135 benchmarks provided in Synolakis et al (Reference 2.4.6-17-9), which are the presently accepted benchmarking standards adopted by the National Tsunami Hazard Mitigation Program (NTHMP) for judging model acceptance for use in development of coastal inundation maps and evacuation plans. Benchmark tests for the Cartesian FUNWAVE-TVD are described in Tehranirad et al (Reference 2.4.6-17-10). The spherical-polar version of the code used here is subjected to several of these benchmarks in order to document consistency and accuracy of the model.

The equations solved by FUNWAVE-TVD consist of a depth-integrated volume conservation equation together with depth-integrated horizontal momentum equations. The equations retain effects to second order in the ratio of water depth to wavelength, accounting for deviations from

depth-uniform horizontal flow up to quadratic terms in the vertical coordinate. The resulting volume conservation equation is given by (Reference 2.4.6-17-3):

$$\frac{1}{\delta}H_t+\frac{1}{\cos\theta}\left\{\left(H\bar{u}\right)_{\phi^*}+\left(H\bar{v}\cos\theta\right)_{\theta^*}\right\}=0 \qquad \text{Eqn 1}$$

where H is the local total water depth, u is Easterly, depth-averaged horizontal velocity and v is depth-averaged Northerly horizontal velocity, θ is latitude in radians, δ is a dimensionless ratio of surface displacement scale to representative water depth, and subscripts t, ϕ^* and θ^* represent a time derivative and spatial derivatives with respect to scaled latitude and longitude (see Reference 2.4.6-17-3 for further details of the derivation).

The corresponding horizontal momentum equations for the Easterly (longitudinal) direction are given by (Reference 2.4.6-17-3):

$$\begin{aligned}&\bar{u}_t-\mu^2 f\bar{v}+\delta\left\{\frac{\bar{u}}{\cos\theta}\bar{u}_{\phi^*}+\overline{vu}_{\theta^*}\right\}+\frac{1}{\cos\theta}\eta_{\phi^*}\\&+\frac{\mu^2}{\cos^2\theta}\left\{\frac{h^2}{6}\left[\bar{u}_{\phi^*\phi^*t}+\left(\bar{v}\cos\theta\right)_{\phi^*\theta^*t}\right]-\frac{h}{2}\left[\left(h\bar{u}_t\right)_{\phi^*\phi^*}+\left(h\cos\theta\bar{v}_t\right)_{\phi^*\theta^*}\right]\right\}\\&+\frac{\mu^2}{\cos\theta}\left(BFT\right)_{\phi^*}-\tau_b^x=O\left(\delta^2,\delta\mu^2,\mu^4\right)\end{aligned} \qquad \text{Eqn 2}$$

The corresponding horizontal momentum equations for the Northerly (latitudinal) direction are given by (Reference 2.4.6-17-3):

$$\begin{aligned}&\bar{v}_t+\mu^2 f\bar{u}+\delta\left\{\frac{\bar{u}}{\cos\theta}\bar{v}_{\phi^*}+\overline{vv}_{\theta^*}\right\}+\eta_{\theta^*}\\&+\mu^2\left\{\frac{h^2}{6}\left[\frac{1}{\cos\theta}\left\{\bar{u}_{\phi^*t}+\left(\bar{v}\cos\theta\right)_{\theta^*t}\right\}\right]_{\theta^*}-\frac{h}{2}\left[\frac{1}{\cos\theta}\left\{\left(h\bar{u}_t\right)_{\phi^*}+\left(h\cos\theta\bar{v}_t\right)_{\theta^*}\right\}\right]_{\theta^*}\right\}\\&+\mu^2\left(BFT\right)_{\theta^*}-\tau_b^y=O\left(\delta^2,\delta\mu^2,\mu^4\right)\end{aligned} \qquad \text{Eqn 3}$$

Here f represents the Coriolis parameter, η represents the water surface displacement from its initial position, h represents local still water depth, and μ is a dimensionless parameter characterizing the ratio of characteristic water depth to characteristic surface wave length. The term *BFT* contains the effect of continuous bottom motion in time, and is not utilized in the present study since bottom displacements are described either as static initial conditions, or are tied to initial surface displacement and velocity field in a separate model computation based on NHWAVE, described below. The term τ_b represents the effect of bottom friction and is given by (Reference 2.4.6-17-3):

$$\tau_b^{x,y}=\frac{1}{H}C_D\left|\mathbf{u}\right|\left(u,v\right) \qquad \text{Eqn 4}$$

where C_D is the drag coefficient and **u** is the horizontal velocity vector. The value of the drag coefficient can range from 0.0008 to 0.0031 on continental shelf and slope environments

(Reference 2.4.6-17-14) and can be as high as 0.005 during breaking and runup (Reference 2.4.6-17-13). Increased roughness of subaerial vegetation and other surface features can lead to higher apparent values of the drag coefficient. For this study, a lower end value of the drag coefficient of $C_D = 0.001$ is used and therefore will result in conservative estimates of runup water levels.

For tsunami applications here, FUNWAVE-TVD is run with closed boundaries and an initial hot start condition consisting of either a surface displacement alone (in the case of static initial conditions) or a surface displacement and initial velocity field (in the case of a dynamic initial condition based on NHWAVE calculations). The choice for each source will be described separately. The model is run from the initial start until past the time when significant wave activity has decayed at the target site.

NHWAVE Model Description

For several of the computations described below, the model NHWAVE is used to describe the early stages of surface displacement and velocity field development associated with an underwater landslide. NHWAVE solves fully non-hydrostatic Navier-Stokes equations in a surface and terrain following (sigma) coordinate system. The model is described in Ma et al (Reference 2.4.6-17-4). The model assumes a single valued water surface and represents turbulent stresses in terms of an eddy viscosity closure. Turbulent stresses are not modeled in the present study, and thus the model is basically solving Euler equations for incompressible flow with a moving surface and bottom.

The governing equations for NHWAVE in Cartesian tensor form are given by (Reference 2.4.6-17-4):

$$\frac{\partial u_i}{\partial x_i^*} = 0 \qquad \text{Eqn 5}$$

and

$$\frac{\partial u_i}{\partial t^*} + u_j \frac{\partial u_i}{\partial x_j^*} = -\frac{1}{\rho}\frac{\partial p}{\partial x_i^*} + g_i + \frac{\partial \tau_{ij}}{\partial x_j^*} \qquad \text{Eqn 6}$$

Here, g_i is the gravitational vector, p is fluid pressure, ρ is the fluid density, u_i is the velocity vector, and τ_{ij} is a tensor representing viscous and turbulent stresses which is not used in the current analysis. The σ coordinate version of the model is described in Ma et al (Reference 2.4.6-17-4). Surface boundary conditions for the model consist of a kinematic constraint on vertical velocity ω, and constraints on tangential and normal stresses (Reference 2.4.6-17-4).

$$\omega|_{z=\eta} = \frac{\partial \eta}{\partial t} + u\frac{\partial \eta}{\partial x} + v\frac{\partial \eta}{\partial y} \qquad \text{Eqn 7}$$

In the absence of turbulent and viscous effects and with no atmospheric forcing, these reduce to the following for normal stress (Reference 2.4.6-17-4):

$$p|_{z=\eta} = 0 \qquad \text{Eqn 8}$$

For tangential stress, these reduce to (Reference 2.4.6-17-4):

$$\frac{\partial u}{\partial \sigma}|_{z=\eta} = \frac{\partial \upsilon}{\partial \sigma}|_{z=\eta} = 0 \qquad \text{Eqn 9}$$

where vertical stretched coordinate $\sigma = (\eta - z)/H$ and H is total depth defined after Equation 1.

At the bottom, zero tangential stress again gives (Reference 2.4.6-17-4):

$$\frac{\partial u}{\partial \sigma}|_{z=-h} = \frac{\partial \upsilon}{\partial \sigma}|_{z=-h} = 0 \qquad \text{Eqn 10}$$

The kinematic constraint on vertical velocity at the bottom is given by (Reference 2.4.6-17-4):

$$\omega|_{z=-h} = -\frac{\partial h}{\partial t} - u\frac{\partial h}{\partial x} - \upsilon\frac{\partial h}{\partial y} \qquad \text{Eqn 11}$$

The condition on normal stress on the moving bottom is derived from the vertical momentum equation and is given by (Reference 2.4.6-17-4):

$$\frac{\partial p}{\partial \sigma}|_{z=-h} = -\rho D\frac{d\omega}{dt}|_{z=-h} \qquad \text{Eqn 12}$$

where *D* represents total water depth. In the current analysis, linearized forms of Equation 11 and Equation 12 are combined to obtain (Reference 2.4.6-17-4):

$$\frac{\partial p}{\partial \sigma}|_{z=-h} = \rho D\frac{\partial^2 h}{\partial t^2} \qquad \text{Eqn 13}$$

This linearized boundary condition is the same as employed in the basic testing of the model against the laboratory data of Enet and Grilli (Reference 2.4.6-17-2) and described in Ma et al (Reference 2.4.6-17-4).

For the present cases, the modeled domain is set up so that the landslide event is centrally located and the generated motion does not reach lateral boundaries during the simulated time. Results from the model at the end of the model run are saved and used in FUNWAVE-TVD as initial conditions.

Model Grid Development and Description

Topographic data were obtained from high resolution LIDAR surveys around the LNP site converted into an ASCII file for use in the computer model. Bathymetric data for the model domains were obtained from the National Geophysical Data Center (NGDC) ETOPO 1 (Reference 2.4.6-17-1) and NGDC Coastal Relief Model (CRM) (Reference 2.4.6-17-5). The computational scheme is comprised of a nesting of three model grids which move the computation for a lower resolution large scale Grid *A* (A_l for landslide cases), through an intermediate resolution Grid *B*, to a high resolution Grid *C* encompassing the study site. All the grids are based on global (latitude-longitude) coordinates.

Grid *A* for the Venezuela seismic tsunami case was generated based on the ETOPO1 data set (Reference 2.4.6-17-1). The data were extracted using GEODAS, a standard tool described in Reference 2.4.6-17-1. ETOPO1 uses Mean Sea Level (MSL) as a vertical datum origin. The grid resolution for Grid *A* is 2 arc-minutes.

Grid A_l for the landslide cases was generated based on ETOPO1 in the same way as the Grid *A* was generated for the Venezuela seismic case. The grid resolution for Grid A_l is 1 arc-minute.

Grid *B*, which is nested within both Grid *A* and A_l, was generated based on Volume 3 of the CRM data set (Reference 2.4.6-17-5). GEODAS is used for data extraction. The CRM also uses MSL as the vertical datum origin. The grid resolution for Grid *B* is 15 arc-seconds.

Grid *C*, which is nested in Grid *B*, was developed from CRM data and the local LIDAR data at the study site. The LIDAR data was first converted into the global horizontal coordinates and the MSL vertical datum using standard tools. The data was merged into the computational grid. The grid resolution for Grid *C* is 3 arc-seconds, or about 90 meters.

Grid *A* and A_l and nested Grids *B* and *C* are presented in Figures 2.4.6-17-1 through 2.4.6-17-4. One-way nesting between Grid *A* (for the Venezuela seismic case) or Grid A_l (for Gulf of Mexico landslide cases), Grid *B* and Grid *C* is performed through the one-way data transfer at nesting boundaries. The grid nesting scheme transfers surface elevation and velocity components calculated from a large domain to a nested small domain through ghost cells at nesting boundaries. A linear interpolation is performed between a large domain and small domain at nesting boundaries.

Vertical Datum and Initial Water Level for Model Runs

The vertical datum used to report maximum water level results near the LNP site is based on North American Vertical Datum 1988 (NAVD88). The vertical datum conversion between MSL and NAVD88 was obtained from National Oceanic and Atmospheric Administration (NOAA) data at Cedar Key, FL (Reference 2.4.6-17-15).

The initial water level used in all simulations is determined by adding the long-term sea level rise to the 10 percent exceedance high tide for this region.

The 10 percent exceedance predicted high tide is determined following the Regulatory Guide 1.59 (RG 1.59) (Reference 2.4.6-17-6). The 10 percent exceedance high tide value of 4.3 ft. MLW for Crystal River is obtained from Table C1 of RG 1.59. This value from RG 1.59 is converted from MLW datum to NAVD88 datum using the datum conversion chart from Reference 2.4.6-17-15. The 10 percent exceedance high tide value is converted to 2.68 ft. NAVD88. This 10 percent exceedance predicted high tide value of 2.68 ft. NAVD88 is combined with initial rise of 0.6 ft. from Table C1 of RG 1.59, to obtain the 10 percent exceedance high tide level of 3.28 ft. NAVD88.

NOAA has evaluated sea level rise trends for each tide station. Reference 2.4.6-17-16 provides the data for the mean sea level trend at the Cedar Key tide gauge, station 8727520. From this reference the mean sea level rise of 0.59 ft. in 100 years is obtained.

By adding the 10 percent exceedance high tide of 3.28 ft. NAVD88 to the long-term sea level rise of 0.59 ft, an initial water level of 3.87 ft. NAVD88 was obtained.

Seismic Source: Venezuela

Source parameters for Venezuela seismic tsunami are based on ten Brink et al (Reference 2.4.6-17-11) and are presented in Table 2.4.6-17-1. There are two fault segments associated with the potential event. The first is the W. Southern Caribbean fault in the north Venezuela subduction zone. This fault is 550 km long and 50 km wide. The strike angle is N53E, the dip angle is 17S, and the rake angle is 90 degrees. The second fault is the E. Southern Caribbean in the north Venezuela subduction zone. It is 200 km long and 50 km wide. The strike, dip and rake angles are N95E, 17S and 90 degrees, respectively. The composite source was used with a slip of 23 m for both of the segments, equivalent to magnitude M_w = 9.0. Figure 2.4.6-17-5 shows the initial source deformation calculated from the Okada formula. Results of the tsunami simulation for the Venezuela seismic source are described later.

Landslide Source: Initial Conditions and Determination of Slide Velocities

Two initial conditions are considered for each landslide source in this analysis. The first is a static source configuration, which ten Brink et al (Reference 2.4.6-17-11) suggest is a conservative approach to conduct a simulated landslide event. For the static source configuration, the initial condition for the numerical simulation is a static surface displacement with a depression over the initial slide location and having the size and shape of the slide volume, and an elevation over the final slide position having the same size and shape. The second condition employs NHWAVE to generate a dynamic source, which specifies both surface displacement and depth averaged horizontal velocity fields. For the dynamic source configuration where initial conditions for landslide sources are determined from NHWAVE, it is necessary to determine a reasonable velocity for the sliding mass, as discussed below.

Slide velocities are estimated following the methods presented by Enet and Grilli (Reference 2.4.6-17-2). The slide shapes given in Reference 2.4.6-17-2 are utilized, with the thickness of the slide relative to a local origin (x,y) = (0,0) given by (Reference 2.4.6-17-2):

$$\zeta = \frac{T}{1-\varepsilon}\left[\operatorname{sech}\left(k_b x\right)\operatorname{sech}\left(k_w y\right) - \varepsilon\right] \qquad \text{Eqn 14}$$

where ζ is the horizontal distribution of slide thickness, T is the maximum slide thickness at the center, $k_b = 2C/b$, $k_w = 2C/w$, b is landslide length in the forward (sliding) direction, w is landslide width in the transverse direction, $C = \operatorname{acosh}(1/\varepsilon)$, and truncation parameter $\varepsilon = 0.7$ as in Reference 2.4.6-17-2. This geometry gives a total slide volume V_b given by (Reference 2.4.6-17-2):

$$V_b = bwT\left(\frac{f^2-\varepsilon}{1-\varepsilon}\right) \quad \text{with} \quad f = \frac{2}{C}a\tan\sqrt{\frac{1-\varepsilon}{1+\varepsilon}} \qquad \text{Eqn 15}$$

The motion of the landslide is estimated from a balance of inertia, gravity force, buoyancy, Coulomb friction and drag force, leading to the balance equation (Reference 2.4.6-17-2):

$$(M_b + \Delta M_b)\frac{d^2 s}{dt^2} = (M_b - \rho_w V_b)(\sin\theta - C_n \cos\theta) g - \frac{1}{2}\rho_w (C_F A_w + C_D A_b)\left(\frac{ds}{dt}\right)^2 \quad \text{Eqn 16}$$

where g is gravitational acceleration, M_b is slide mass, s is downslope slide displacement, ρ_w is water density, θ is bed slope angle, ΔM_b, A_w and A_b are slide added mass, wetted surface area and main cross-section perpendicular to the direction of motion, respectively. The remaining parameters are C_F, the skin friction coefficient, C_D, the form drag coefficient, and C_n, the basal Coulomb friction coefficient. Based on this model, a terminal velocity of the slide is calculated using the following equation with the assumption that the slide moves forward a distance equal to its initial width b in the slide direction (Reference 2.4.6-17-2):

$$u_t = \sqrt{gb\sin\theta\left(1 - \frac{\tan\phi}{\tan\theta}\right)\left(\frac{\gamma - 1}{C_d'}\right)\frac{2\left(f^2 - \varepsilon\right)}{f - \varepsilon}} \quad \text{Eqn 17}$$

The parameter $\gamma = \rho_s / \rho_w$ is the specific gravity of the sliding material, which is taken to be 2.65. Following Reference 2.4.6-17-2, the global drag coefficient $C'_d = 1.0$.

Landslide Source: Mississippi Canyon

The Mississippi Canyon landslide event was chosen as the largest credible event occurring in the Gulf of Mexico basin. The description of the Mississippi Canyon landslide source is based on the discussion in ten Brink et al (Reference 2.4.6-17-11). The bathymetric evidence for the event is illustrated in Figure 2.4.6-17-6, where the source region is outlined. Ten Brink et al (Reference 2.4.6-17-11) estimates that the initial slide has an area A = 3687 km^2 and volume V_b = 425.5 km^3. From the outlined region in Figure 2.4.6-17-6, the slide source's length b is estimated to be 150 km. Using the geometric description in the previous section, a slide width w is estimated to be 31.3 km, and a maximum slide thickness T is estimated to be 0.306 km, which corresponds well with the reported excavation depth of approximately 300 m given in ten Brink et al (Reference 2.4.6-17-11). The source parameters for the Mississippi Canyon landslide event are presented in Table 2.4.6-17-2.

Two initial conditions are considered for the Mississippi Canyon landslide simulation. The first is a static source configuration, for which it is assumed that the initial slide volume described above translates downslope along its major axis a distance equal to its initial length, 150 km. The initial and final positions of the slide are displayed in Figure 2.4.6-17-6. The water depths at the slides initial and final centroids are 1000 m and 2450 m, respectively, giving an effective local slope (delta) h/b = 0.01. The runout distance of 150 km is less than the estimates based on measured bathymetry given in ten Brink et al (Reference 2.4.6-17-11), but the spreading and flattening of the sliding mass during the slide process is neglected in the present simulations. This gives a higher and narrower initial elevation hump at the final slide location than would occur if the slide were allowed to deform, but the initial displaced water volume is equivalent in either case. The resulting initial surface displacement for input into FUNWAVE-TVD is shown in Figure 2.4.6-17-7.

The second initial condition employs the model NHWAVE to generate an initial surface displacement and horizontal velocity field based on direct modeling of the sliding mass described above. Input to NHWAVE includes bathymetric grid, initial slide position and orientation, total sliding distance, and down-slope translation velocity of the slide. Equation 17

is used to estimate a terminal velocity u_t = 151.4 m/s. In the simulation, the slide is translated at this velocity for the entire slide event. The duration of the event is then (delta) $t = b/u_t = 990.7$ seconds. The model is run for this duration, and the final surface displacement field and horizontal velocity fields are saved for input into FUNWAVE-TVD. The resulting surface displacement at the end of the NHWAVE run is shown in Figure 2.4.6-17-8.

Using either the static or dynamic source as initial condition, FUNWAVE-TVD is run using one-way nesting using Grids A_l, B and C. Results of the tsunami simulation for the Mississippi Canyon source are described later.

Landslide Source: Florida Escarpment

The Florida Escarpment landslide event is the closest large event to LNP site, chosen since landslide tsunami impact is often most severe on adjacent shorelines. The Florida Escarpment landslide event is based on a collapse of the shelf break slope of the carbonate platform which forms the continental shelf on the western side of the Florida peninsula. The description of the Florida Escarpment landslide source is based on the discussion in ten Brink et al (Reference 2.4.6-17-11). The bathymetric evidence for the event is illustrated in Figure 2.4.6-17-9, where the source region is outlined, following on information presented in Figure 3-6 in ten Brink et al (Reference 2.4.6-17-11). Ten Brink et al (Reference 2.4.6-17-11) estimate that the initial slide has an area A = 647.47 km^2, width w = 42.94 km and volume V_b = 16.2 km^3. From the outlined region in Figure 2.4.6-17-9 the slide source's length b is estimated to be 19.2 km, and a maximum slide thickness T is estimated to be 58 m, which differs from the estimate of 150 m given in ten Brink et al (Reference 2.4.6-17-11), but results from the very uneven excavation pattern in the actual slide. The source parameters for the Florida Escarpment landslide event are presented in Table 2.4.6-17-2.

As in the Mississippi Canyon landslide event, two initial conditions are considered for the Florida Escarpment landslide simulation. For both, it is assumed that the initial source translated a downslope distance equal to its initial downslope length. Ten Brink et al (Reference 2.4.6-17-11) discuss this translation and point out that it is presently impossible to determine the configuration of the slide deposit from existing sonar data as the volume is buried under later deposits. The initial and final positions of the slide in the simulations are displayed in Figure 2.4.6-17-9. The water depths at the initial and final centroids of the slides are 1548 m and 3305 m, respectively, giving an effective local slope (delta) h/b = 0.09. For the dynamic source determination, Equation 17 is used to estimate a terminal velocity u_t = 175.3 m/s. In the simulation, the slide is translated at this velocity for the entire slide event. The duration of the event is then (delta) $t = b/u_t = 109.5$ seconds. The model is run for this duration, and the final surface displacement field and horizontal velocity fields are saved for input into FUNWAVE-TVD. Initial surface displacements for FUNWAVE-TVD for the static and dynamic sources are shown in Figure 2.4.6-17-10 and Figure 2.4.6-17-11, respectively.

Using either the static or dynamic sources as initial conditions, FUNWAVE-TVD is run using one-way nesting using Grids A_l, B and C. Results of the tsunami simulation for the Florida Escarpment source are described later.

Model Results: Venezuela Seismic Event Simulation

Figure 2.4.6-17-12 shows snapshots for the propagation of the tsunami in the Venezuela Grid A at 40 minutes and 80 minutes after the start of the model. Figure 2.4.6-17-13 shows a plot of

the maximum water level occurring in Grid *A*, and shows that tsunami runup height on the west Florida shelf is on the order of 20 to 30 cm. Figure 2.4.6-17-14 shows snapshots, at 440 minutes and 520 minutes after the start of the model, of the tsunami wave crossing the shelf region (Grid *B*) and making landfall on the west coast of Florida. Maximum tsunami amplitudes are greatly reduced by frictional effects over the shelf, and are limited to values on the order of 15 cm along the coast covered by Grid *B* (Figure 2.4.6-17-15). Figure 2.4.6-17-16 and Figure 2.4.6-17-17 show propagation and maximum water level in Grid *C*, respectively, and show that tsunami runup in the vicinity of the LNP site reaches levels on the order of 30 cm. Surface displacements in Figures 2.4.6-17-12 through 2.4.6-17-17 are with respect to model initial water level, which includes MSL plus 10 percent exceedence high tide plus the long-term sea level rise.

Figure 2.4.6-17-18 shows a plot of the initial MSL shoreline and maximum extent of tsunami inundation superimposed on a topographic contour map of the Grid C region. The extent of tsunami runup in the inundated region is illustrated in Figure 2.4.6-17-19, which shows a vertical section through Grid C at latitude 29.075N, representing an east-west line through the location of the LNP site, indicated on the figure. Results, including maximum water levels and inland distance of inundation, are summarized in Table 2.4.6-17-3. It should be noted that the elevations of the Levy site shown on Figures 2.4.6-17-18 and 2.4.6-17-19 and other topographical maps contained in following descriptions of model results represent the existing grade of approximately 41 ft. to 49 ft. NAVD88, as opposed to the plant grade elevation of 50 ft. NAVD88.

Model Results: Mississippi Canyon Landslide Event Simulation

The Mississippi Canyon landslide source was run using two different source configurations: a static source following the procedure in Reference 2.4.6-17-11, and a dynamic source using the NHWAVE model and the determination of slide. Results of the tsunami simulation based on the static source are displayed in Figures 2.4.6-17-20 through 2.4.6-17-27, and results based on the dynamic source are displayed in Figures 2.4.6-17-28 through 2.4.6-17-35.

Although the methodology described in Reference 2.4.6-17-11 is aimed at giving the most conservative estimate of tsunami wave amplitude for a given source configuration, results of these simulations indicate that the geometry for the source also plays a role in determining the susceptibility of any segment of coastline to tsunami attack. For example, a comparison of Figure 2.4.6-17-20 (for the static source) and Figure 2.4.6-17-28 (for the dynamic source) show a tendency for wave energy to be directed in a more southerly direction for the dynamic source. The resulting patterns of maximum wave amplitude for Grid A_1 for the two sources, shown in Figure 2.4.6-17-21 and Figure 2.4.6-17-29, show that the tsunami wave height arriving at the west Florida shelf break is significantly larger for the dynamic source than for the static source.

The evolution of the landward propagating wave for either source is controlled by strong wave breaking dissipation over the shallow and broad extent of the shelf. A comparison of the maximum wave heights for the two sources over Grid *B*, presented in Figure 2.4.6-17-23 and Figure 2.4.6-17-31, show that the dynamic source produces higher waves over the inner shelf region, but that wave height is significantly reduced by the time waves reach the inner Grid *C* region. Results for the two sources over Grid *C* are very similar, as revealed by plot plans in Figure 2.4.6-17-26 and Figure 2.4.6-17-34 and transect plots in Figure 2.4.6-17-27 and Figure 2.4.6-17-35. Inundation depth offshore reaches about 15 ft. NAVD88 in both cases, and there is significant inland flooding which reaches the base of the steeper terrain surrounding the LNP

site. Details of the spatial distribution of maximum runup elevation differ for the two cases, although neither is likely to be strictly accurate due to the relatively inaccurate nature of the CRM bathymetry for the subaerial regions fronting the LNP site.

The maximum water level near the LNP site due to a tsunami caused by the simulated Mississippi Canyon landslide event is 12.94 ft. NAVD88, considering both the static and dynamic source configurations. The inundation due to this tsunami reaches a location approximately 9.7 miles inland and approximately 3.7 miles from the LNP site. Tsunami simulation results are summarized in Table 2.4.6-17-3.

Model Results: Florida Escarpment Landslide Event Simulation

The tsunami simulation results for both static and dynamic source configurations for the Florida Escarpment landslide event are similar. Therefore, the time-wise simulation results for the static case only are presented in Figures 2.4.6-17-36 through 2.4.6-17-43. For comparison with the static source case, only the inland extent of inundation is provided for the dynamic case as presented in Figure 2.4.6-17-44.

The maximum water level near the LNP site due to a tsunami caused by the simulated Florida Escarpment landslide event is 4.33 ft. NAVD88, considering both the static and dynamic source configurations. The inundation due to this tsunami reaches a location approximately 4.2 miles inland and approximately 9.2 miles from the LNP site. Results for all of the tsunami simulations are summarized in Table 2.4.6-17-3.

PMT Maximum Water Level near LNP 1 and 2 Site

The results of maximum water level and inundation distance for each of the simulated tsunami scenarios and source configurations are presented in Table 2.4.6-17-3. Based on the discussion of tsunami simulation results, the most severe PMT event is associated with the large scale Mississippi Canyon landslide event in the Gulf of Mexico. This event produced the highest runup and farthest extent of onshore inundation in the vicinity of the LNP site.

The maximum PMT runup elevation due to the Mississippi Canyon landslide was computed to be 12.94 ft. NAVD88, which is the most conservative of all the simulation scenarios. The PMT runup includes the initial water level due to the 10 percent exceedance high tide and the long-term sea level rise. The maximum PMT runup elevation is below the plant grade elevation of 50 ft. NAVD88. The extent of inundation due to the PMT closest to the LNP site is 3.7 miles west of the LNP Units 1 and 2. Therefore, the safety-related systems and components of LNP Units 1 and 2 will not be affected by the PMT in the Gulf of Mexico.

References

2.4.6-17-1. Amante, C. and B. W. Eakins, ETOPO1 1 Arc-Minute Global Relief Model: Procedures, Data Sources and Analysis. National Oceanic and Atmospheric Administration (NOAA) Technical Memorandum NESDIS NGDC-24, 19 pp, 2009, Available at: http://www.ngdc.noaa.gov/mgg/global/global.html.

2.4.6-17-2. Enet, F. and Grilli, S. T., "Experimental study of tsunami generation by three-dimensional rigid underwater landslides," *J. Waterway, Port, Coastal and Ocean Engineering*, 133, 442-454, 2007.

2.4.6-17-3. Kirby, J. T., Shi, F., Harris, J. C. and Grilli, S. T., "Sensitivity analysis of trans-oceanic tsunami propagation to dispersive and Coriolis effects," draft manuscript, 2011.

2.4.6-17-4. Ma, G., Shi, F. and Kirby, J. T., "Shock-capturing Non-hydrostatic Model for Fully Dispersive Surface Wave Processes," submitted to *Ocean Modelling*, June, 2011.

2.4.6-17-5. National Oceanic and Atmospheric Administration (NOAA) National Geophysical Data Center (NGDC), U.S. Coastal Relief Model, Volume 3, Date Retrieved: June 13 and June 17, 2011, http://www.ngdc.noaa.gov/mgg/coastal/crm.html.

2.4.6-17-6. U.S. Nuclear Regulatory Commission, Regulatory Guide 1.59, Design Basis Floods for Nuclear Power Plants, Revision 2, August 1977.

2.4.6-17-7. Shi, F., Kirby, J. T., Harris, J. C., Geiman, J. D. and Grilli, S. T., "A High-Order Adaptive Time-Stepping TVD Solver for Boussinesq Modeling of Breaking Waves and Coastal Inundation," Manuscript in preparation for *Ocean Modelling*, 2011.

2.4.6-17-8. Shi, F., Kirby, J. T., Tehranirad, B., Harris, J. C. and Grilli, S. T., "FUNWAVE-TVD Version 1.0, Fully Nonlinear Boussinesq Wave Model with TVD Solver, Documentation and User's Manual," Research Report No. CACR-11-04, Center for Applied Coastal Research, University of Delaware, Newark. (DRAFT), 2011.

2.4.6-17-9. Synolakis, C. E., Bernard, E. N., Titov, V. V., Kanoglu, U. and Gonzalez, F. I., Standards, Criteria, and Procedures for NOAA Evaluation of Tsunami Numerical Models, National Oceanic and Atmospheric Administration (NOAA) Technical Memorandum OAR PMEL-135, Pacific Marine Environmental Laboratory, Seattle, 2007.

2.4.6-17-10. Tehranirad, B., Shi, F., Kirby, J. T., Harris, J. C. and Grilli, S. T., "Tsunami Benchmark Results for Fully Nonlinear Boussinesq Wave Model FUNWAVE-TVD, Version 1.0," Research Report No. CACR-11-02, Center for Applied Coastal Research, University of Delaware, Newark. (DRAFT), 2011.

2.4.6-17-11. ten Brink, U., Twichell, D., Lynett, P., Geist, E., Chaytor, J., Lee, H., Buczkowski, B. and Flores, C., "Regional assessment of tsunami potential in the Gulf of Mexico," U. S. Geological Survey Administrative Report, 2009.

2.4.6-17-12. Okada, Y., "Surface Deformation Due to Shear and Tensile Faults in a Half-Space," Bulletin of the Seismological Society of America, Vol. 75, No. 4, pp. 1135-1154, August 1985.

2.4.6-17-13. Satake, K., "Linear and Nonlinear Computations of the 1992 Nicaragua Earthquake Tsunami," *Pure and Applied Geophysics*, 144, 455-470, 1995.

2.4.6-17-14. Soulsby, R. L., "The Bottom Boundary Layer of Shelf Seas," in B. Johns (ed), Physical Oceanography of Coastal and Shelf Seas, Elsevier, 189-266, 1983.

2.4.6-17-15. National Oceanic and Atmospheric Administration (NOAA), Tides and Currents, Datums, Cedar Key, Florida, Station ID: 8727520, Datums, Accessed in June 2010, *http://tidesandcurrents.noaa.gov/data_menu.shtml?stn=8727520%20Cedar%20Key,%20FL&type=Datums*.

2.4.6-17-16. National Oceanic and Atmospheric Administration (NOAA), Mean Sea Level Trend, 8727520 Cedar Key, Florida, Accessed in June 2010, *http://tidesandcurrents.noaa.gov/sltrends/sltrends_station.shtml?stnid=8727520*.

Table 2.4.6-17-1
Tsunami Source Parameters for the Venezuela Seismic Source

Seismic Source: Fault	Fault Length (km)	Fault Width (km)	Strike Angle	Dip Angle	Rake Angle (°)
Venezuela: W. Southern Caribbean	550	50	N53E	17S	90
Venezuela: E. Southern Caribbean	200	50	N95E	17W	90

Source: Reference 2.4.6-17-11

Table 2.4.6-17-2
Tsunami Source Parameters for the Landslide Sources

Landslide Source	Total Volume V_b (km^3)	Area A (km^2)	Excavation Depth (m)	Runout Distance (km from toe)
Mississippi Canyon	425.54	3687.26	~300	297
Florida Escarpment	16.2	647.57	~150	Uncertain

Source: Reference 2.4.6-17-11

Table 2.4.6-17-3
Probable Maximum Tsunami Simulation Results Using FUNWAVE

Scenario	Maximum Wave Amplitude at Five Miles Offshore (Feet) (1)	Maximum Wave Amplitude at Shoreline (Feet) (1)	Maximum Extent of Inundation Distance from Shoreline (Miles) (2)	Maximum Extent of Inundation Distance from LNP Site (Miles) (2)	Maximum Water Level Nearest the LNP Site (Feet NAVD88)	Grade Elevation / Floor Elevation of LNP Safety-Related Facilities (Feet NAVD88)
Venezuela Seismic Source	0.22	0.30	4.2	9.2	4.27	50.0 / 51.0
Mississippi Canyon Landslide – Static Source	9.93	9.11	9.7	3.7	12.94	50.0 / 51.0
Mississippi Canyon Landslide – Dynamic Source	10.05	8.93	9.6	3.8	11.66	50.0 / 51.0
Florida Escarpment Landslide – Static Source	0.27	0.29	4.2	9.2	4.33	50.0 / 51.0
Florida Escarpment Landslide – Dynamic Source	0.25	0.27	4.2	9.2	4.30	50.0 / 51.0

Notes:
(1) The tsunami wave amplitudes presented in the table are measured above the initial water level of 3.87 feet NAVD88.
(2) The distances presented in the table are measured along latitude 29.075N. The LNP site is located approximately 13.4 miles from the shoreline.

Associated LNP COL Application Revisions:

The following changes will be made in a future revision to Part 2, FSAR of the LNP COLA:

1. Text for FSAR Subsection 2.4.6.6.3 (including Subsections 2.4.6.6.3.1 through 2.4.6.6.3.10) (updated in response to NRC Letter 094, RAI 02.04.06-16 (NPD-NRC-2010-083, L-0867)) will be deleted.
2. Text for FSAR Subsection 2.4.6.7 (updated in response to NRC Letter 094, RAI 02.04.06-16 (NPD-NRC-2010-083, L-0867)) will be replaced with the text presented in Attachment RAI 02.04.06-17-A.
3. Text for FSAR Subsection 2.4.16 will be revised to replace References 2.4.6-228 through 2.4.6-241 with new References 2.4.6-228 through 2.4.6-241 as presented in Attachment RAI 02.04.06-17-A.
4. Text for FSAR Subsection 2.4.16 will be revised to add References 2.4.6-242 and 2.4.6-243 as presented in Attachment RAI 02.04.06-17-A
5. FSAR Table 2.4.6-206 (updated in response to NRC Letter 094, RAI 02.04.06-16 (NPD-NRC-2010-083, L-0867)) will be replaced with new Table 2.4.6-206 as presented in Attachment RAI 02.04.06-17-B.
6. FSAR Table 2.4.6-207 (updated in response to NRC Letter 094, RAI 02.04.06-16 (NPD-NRC-2010-083, L-0867)) will be replaced with new Table 2.4.6-207 as presented in Attachment RAI 02.04.06-17-B.
7. FSAR Table 2.4.6-208 (updated in response to NRC Letter 094, RAI 02.04.06-16 (NPD-NRC-2010-083, L-0867)) will be replaced with new Table 2.4.6-208 as presented in Attachment RAI 02.04.06-17-B.
8. FSAR Table 2.4.6-209 through Table 2.4.6-211 (updated in response to NRC Letter 094, RAI 02.04.06-16 (NPD-NRC-2010-083, L-0867)) will be deleted.
9. FSAR Figure 2.4.6-228 will be replaced with new Figure 2.4.6-228 as presented in Attachment RAI 02.04.06-17-C.
10. FSAR Figure 2.4.6-229 will be replaced with new Figure 2.4.6-229 as presented in Attachment RAI 02.04.06-17-C.
11. FSAR Figure 2.4.6-230 presented in response to NRC Letter 094, RAI 02.04.06-16 (NPD-NRC-2010-083, L-0867) will be replaced with new Figure 2.4.6-230 as presented in Attachment RAI 02.04.06-17-C.
12. FSAR Figure 2.4.6-231 through Figure 2.4.6-271 will be added as presented in Attachment RAI 02.04.06-17-C.

Attachments/Enclosures:

1. Enclosure 2: Figures RAI 2.4.6-17-1 through RAI 2.4.6-17-44 [45 pages]
2. Attachment RAI 02.04.06-17-A: FSAR Text Revisions [14 pages]
3. Attachment RAI 02.04.06-17-B: New FSAR Tables (Table 2.4.6-206 through Table 2.4.6-208) [3 pages]
4. Attachment RAI 02.04.06-17-C: New FSAR Figures (Figure 2.4.6-228 through Figure 2.4.6-271) [44 pages]
5. Attachment RAI 02.04.06-17-D: DVD Model Input and Output Files for the PMT Analysis
6. Appendix 1: Verification and Validation Document (Appendix 1 in Calculation No. LNP-0000-X7C-051) [334 pages]

Figures

RAI 2.4.6-17-1

through

RAI 2.4.6-17-44

[45 pages including this cover page]

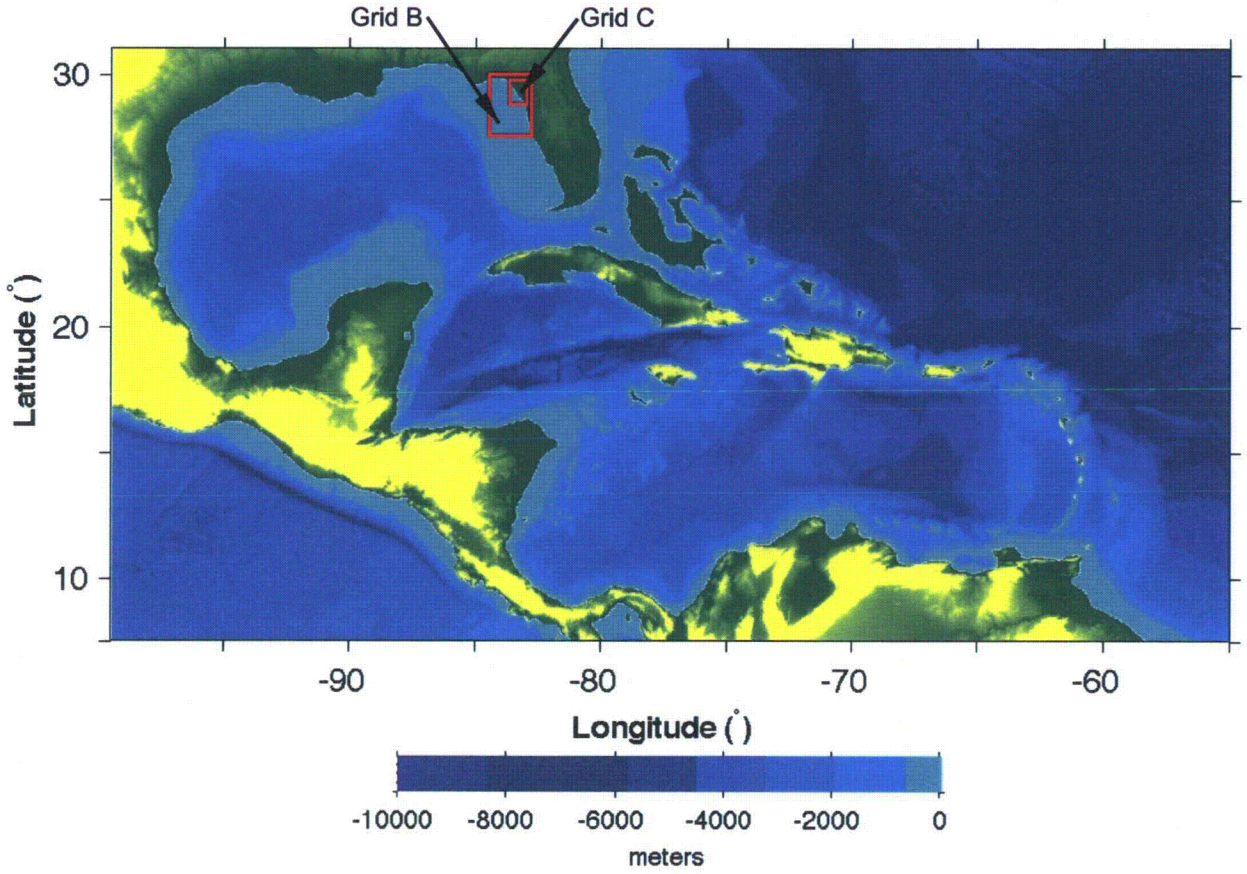

Progress Energy Florida
Levy Nuclear Plant
Units 1 and 2
Part 2, Final Safety Analysis Report

Venezuela Seismic Event Simulation:
Geometry of Grid *A*

FIGURE RAI 2.4.6-17-1 Rev 0

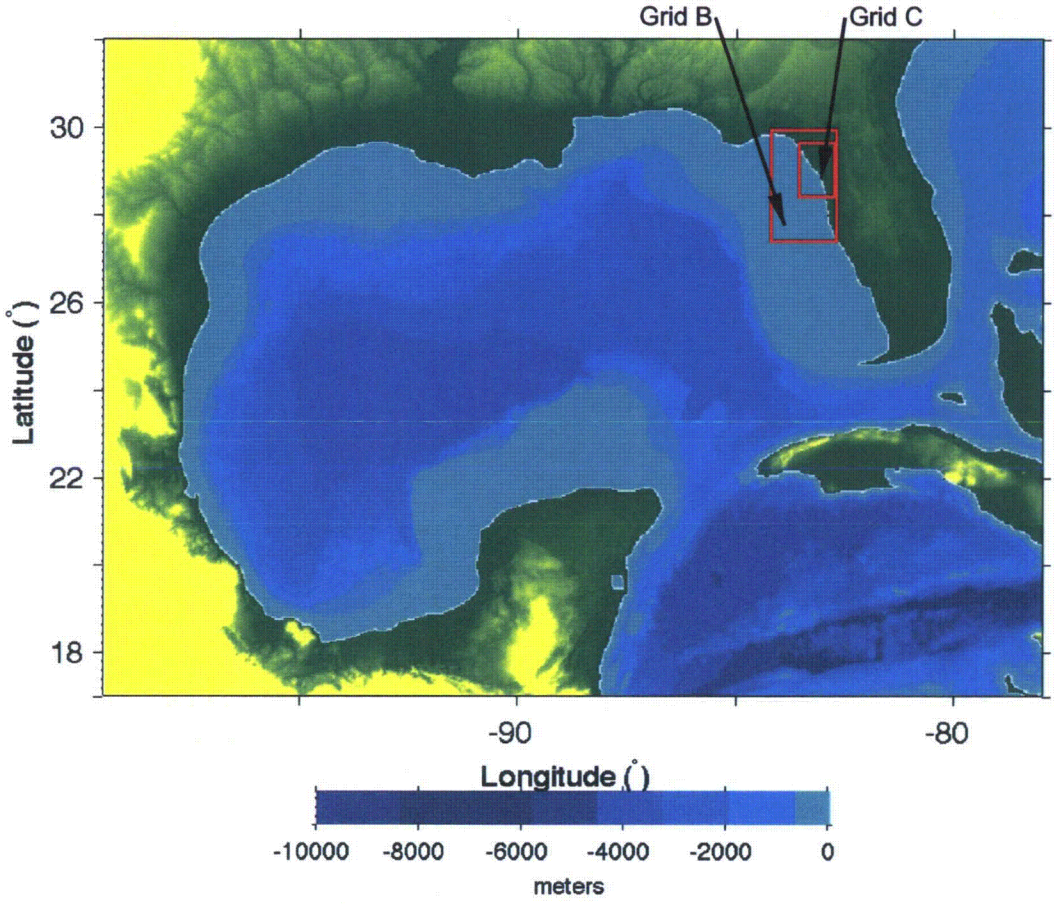

Progress Energy Florida
Levy Nuclear Plant
Units 1 and 2
Part 2, Final Safety Analysis Report

Mississippi Canyon and Florida Escarpment
Landslide Event Simulations:
Geometry of Grid A_f

FIGURE RAI 2.4.6-17-2 Rev 0

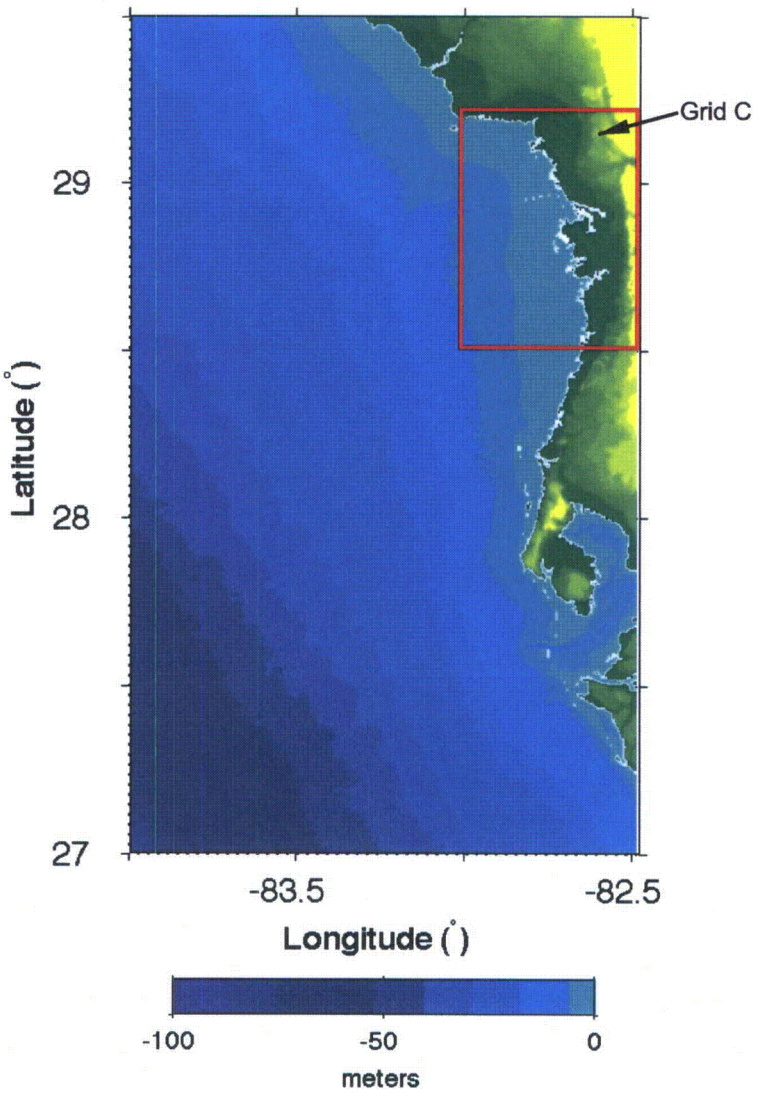

Progress Energy Florida
Levy Nuclear Plant
Units 1 and 2
Part 2, Final Safety Analysis Report

Geometry of Nested Grid *B*
for all Simulated Events

FIGURE RAI 2.4.6-17-3 Rev 0

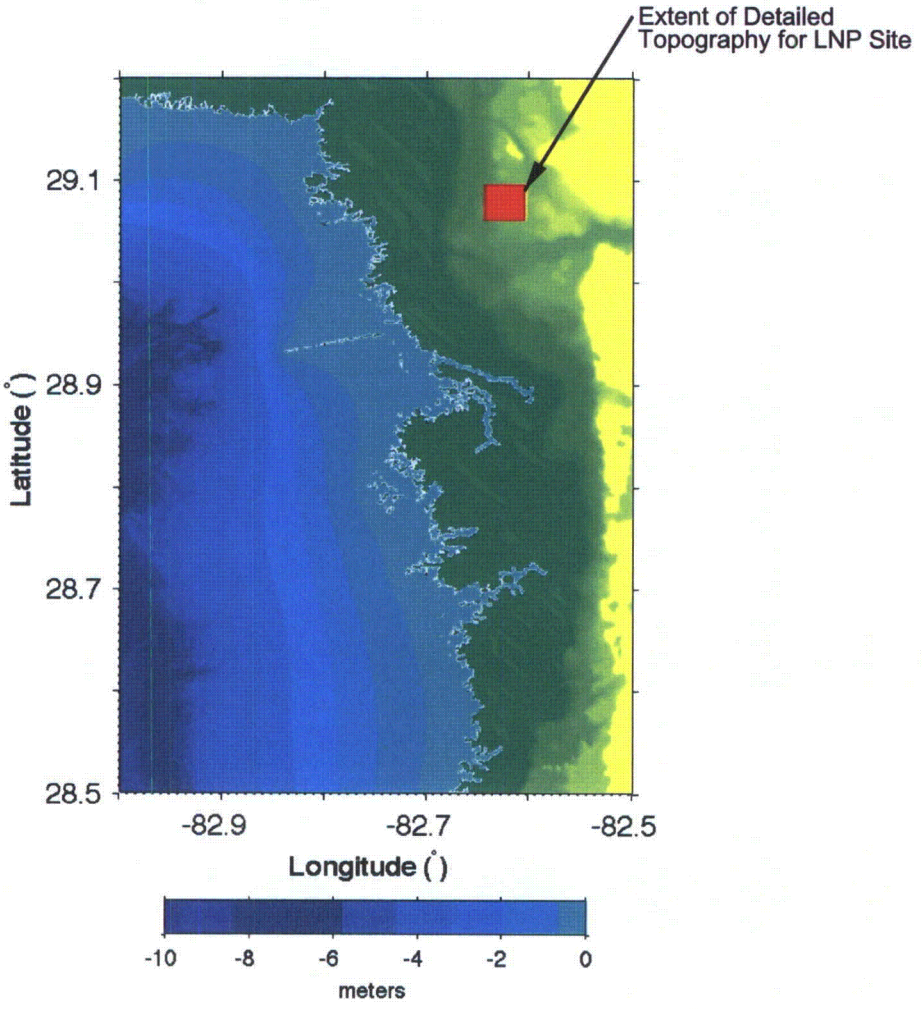

Progress Energy Florida
Levy Nuclear Plant
Units 1 and 2
Part 2, Final Safety Analysis Report

Geometry of Nested Grid *C*
for all Simulated Events

FIGURE RAI 2.4.6-17-4 Rev 0

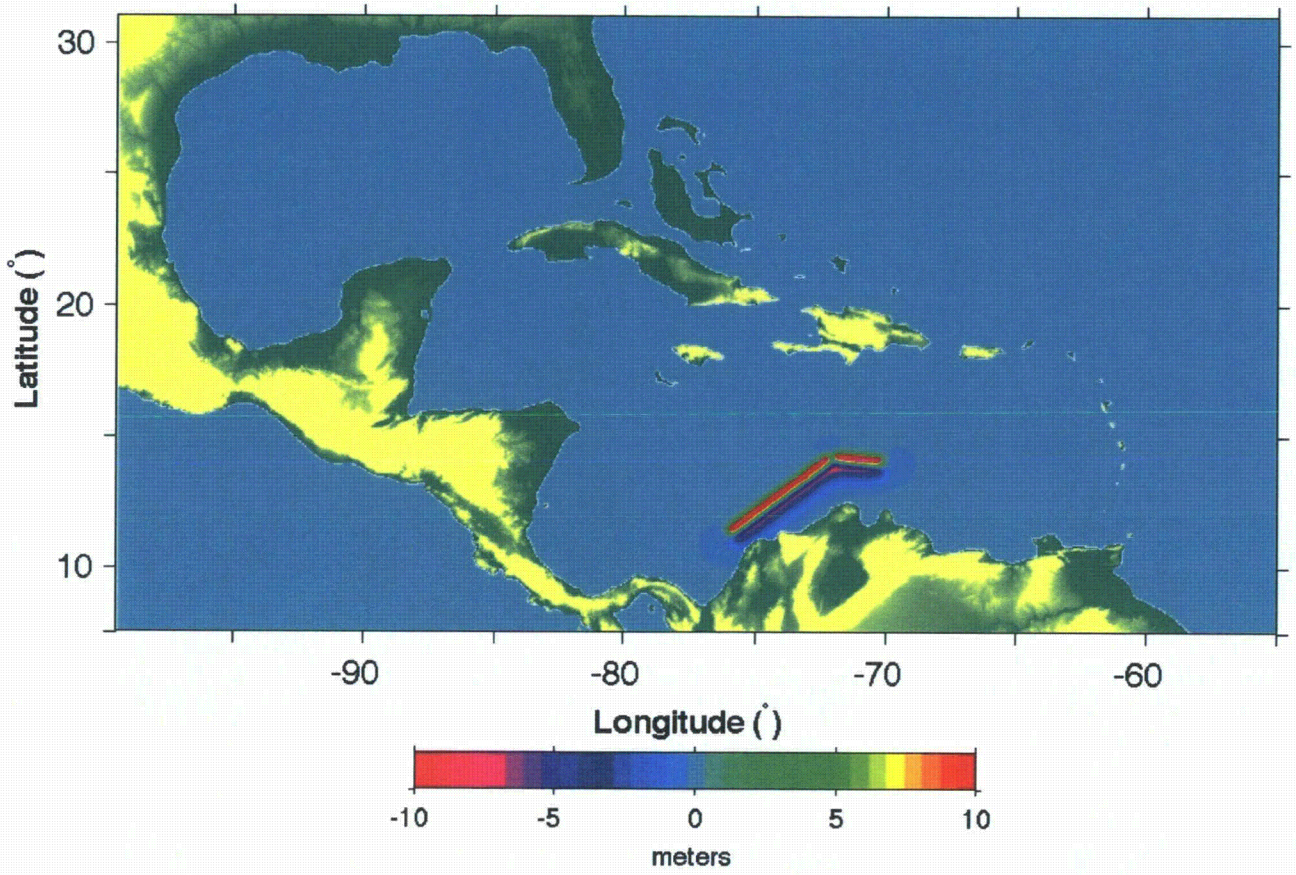

Progress Energy Florida
Levy Nuclear Plant
Units 1 and 2
Part 2, Final Safety Analysis Report

Venezuela Seismic Event Simulation:
Static Seismic Source,
Initial Bottom and Sea Surface Deformation

FIGURE RAI 2.4.6-17-5 Rev 0

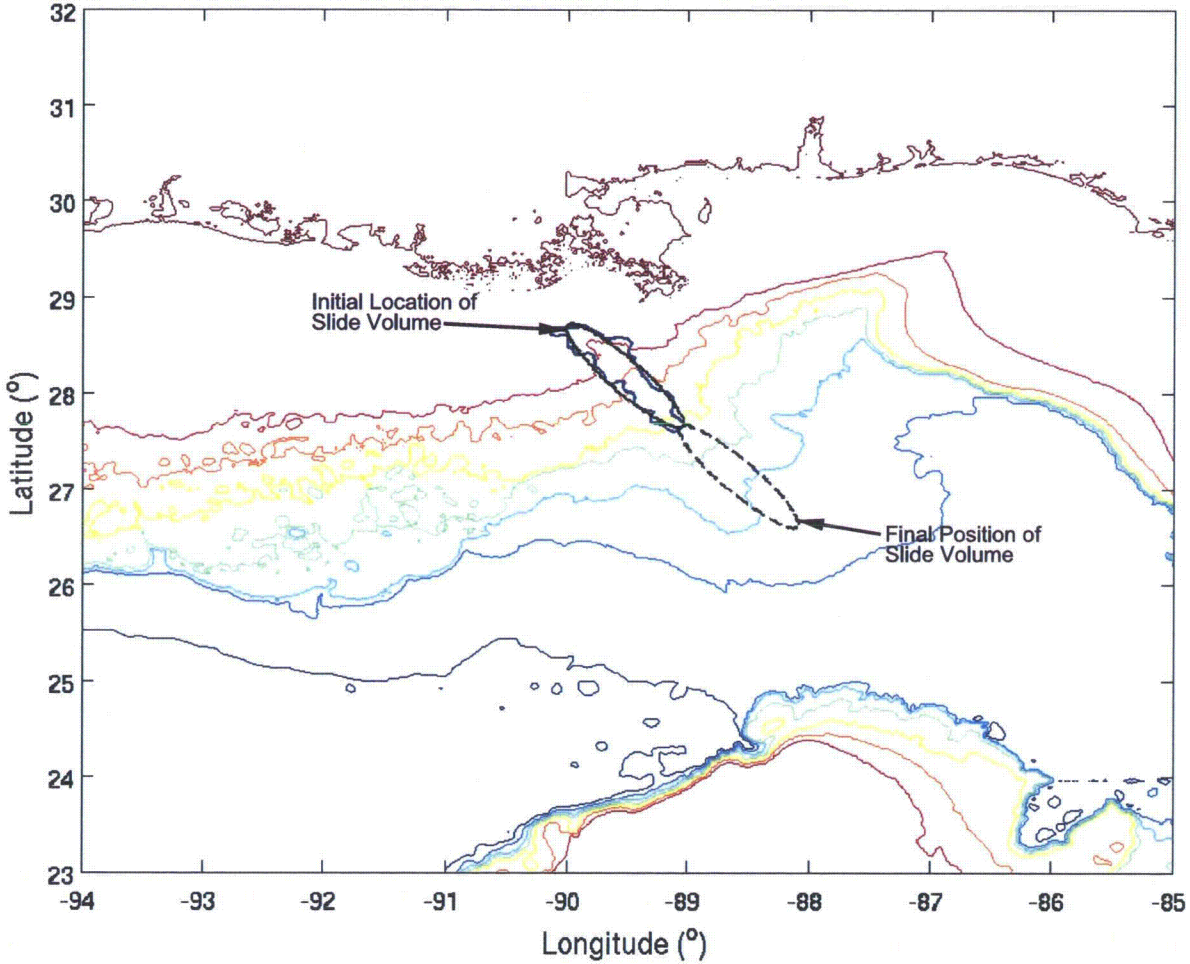

Progress Energy Florida
Levy Nuclear Plant
Units 1 and 2
Part 2, Final Safety Analysis Report

Mississippi Canyon Landslide Event Simulation:
Geometry of Slide Area Superimposed on
ETOPO1 Bathymetry

FIGURE RAI 2.4.6-17-6 Rev 0

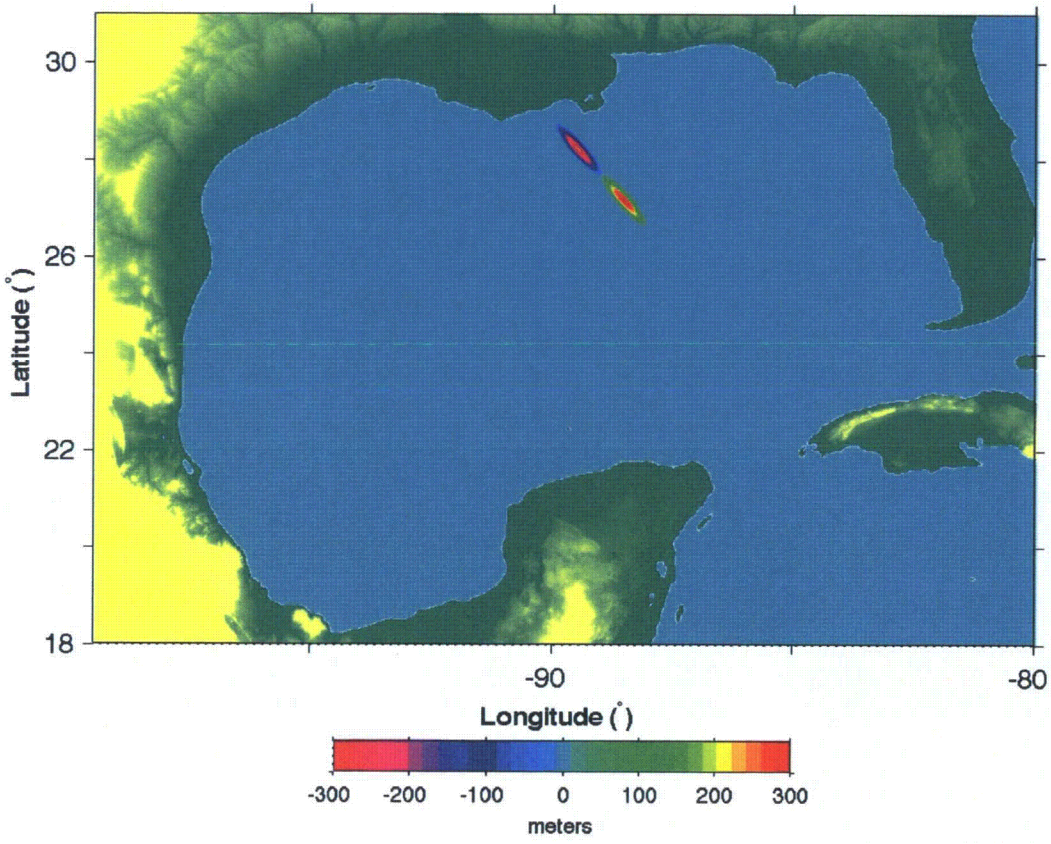

Progress Energy Florida
Levy Nuclear Plant
Units 1 and 2
Part 2, Final Safety Analysis Report

Mississippi Canyon Landslide Event Simulation:
Initial Static Source,
Initial Sea Surface Displacement (Grid A_I)

FIGURE RAI 2.4.6-17-7 Rev 0

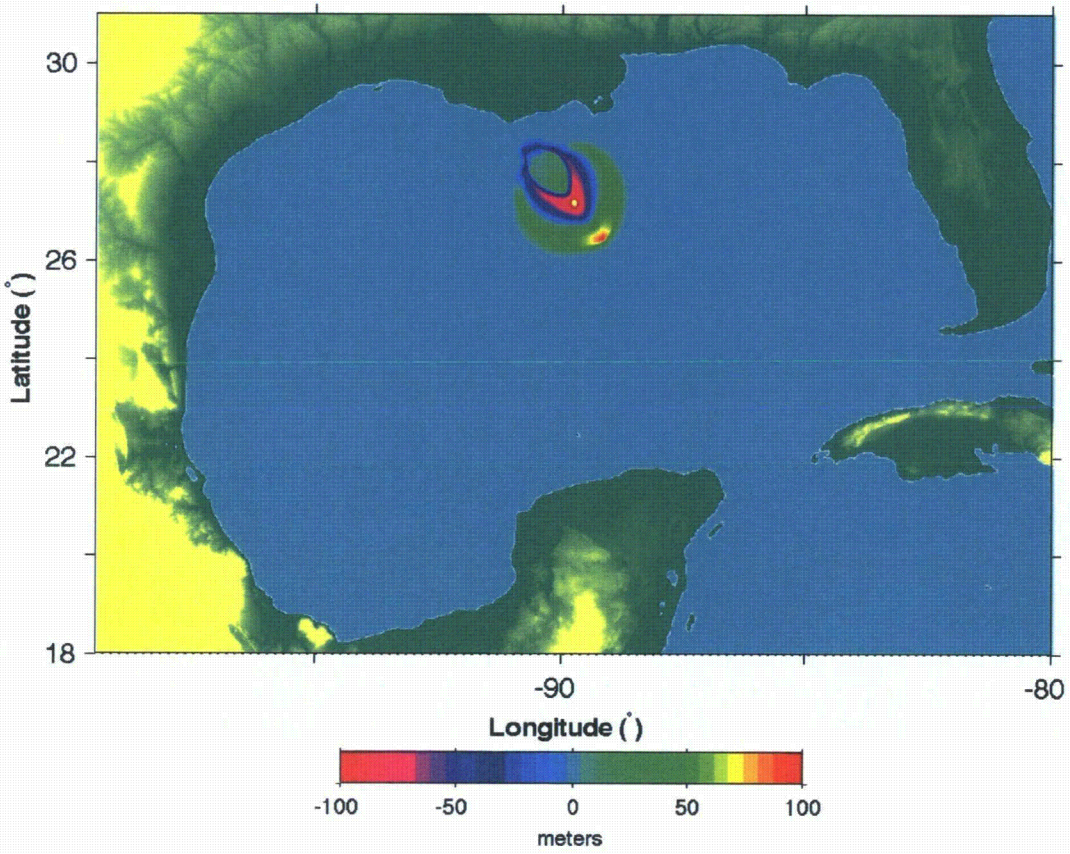

Progress Energy Florida
Levy Nuclear Plant
Units 1 and 2
Part 2, Final Safety Analysis Report

Mississippi Canyon Landslide Event Simulation:
Initial Dynamic Source, Sea Surface Displacement
at the end of NHWAVE Run (Grid A_1)

FIGURE RAI 2.4.6-17-8 Rev 0

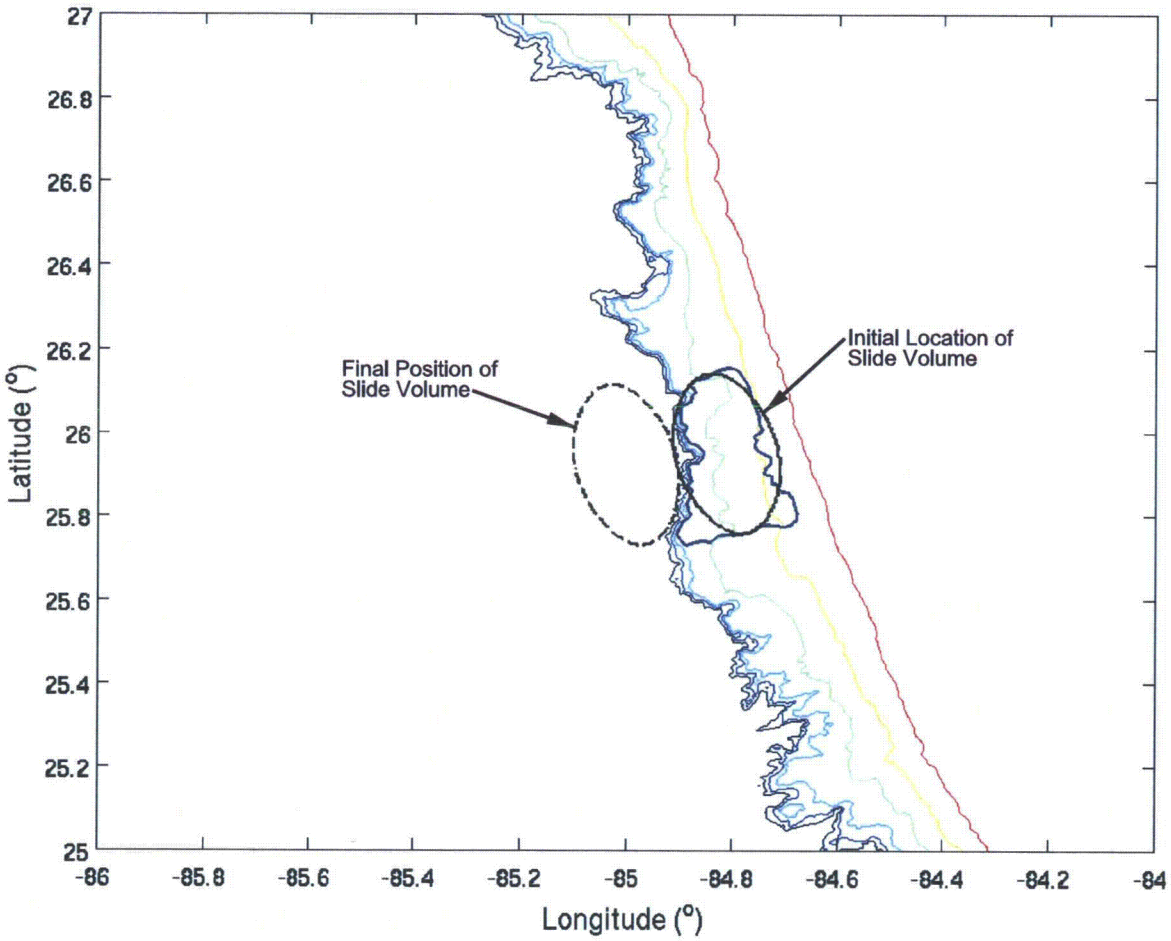

Progress Energy Florida
Levy Nuclear Plant
Units 1 and 2
Part 2, Final Safety Analysis Report

Florida Escarpment Landslide Event Simulation:
Geometry of Slide Configuration
Superimposed on CRM Bathymetry

FIGURE RAI 2.4.6-17-9 Rev 0

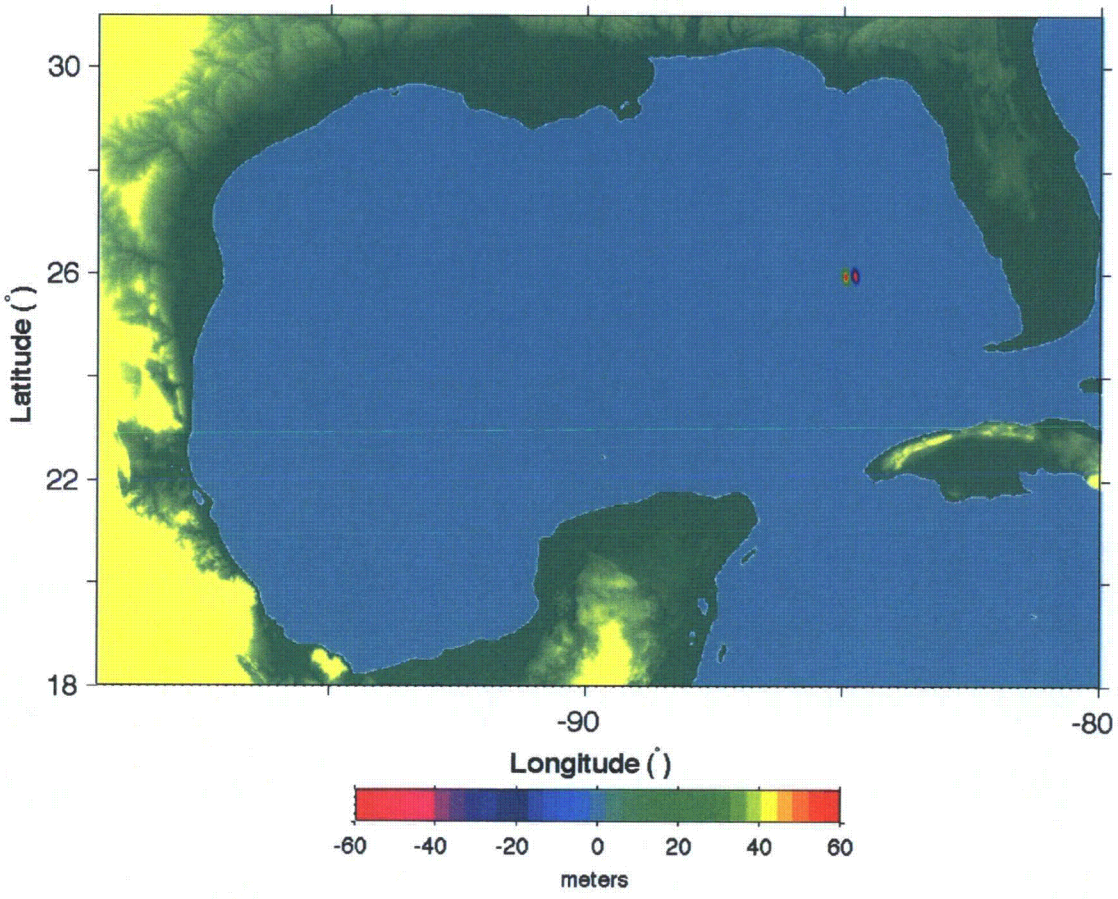

Progress Energy Florida
Levy Nuclear Plant
Units 1 and 2
Part 2, Final Safety Analysis Report

Florida Escarpment Landslide Event Simulation:
Initial Static Source,
Initial Sea Surface Displacement (Grid A_i)

FIGURE RAI 2.4.6-17-10 Rev 0

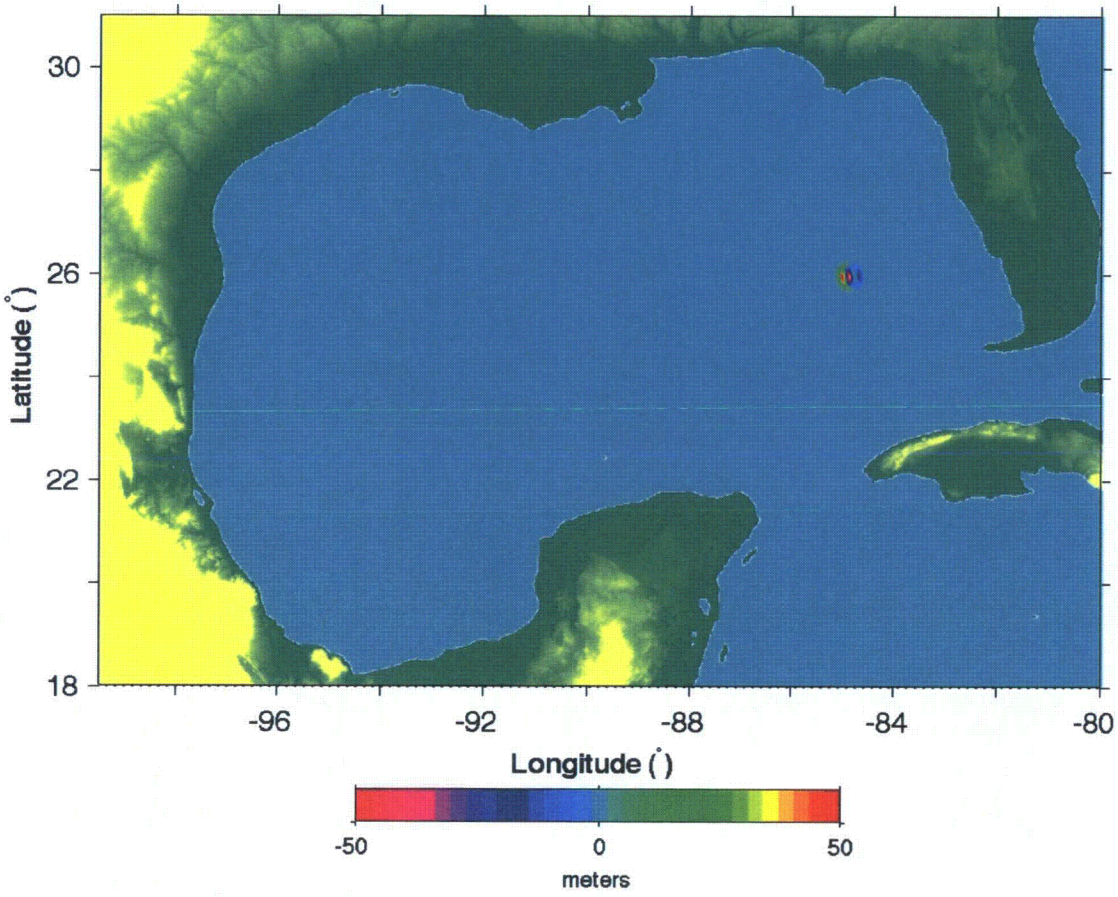

Progress Energy Florida
Levy Nuclear Plant
Units 1 and 2
Part 2, Final Safety Analysis Report

Florida Escarpment Landslide Event Simulation:
Initial Dynamic Source, Sea Surface Displacement
at the end of NHWAVE Run (Grid A_I)

FIGURE RAI 2.4.6-17-11 Rev 0

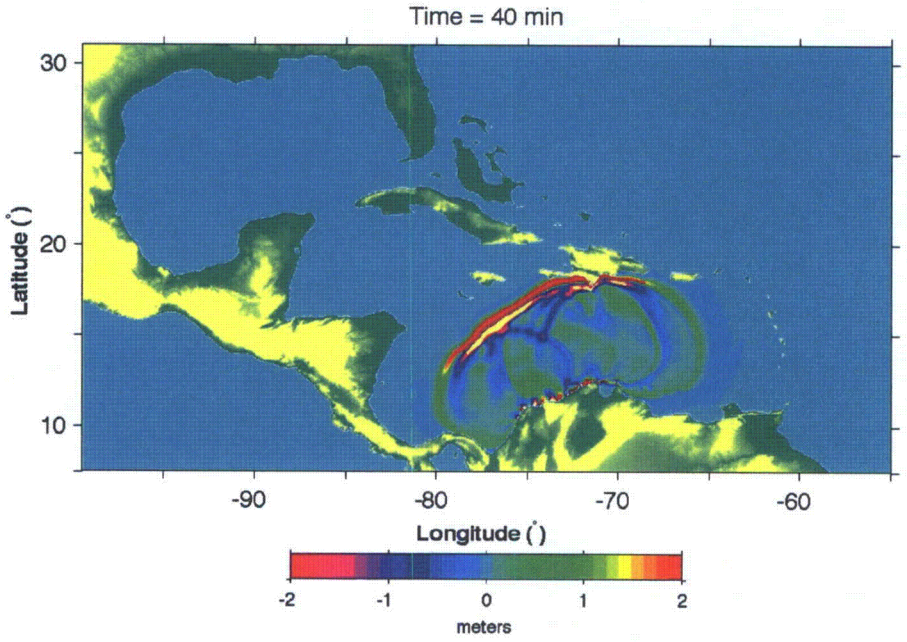

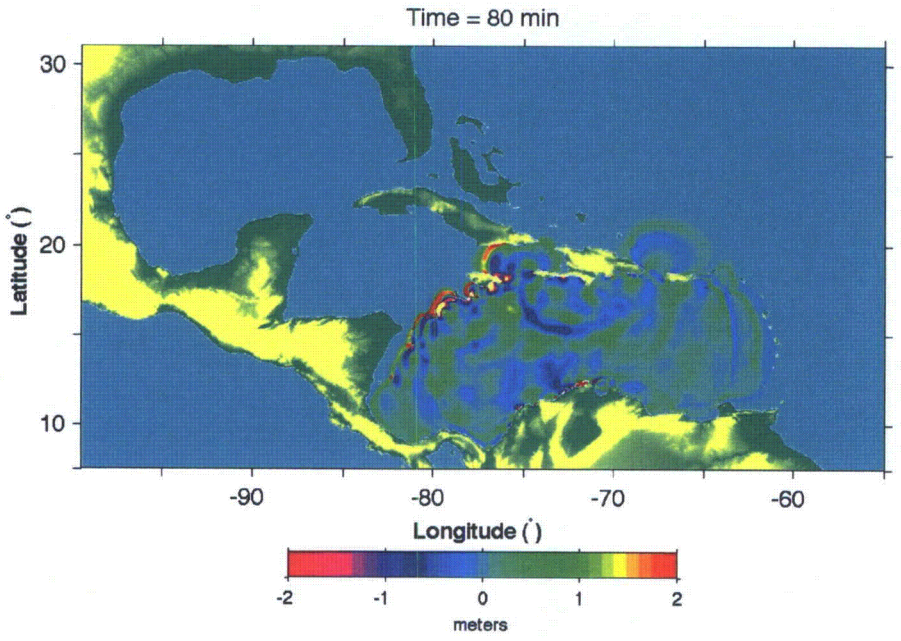

Progress Energy Florida
Levy Nuclear Plant
Units 1 and 2
Part 2, Final Safety Analysis Report

Venezuela Seismic Event Simulation:
Instantaneous Surface Displacement (Grid *A*)
at T = 40 min and T = 80 min

FIGURE RAI 2.4.6-17-12 Rev 0

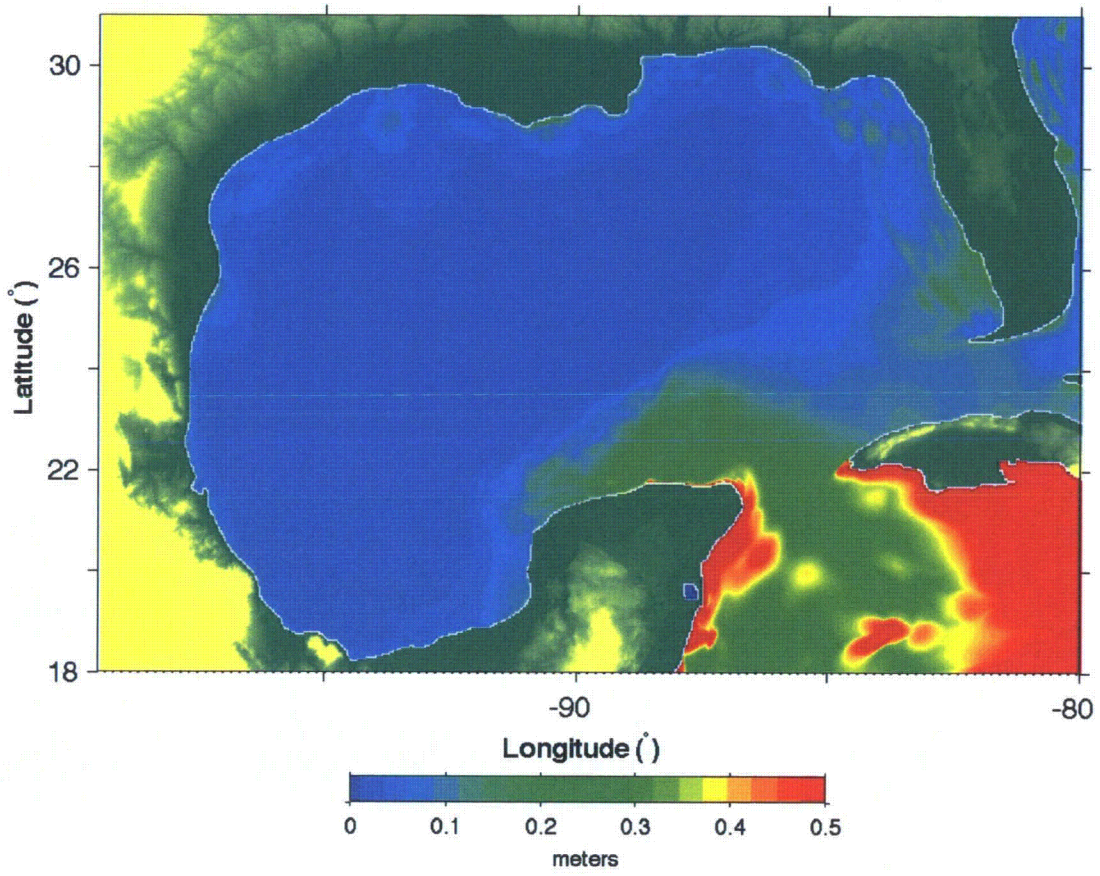

Progress Energy Florida
Levy Nuclear Plant
Units 1 and 2
Part 2, Final Safety Analysis Report

Venezuela Seismic Event Simulation:
Maximum Water Level
Generated During Simulation (Grid *A*)

FIGURE RAI 2.4.6-17-13 Rev 0

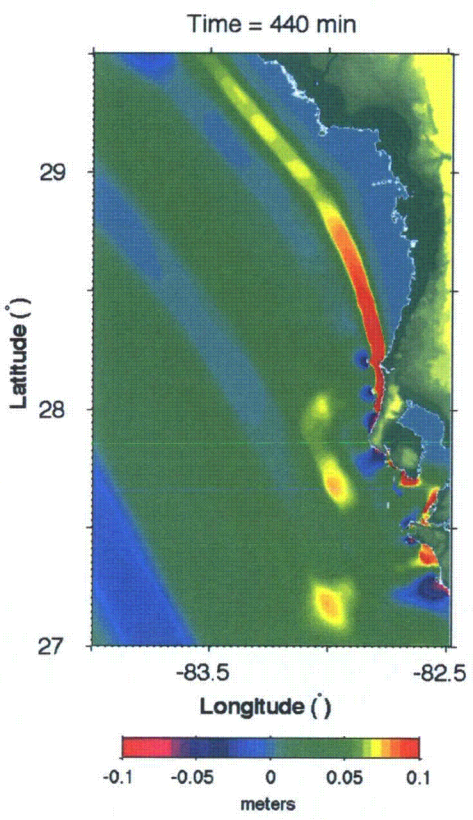

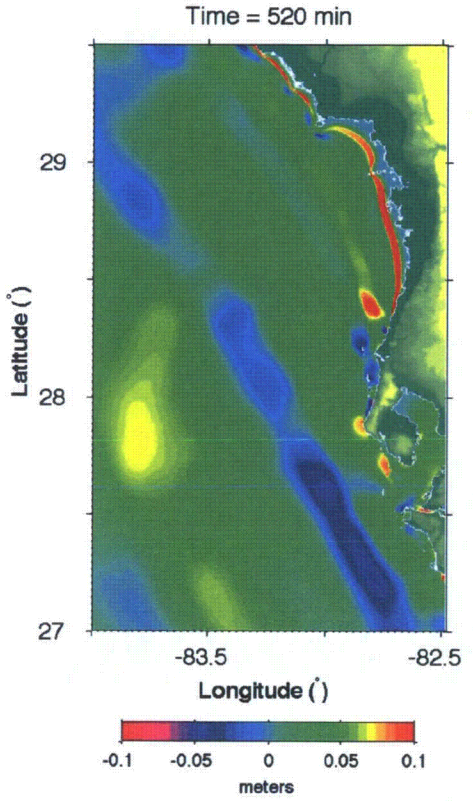

Progress Energy Florida
Levy Nuclear Plant
Units 1 and 2
Part 2, Final Safety Analysis Report

Venezuela Seismic Event Simulation:
Instantaneous Surface Displacement (Grid *B*)
at T = 440 min and T = 520 min

FIGURE RAI 2.4.6-17-14 Rev 0

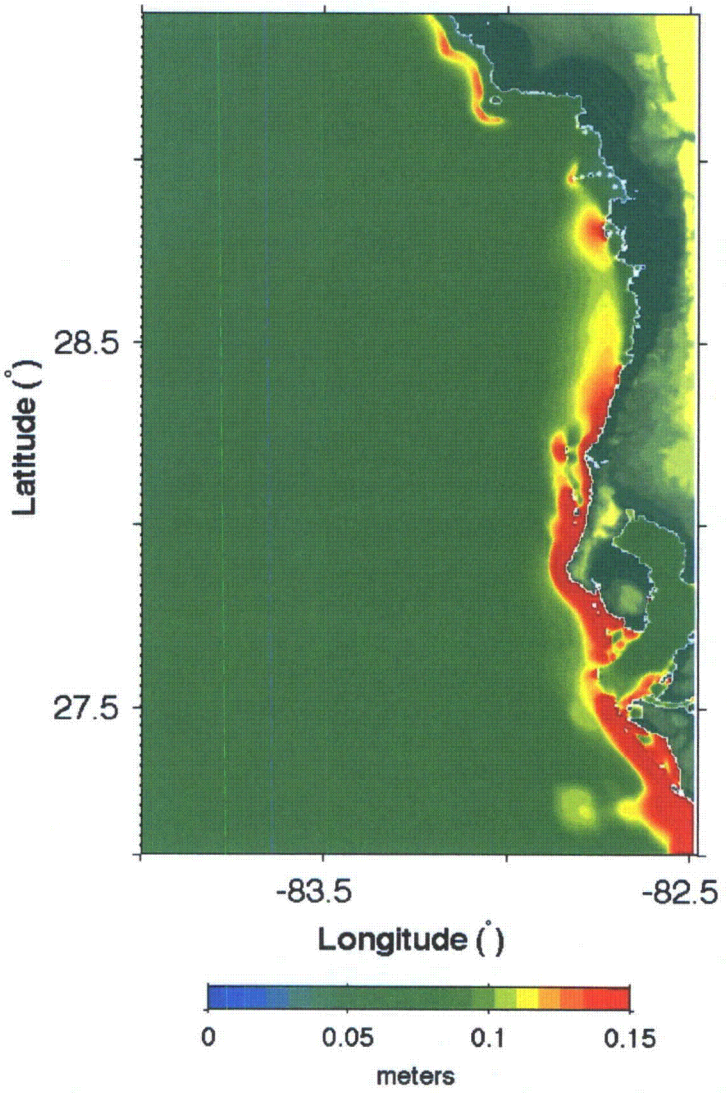

Progress Energy Florida
Levy Nuclear Plant
Units 1 and 2
Part 2, Final Safety Analysis Report

Venezuela Seismic Event Simulation:
Maximum Water Level
Generated During Simulation (Grid *B*)

FIGURE RAI 2.4.6-17-15 Rev 0

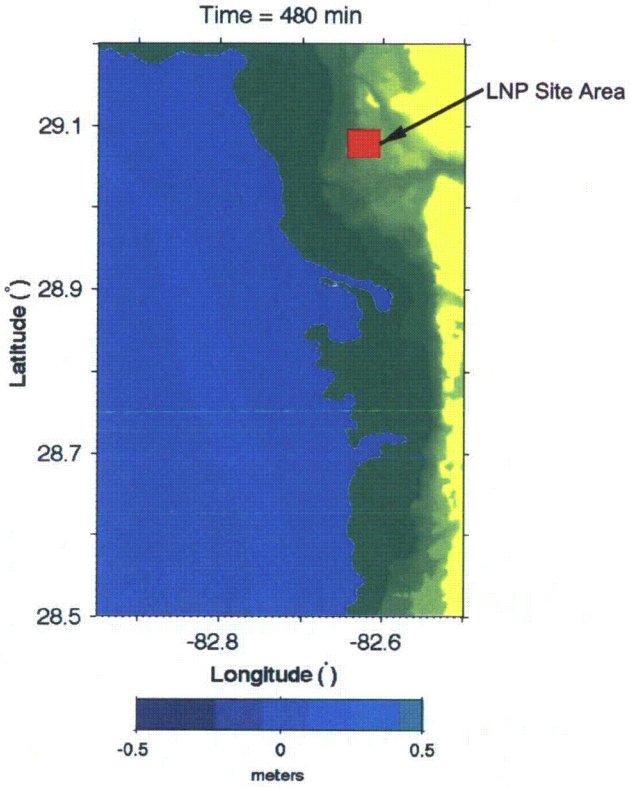

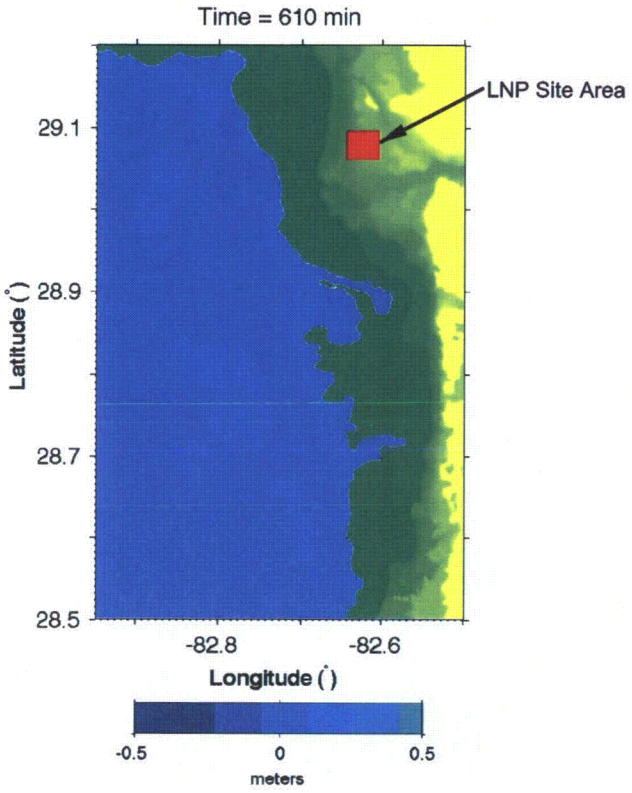

Progress Energy Florida
Levy Nuclear Plant
Units 1 and 2
Part 2, Final Safety Analysis Report

Venezuela Seismic Event Simulation:
Instantaneous Surface Displacement (Grid *C*)
at T = 480 min and T = 610 min

FIGURE RAI 2.4.6-17-16 Rev 0

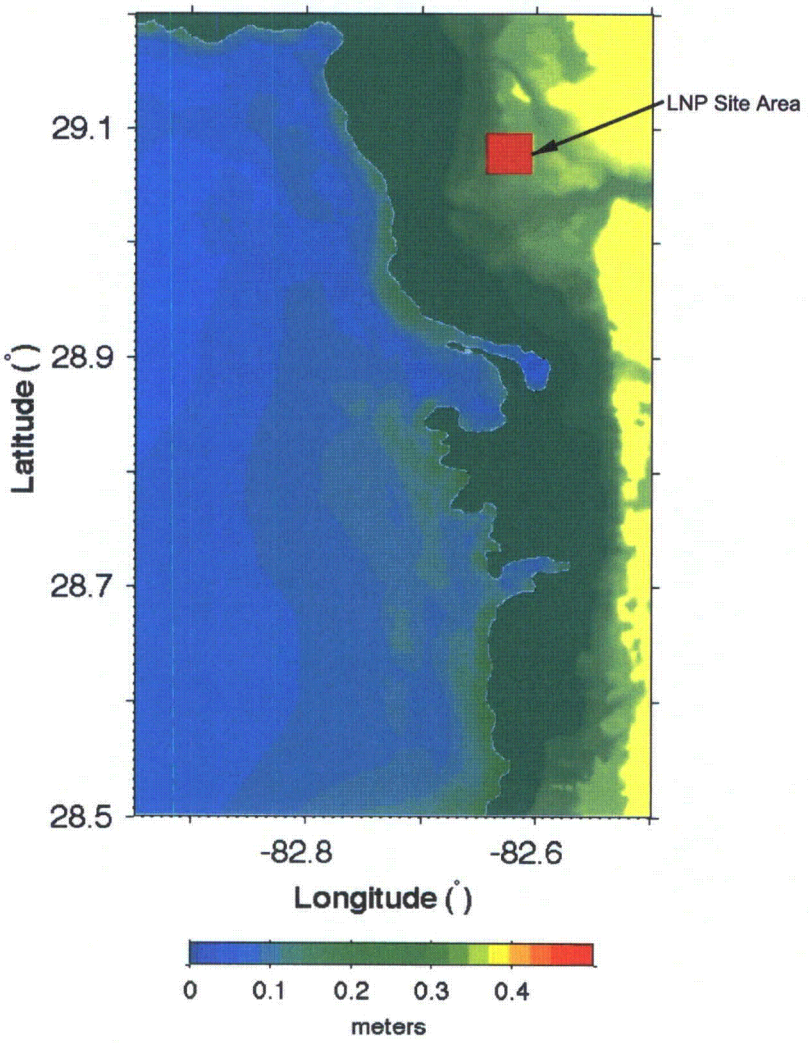

Progress Energy Florida
Levy Nuclear Plant
Units 1 and 2
Part 2, Final Safety Analysis Report

Venezuela Seismic Event Simulation:
Maximum Water Level
Generated During Simulation (Grid *C*)

FIGURE RAI 2.4.6-17-17 Rev 0

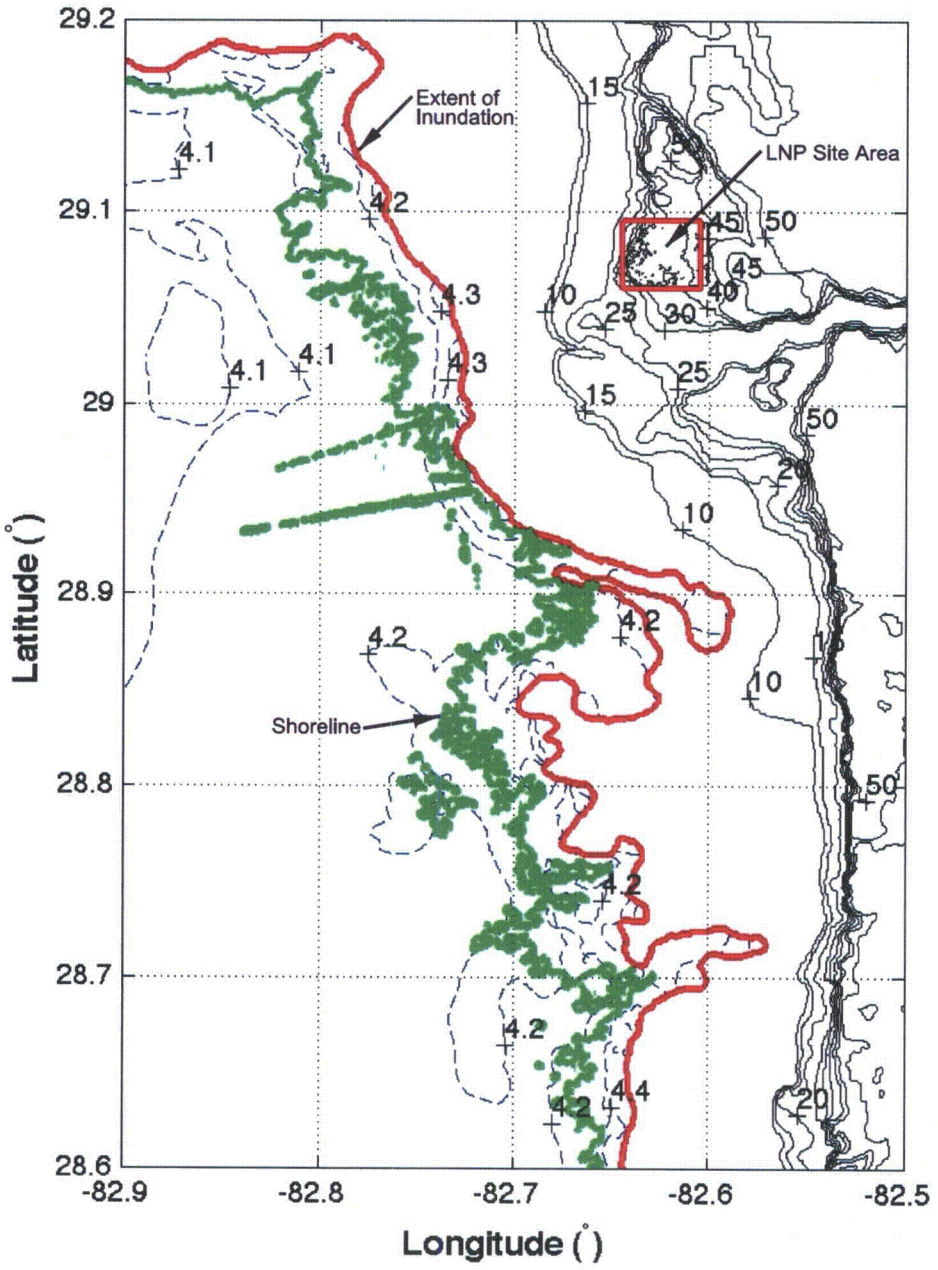

NOTE:
Contour elevations are given in feet NAVD 88.

Progress Energy Florida
Levy Nuclear Plant
Units 1 and 2
Part 2, Final Safety Analysis Report

Venezuela Seismic Event Simulation:
Maximum Extent of Inundation

FIGURE RAI 2.4.6-17-18 Rev 0

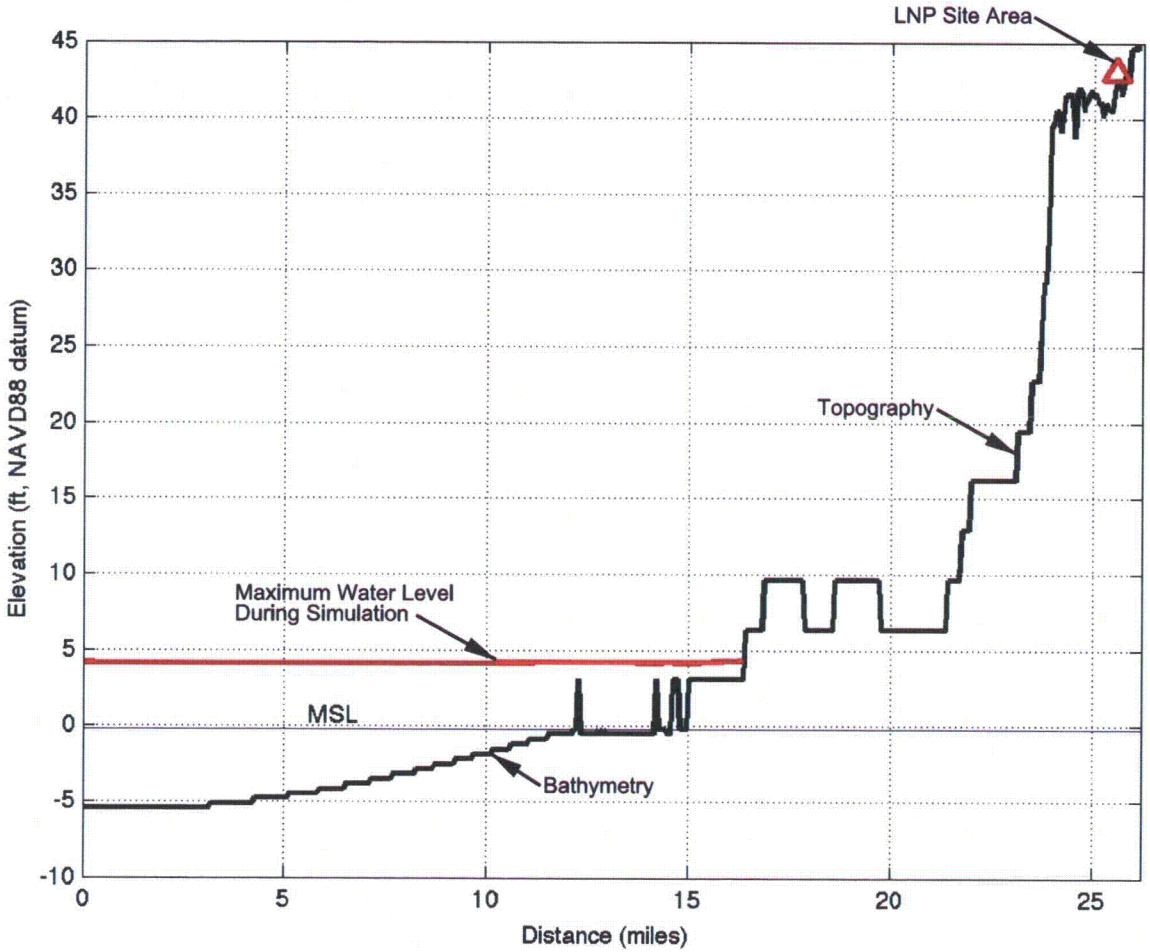

NOTE:
The existing grade elevation at the LNP site location is approximately 43 feet NAVD 88. The final grade elevation of LNP Units 1 & 2 will be raised to 50 feet NAVD 88.

Progress Energy Florida
Levy Nuclear Plant
Units 1 and 2
Part 2, Final Safety Analysis Report

Venezuela Seismic Event Simulation:
Profile at Latitude = 29.075 N

FIGURE RAI 2.4.6-17-19 Rev 0

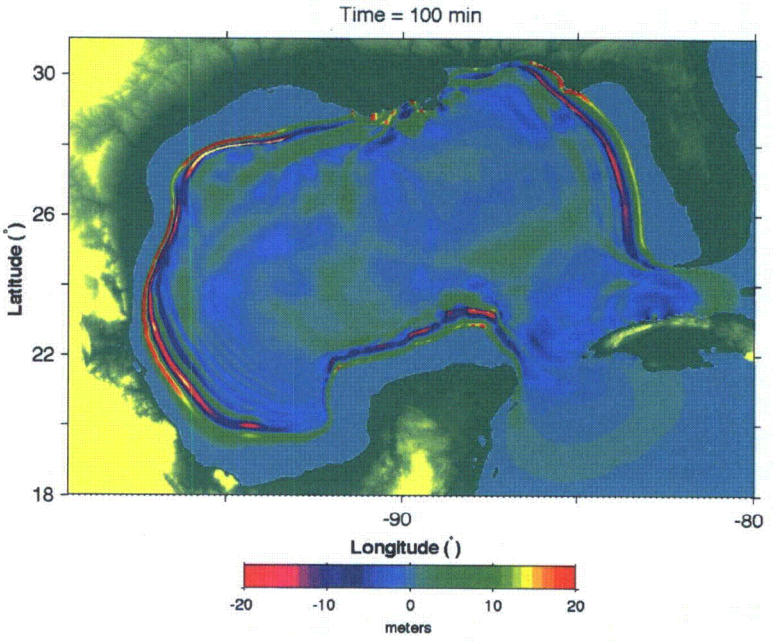

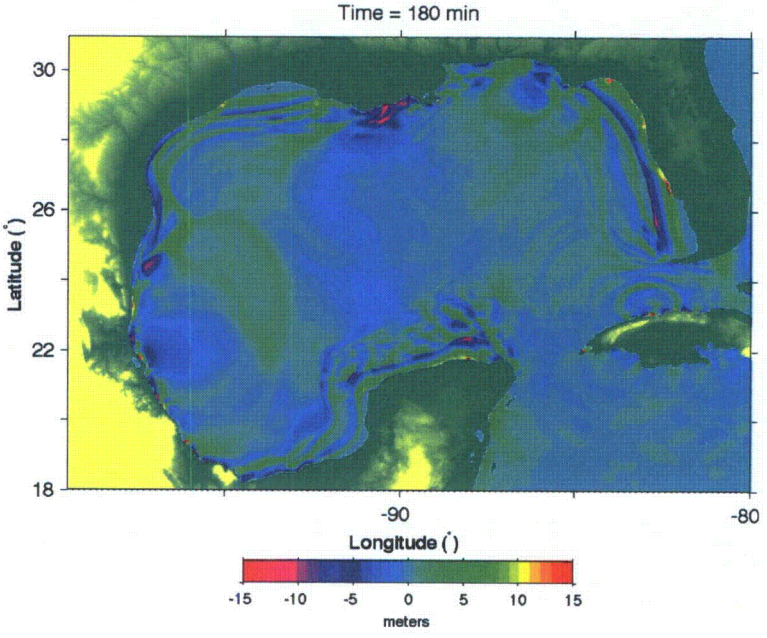

Progress Energy Florida
Levy Nuclear Plant
Units 1 and 2
Part 2, Final Safety Analysis Report

Mississippi Canyon Landslide Event Simulation,
Static Source:
Instantaneous Surface Displacement (Grid A_I)
at T = 100 min and T = 180 min
FIGURE RAI 2.4.6-17-20 Rev 0

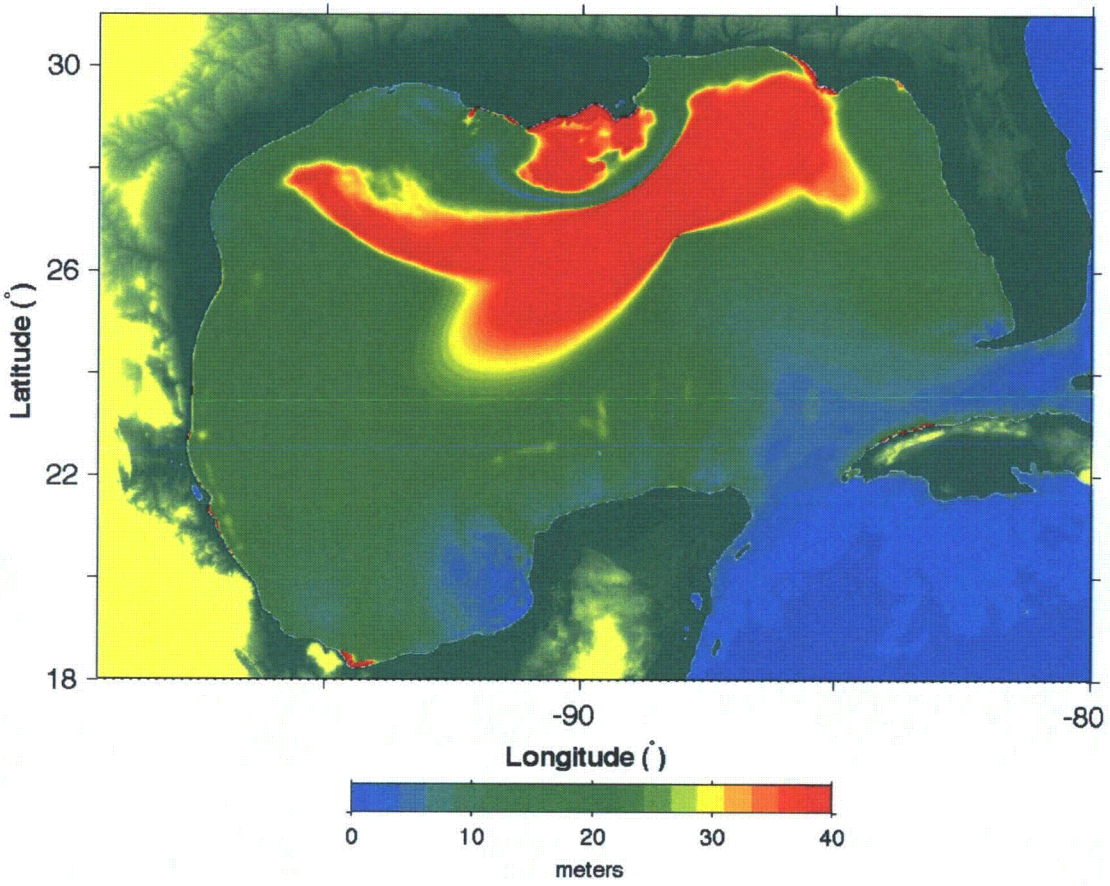

Progress Energy Florida
Levy Nuclear Plant
Units 1 and 2
Part 2, Final Safety Analysis Report

Mississippi Canyon Landslide Event Simulation,
Static Source: Maximum Water Level
Generated During Simulation (Grid A_l)

FIGURE RAI 2.4.6-17-21 Rev 0

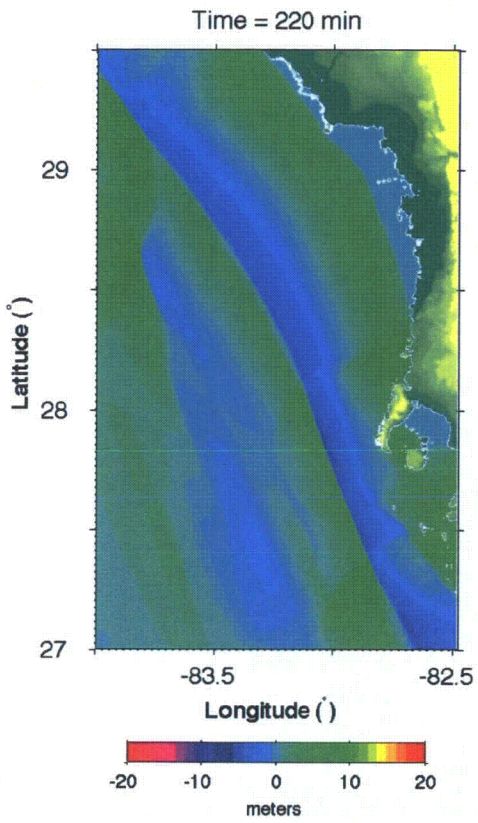

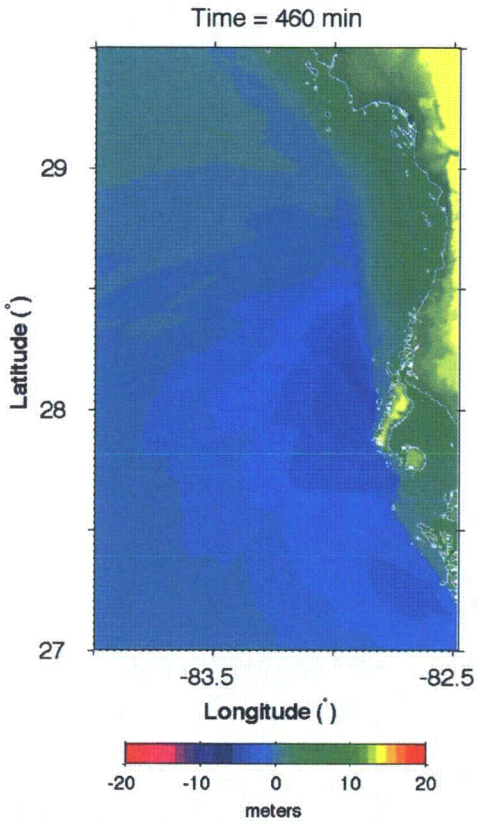

Progress Energy Florida
Levy Nuclear Plant
Units 1 and 2
Part 2, Final Safety Analysis Report

Mississippi Canyon Landslide Event Simulation,
Static Source:
Instantaneous Surface Displacement (Grid *B*)
at T = 220 min and T = 460 min
FIGURE RAI 2.4.6-17-22 Rev 0

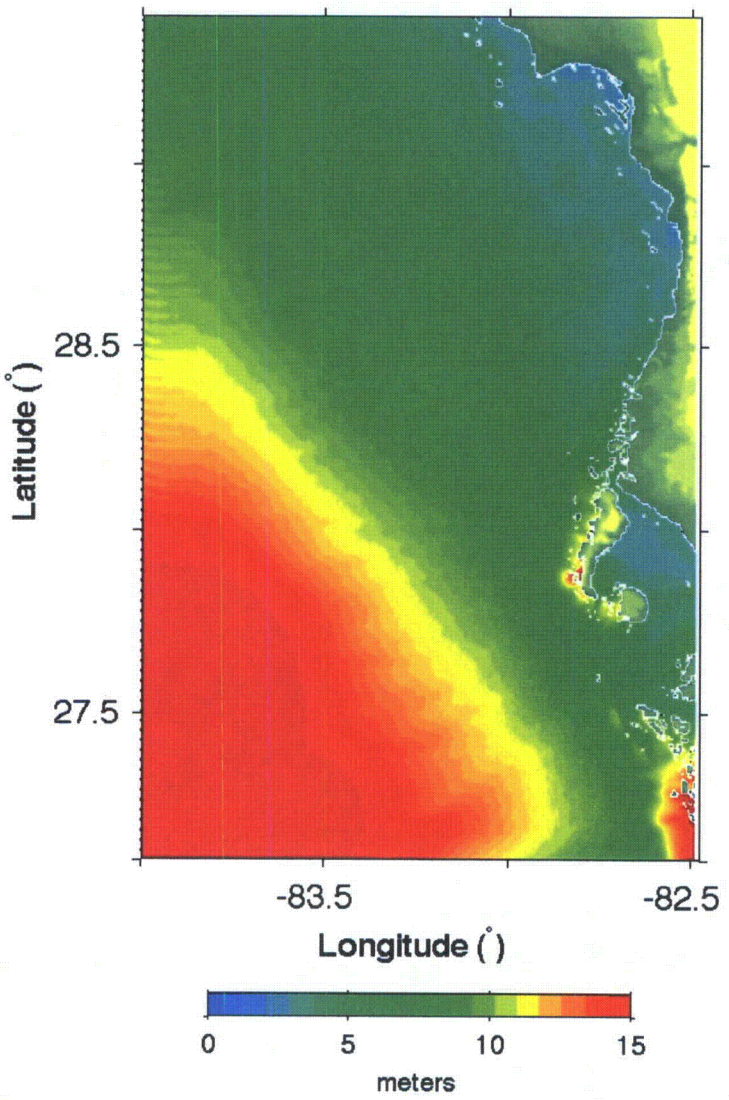

Progress Energy Florida
Levy Nuclear Plant
Units 1 and 2
Part 2, Final Safety Analysis Report

Mississippi Canyon Landslide Event Simulation,
Static Source: Maximum Water Level
Generated During Simulation (Grid *B*)

FIGURE RAI 2.4.6-17-23 Rev 0

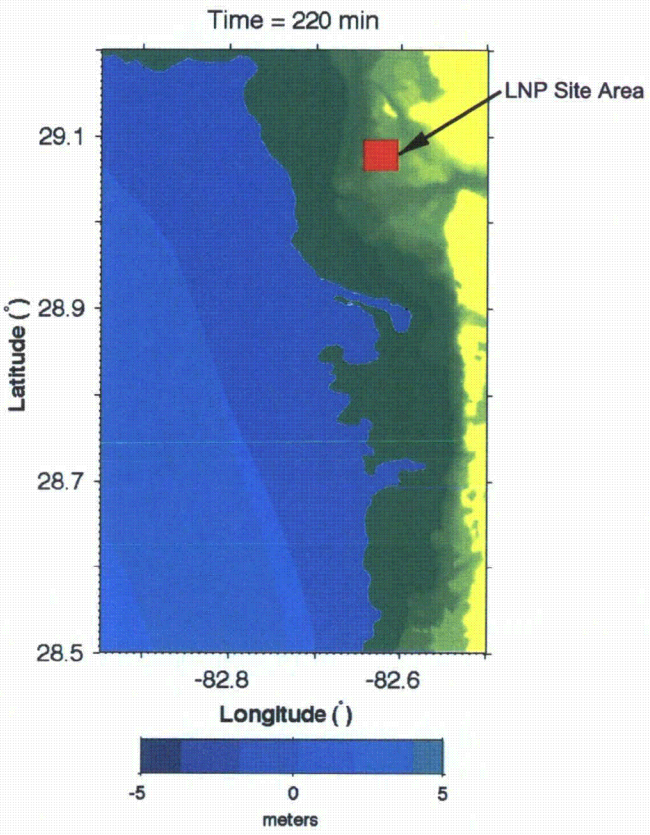

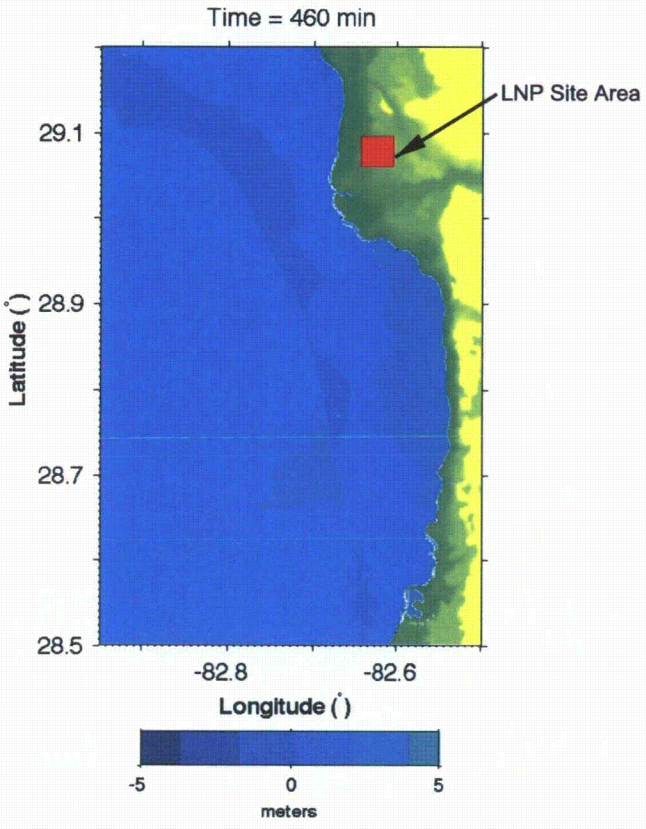

Progress Energy Florida
Levy Nuclear Plant
Units 1 and 2
Part 2, Final Safety Analysis Report

Mississippi Canyon Landslide Event Simulation,
Static Source:
Instantaneous Surface Displacement (Grid *C*)
at T = 220 min and T = 460 min
FIGURE RAI 2.4.6-17-24 Rev 0

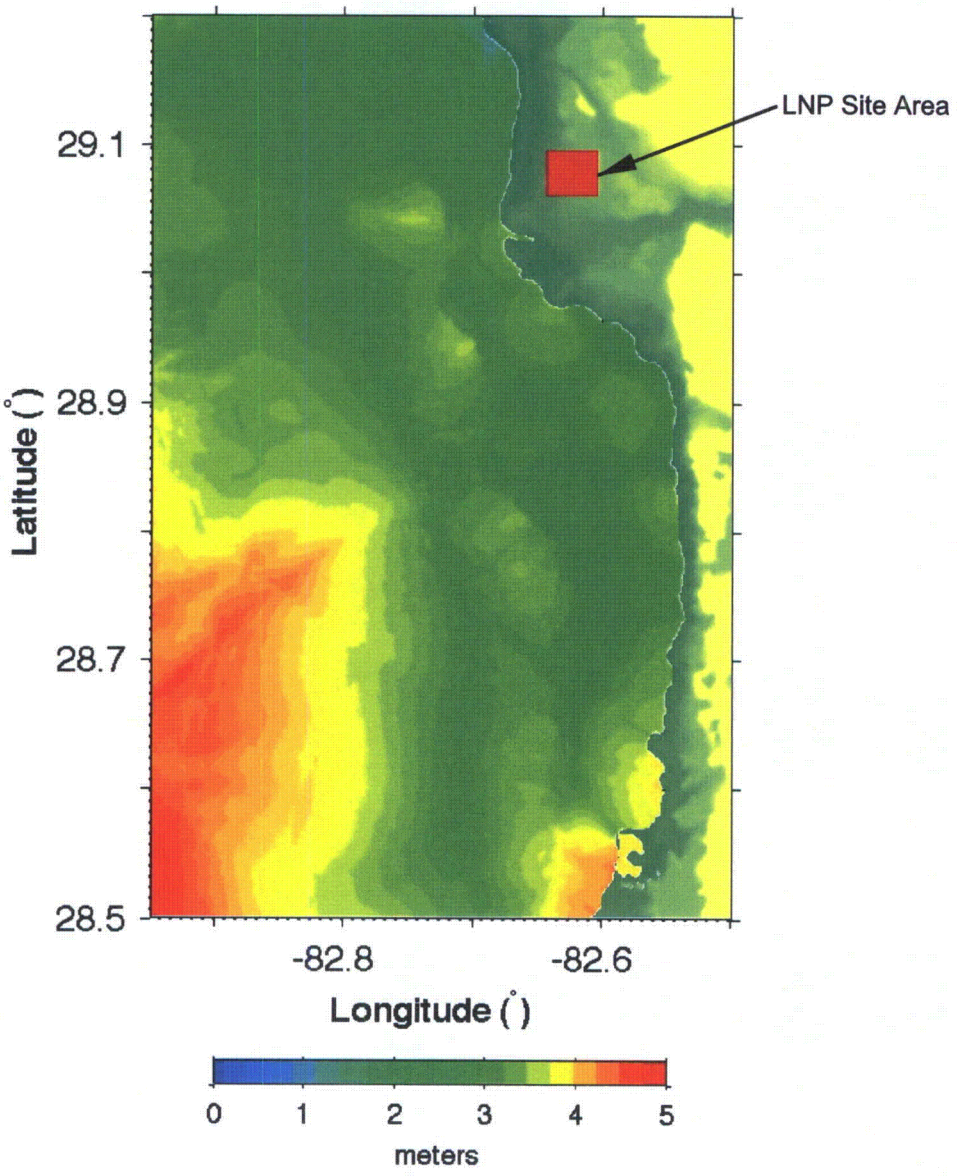

Progress Energy Florida
Levy Nuclear Plant
Units 1 and 2
Part 2, Final Safety Analysis Report

Mississippi Canyon Landslide Event Simulation,
Static Source: Maximum Water Level
Generated During Simulation (Grid *C*)

FIGURE RAI 2.4.6-17-25 Rev 0

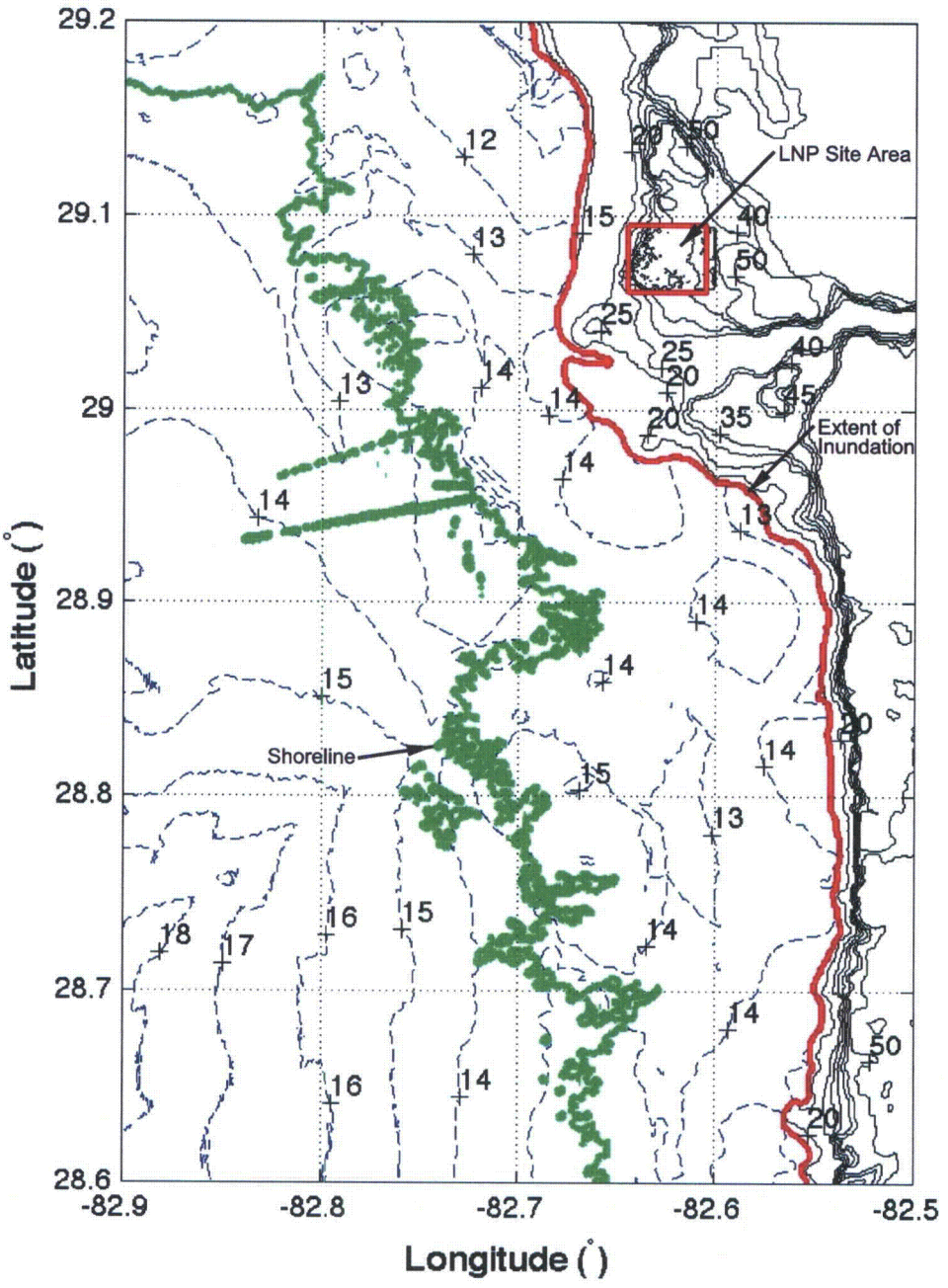

NOTE:
Contour elevations are given in feet NAVD 88.

Progress Energy Florida
Levy Nuclear Plant
Units 1 and 2
Part 2, Final Safety Analysis Report

Mississippi Canyon Landslide Event Simulation,
Static Source:
Maximum Extent of Inundation

FIGURE RAI 2.4.6-17-26 Rev 0

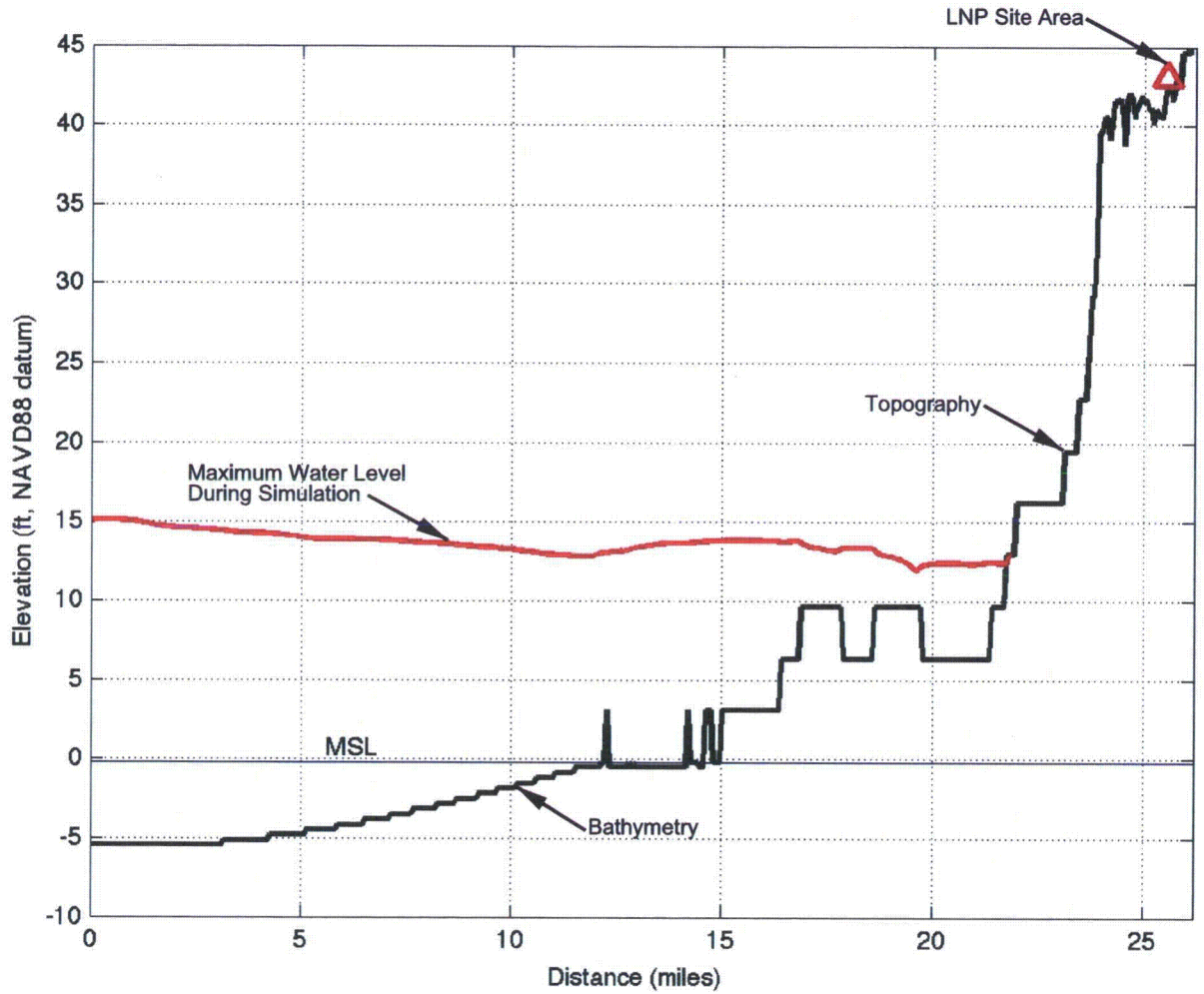

NOTE:
The existing grade elevation at the LNP site location is approximately 43 feet NAVD 88. The final grade elevation of LNP Units 1 & 2 will be raised to 50 feet NAVD 88.

Progress Energy Florida
Levy Nuclear Plant
Units 1 and 2
Part 2, Final Safety Analysis Report

Mississippi Canyon Landslide Event Simulation,
Static Source:
Profile at Latitude = 29.075 N

FIGURE RAI 2.4.6-17-27 Rev 0

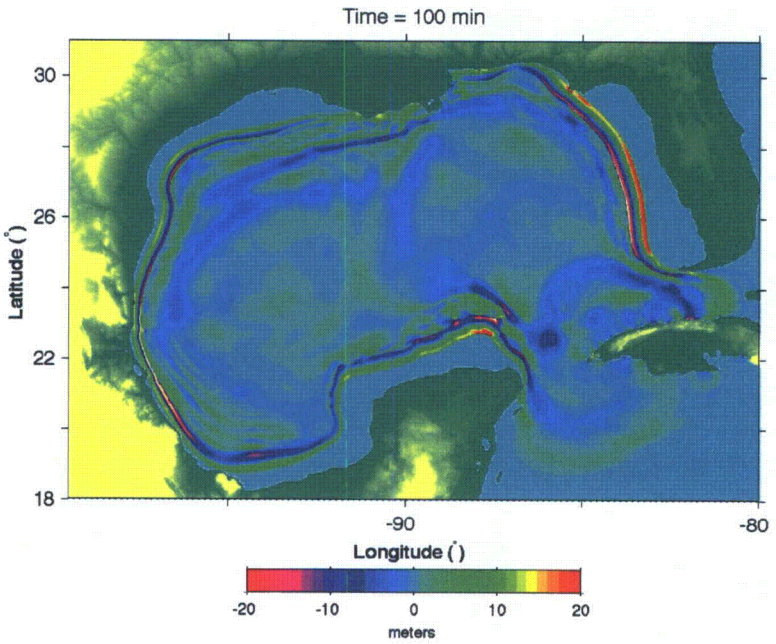

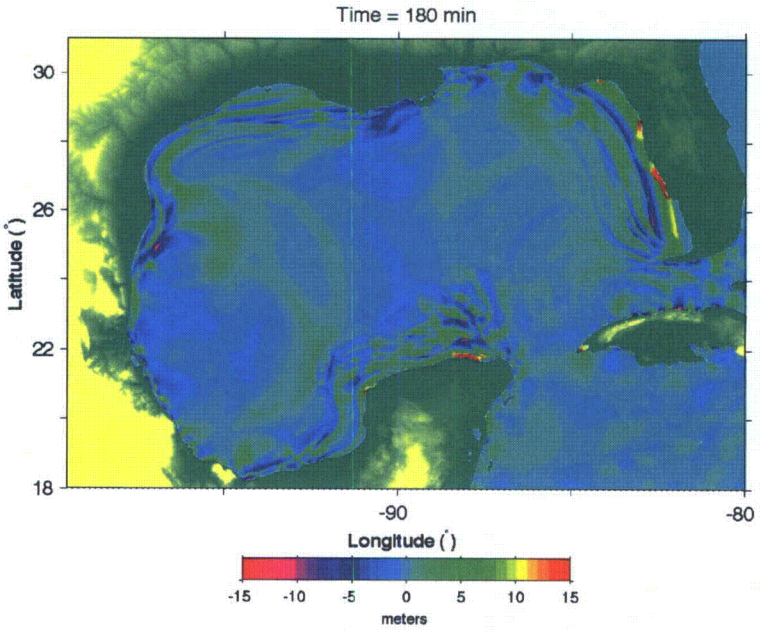

Progress Energy Florida
Levy Nuclear Plant
Units 1 and 2
Part 2, Final Safety Analysis Report

Mississippi Canyon Landslide Event Simulation,
Dynamic (NHWAVE) Source:
Instantaneous Surface Displacement (Grid A_1)
at T = 100 min and T = 180 min
FIGURE RAI 2.4.6-17-28 Rev 0

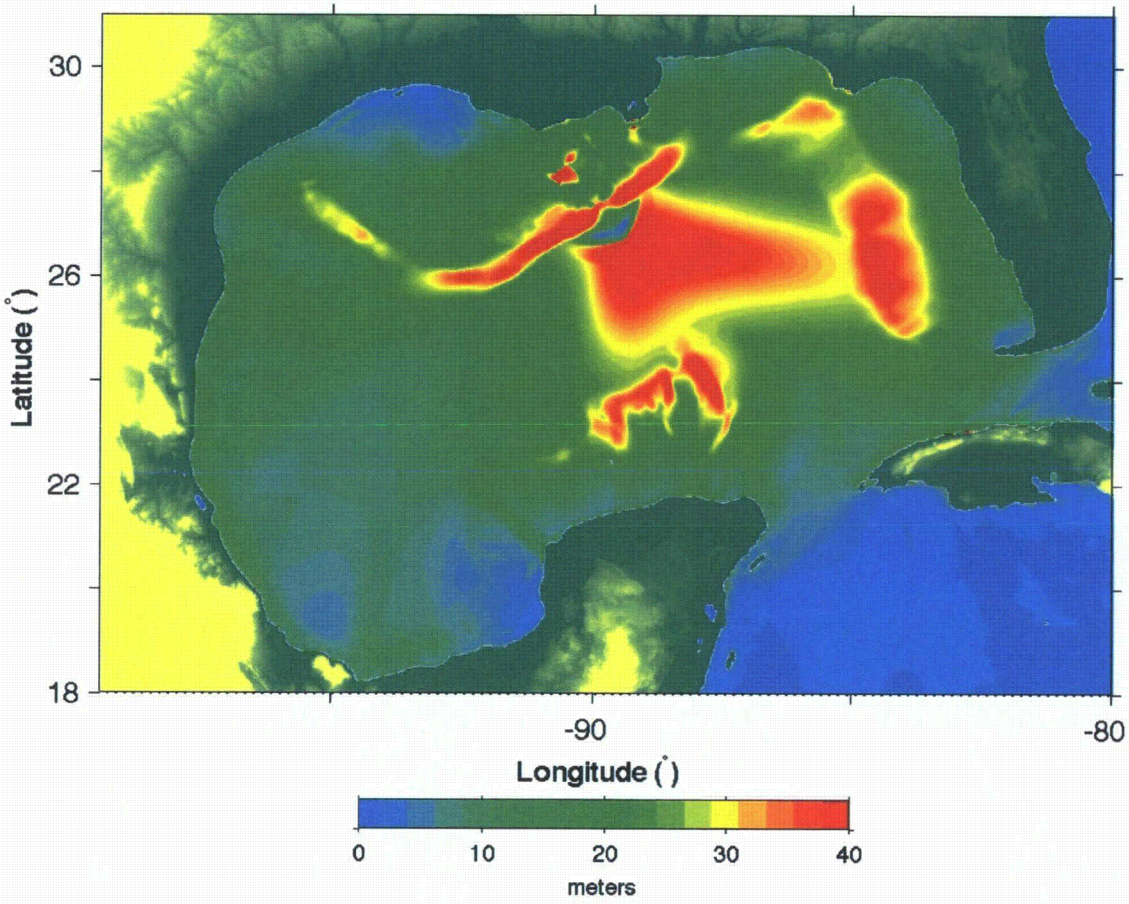

Progress Energy Florida
Levy Nuclear Plant
Units 1 and 2
Part 2, Final Safety Analysis Report

Mississippi Canyon Landslide Event Simulation,
Dynamic (NHWAVE) Source:
Maximum Water Level
Generated During Simulation (Grid A_I)
FIGURE RAI 2.4.6-17-29 Rev 0

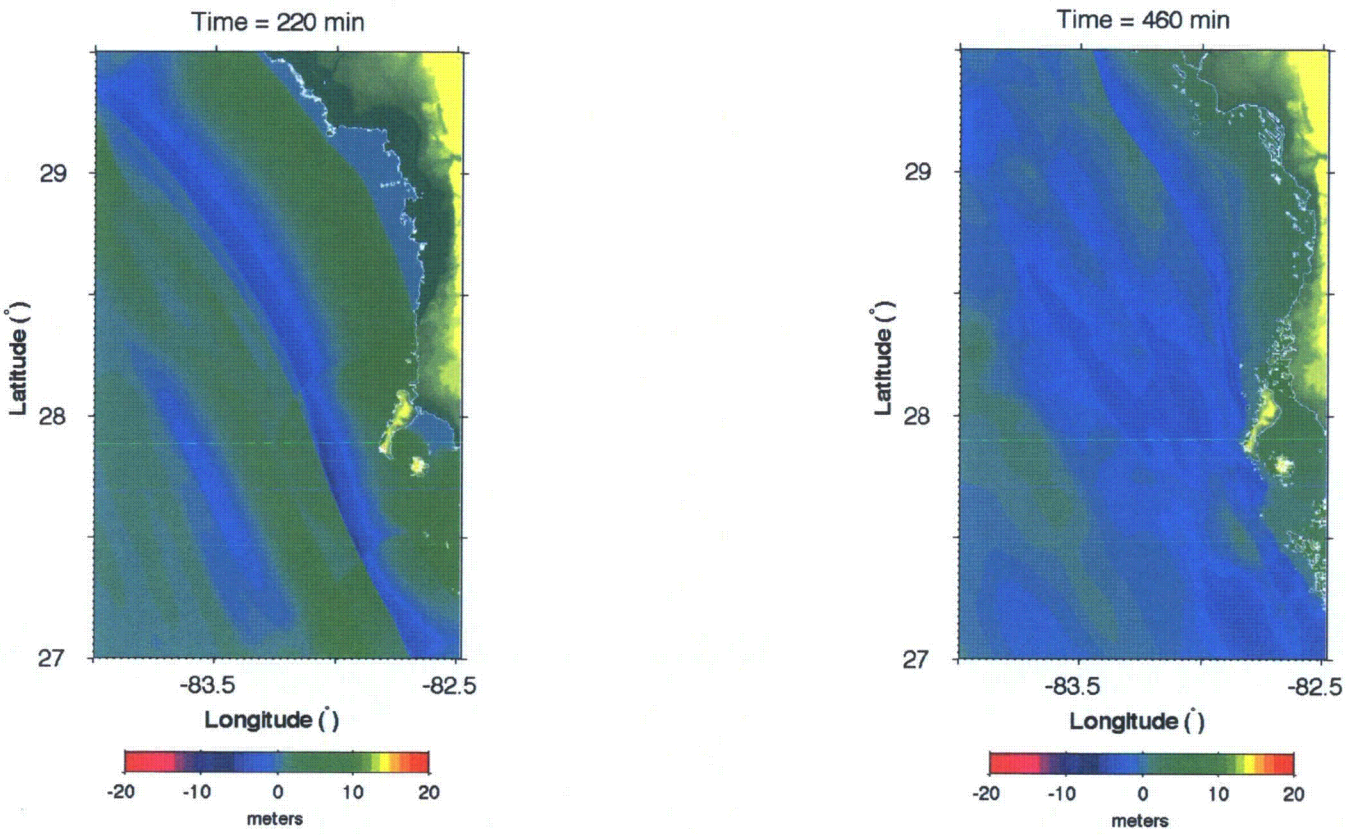

Progress Energy Florida
Levy Nuclear Plant
Units 1 and 2
Part 2, Final Safety Analysis Report

Mississippi Canyon Landslide Event Simulation,
Dynamic (NHWAVE) Source:
Instantaneous Surface Displacement (Grid *B*)
at T = 220 min and T = 460 min
FIGURE RAI 2.4.6-17-30 Rev 0

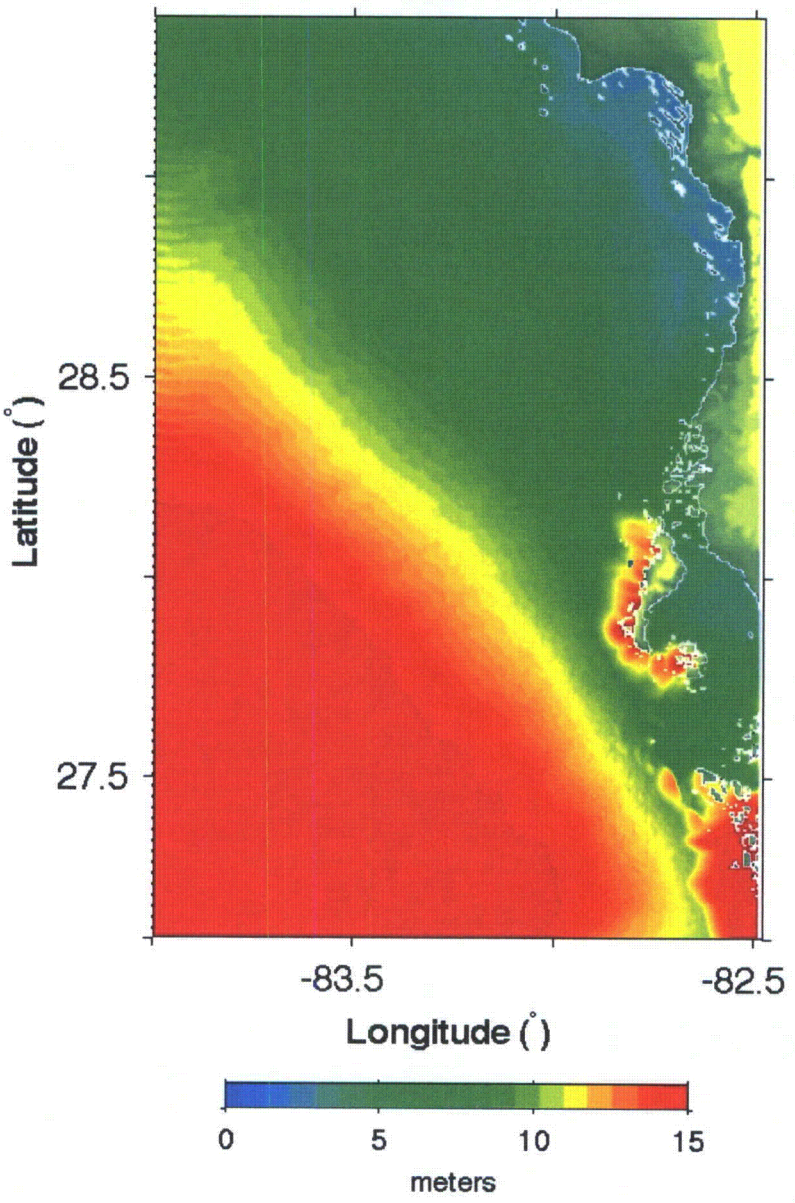

Progress Energy Florida
Levy Nuclear Plant
Units 1 and 2
Part 2, Final Safety Analysis Report

Mississippi Canyon Landslide Event Simulation,
Dynamic (NHWAVE) Source:
Maximum Water Level
Generated During Simulation (Grid *B*)
FIGURE RAI 2.4.6-17-31 Rev 0

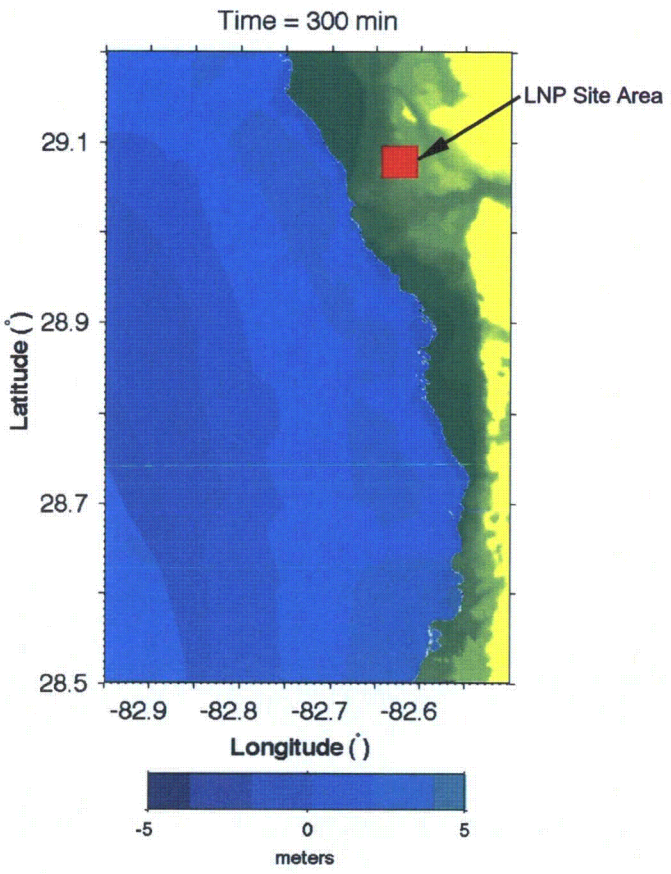

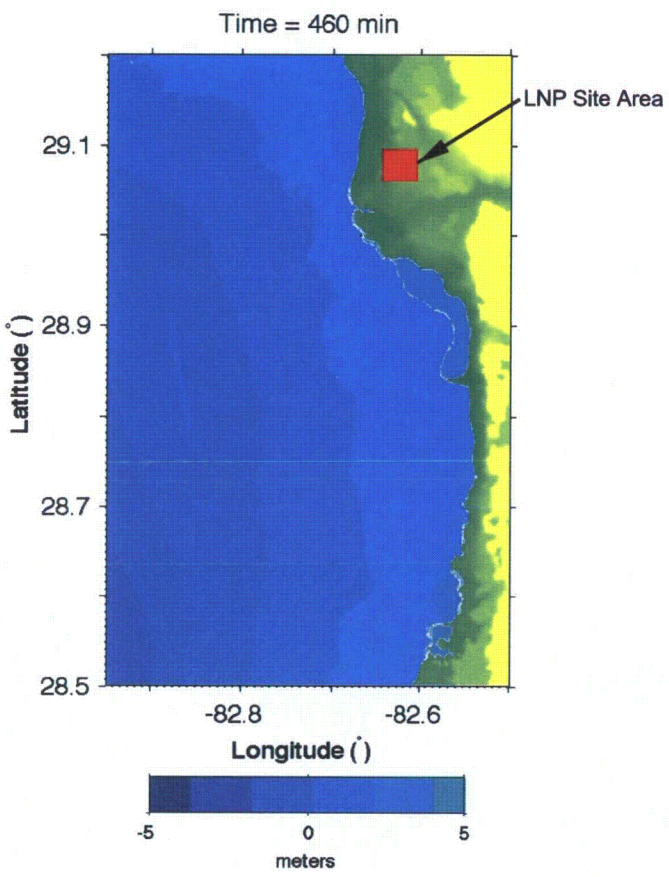

Progress Energy Florida
Levy Nuclear Plant
Units 1 and 2
Part 2, Final Safety Analysis Report

Mississippi Canyon Landslide Event Simulation,
Dynamic (NHWAVE) Source:
Instantaneous Surface Displacement (Grid *C*)
at T = 300 min and T = 460 min
FIGURE RAI 2.4.6-17-32 Rev 0

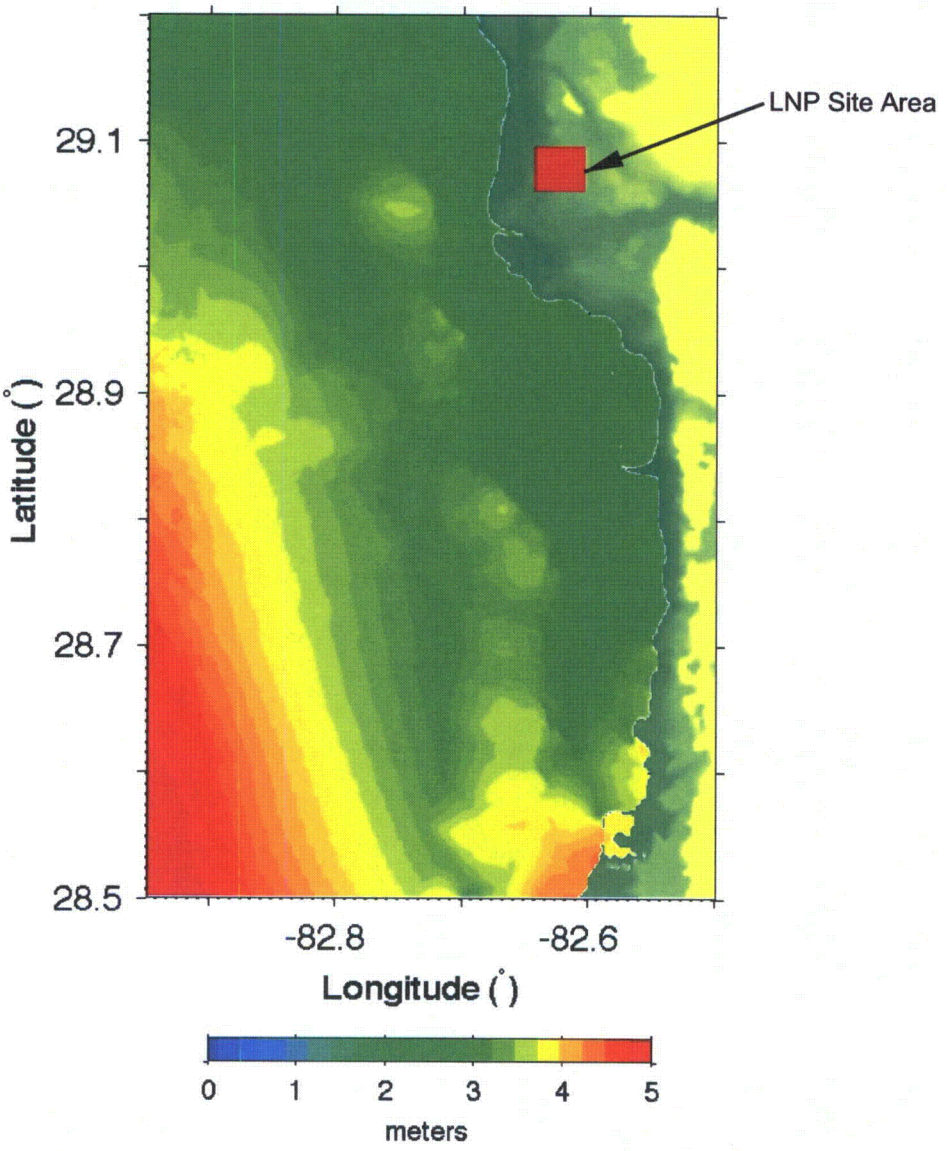

Progress Energy Florida
Levy Nuclear Plant
Units 1 and 2
Part 2, Final Safety Analysis Report

Mississippi Canyon Landslide Event Simulation,
Dynamic (NHWAVE) Source:
Maximum Water Level
Generated During Simulation (Grid *C*)
FIGURE RAI 2.4.6-17-33 Rev 0

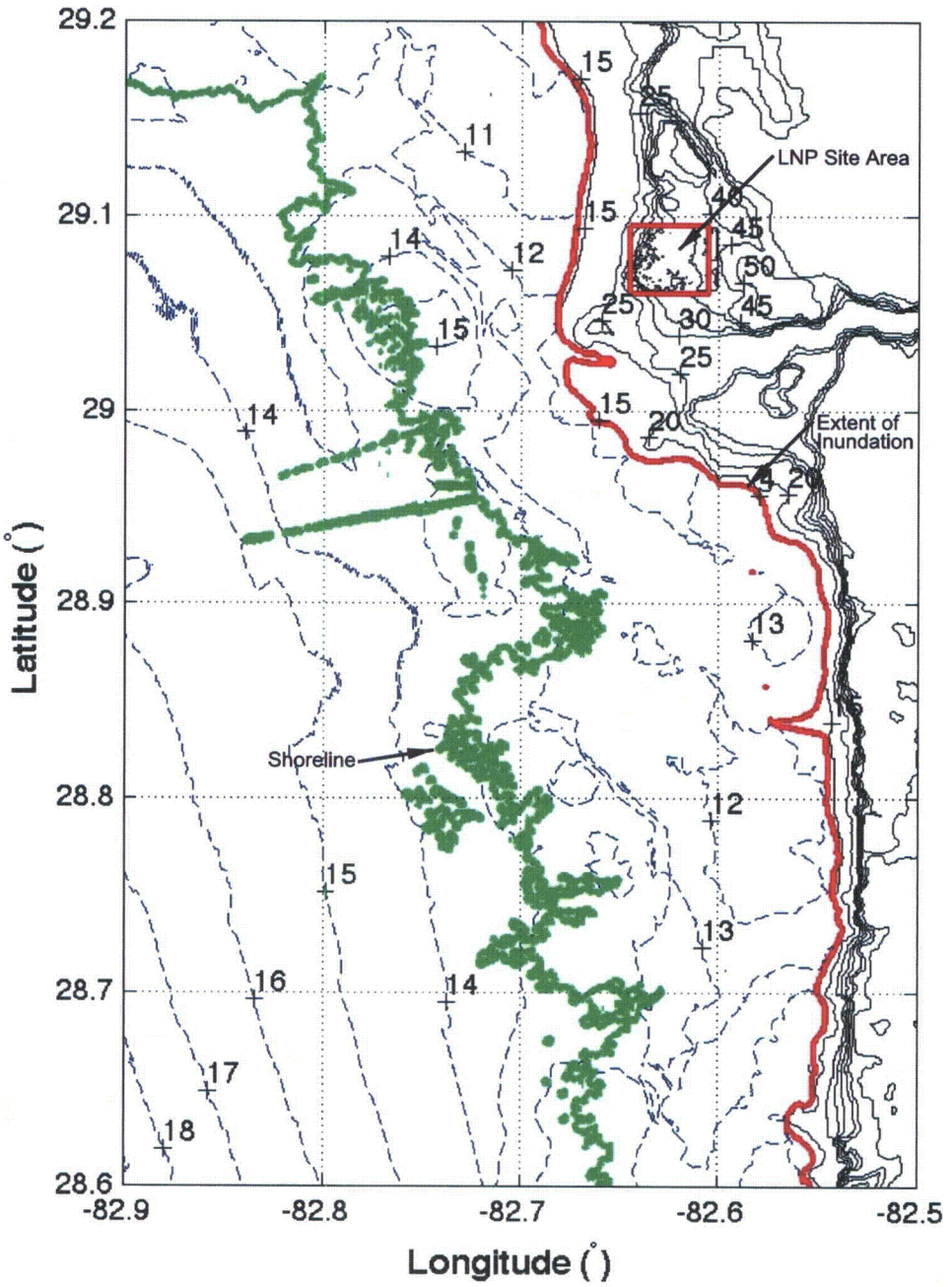

NOTE:
Contour elevations are given in feet NAVD 88.

Progress Energy Florida
Levy Nuclear Plant
Units 1 and 2
Part 2, Final Safety Analysis Report

Mississippi Canyon Landslide Event Simulation,
Dynamic (NHWAVE) Source:
Maximum Extent of Inundation

FIGURE RAI 2.4.6-17-34 Rev 0

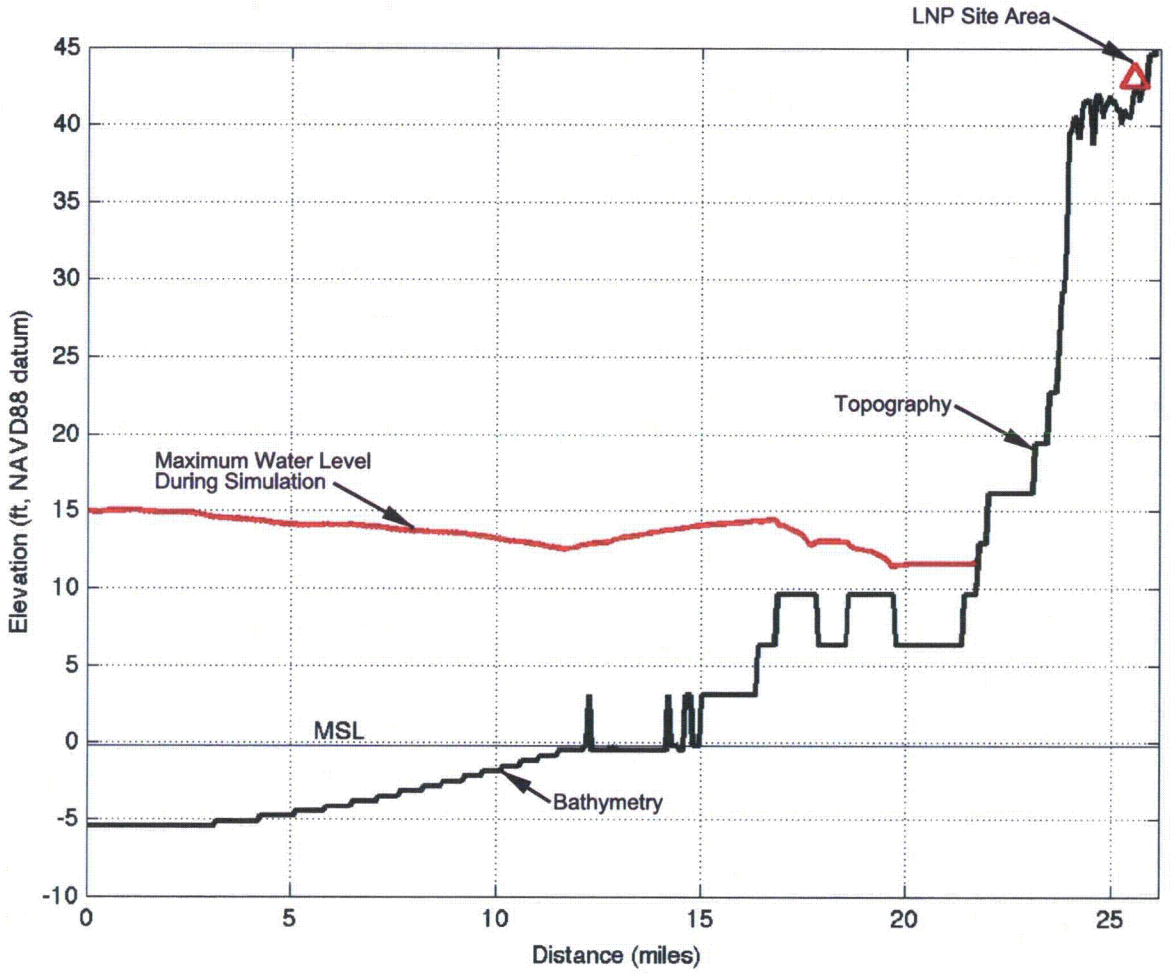

NOTE:
The existing grade elevation at the LNP site location is approximately 43 feet NAVD 88. The final grade elevation of LNP Units 1 & 2 will be raised to 50 feet NAVD 88.

Progress Energy Florida
Levy Nuclear Plant
Units 1 and 2
Part 2, Final Safety Analysis Report

Mississippi Canyon Landslide Event Simulation,
Dynamic (NHWAVE) Source:
Profile at Latitude = 29.075 N

FIGURE RAI 2.4.6-17-35 Rev 0

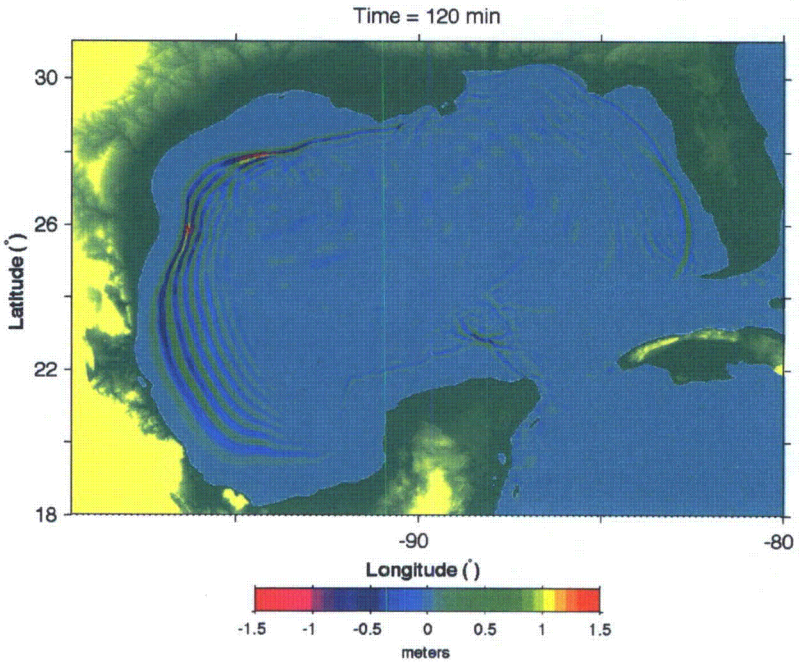

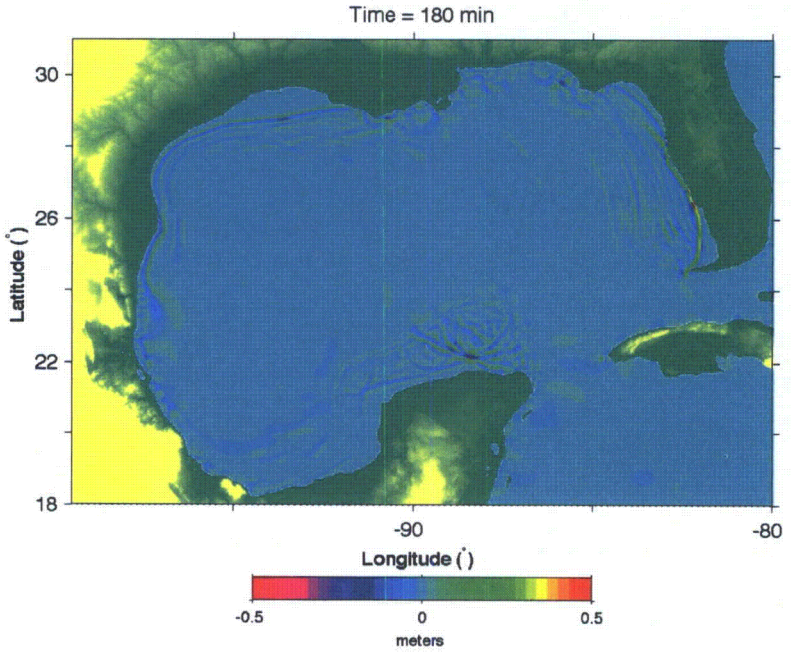

Progress Energy Florida
Levy Nuclear Plant
Units 1 and 2
Part 2, Final Safety Analysis Report

Florida Escarpment Landslide Event Simulation,
Static Source:
Instantaneous Surface Displacement (Grid A_l)
at T = 120 min and T = 180 min
FIGURE RAI 2.4.6-17-36 Rev 0

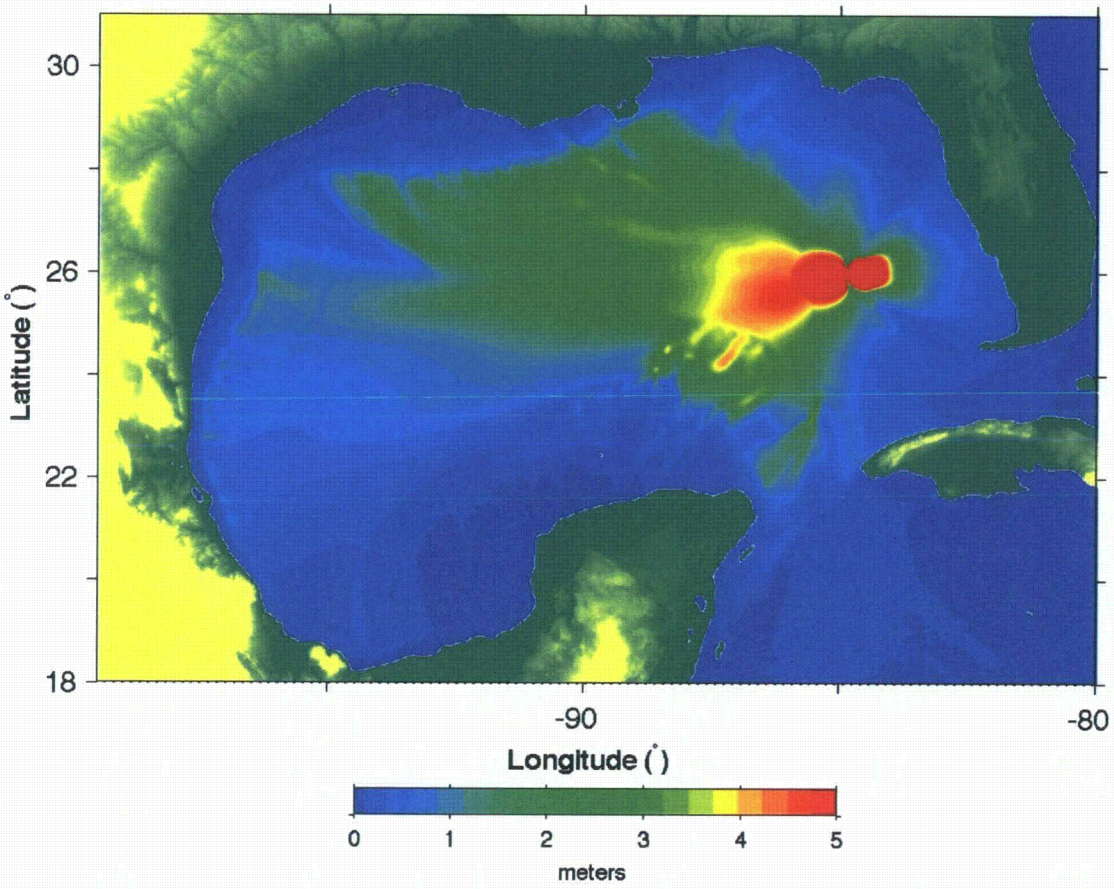

Progress Energy Florida
Levy Nuclear Plant
Units 1 and 2
Part 2, Final Safety Analysis Report

Florida Escarpment Landslide Event Simulation,
Static Source: Maximum Water Level
Generated During Simulation (Grid A_l)

FIGURE RAI 2.4.6-17-37 Rev 0

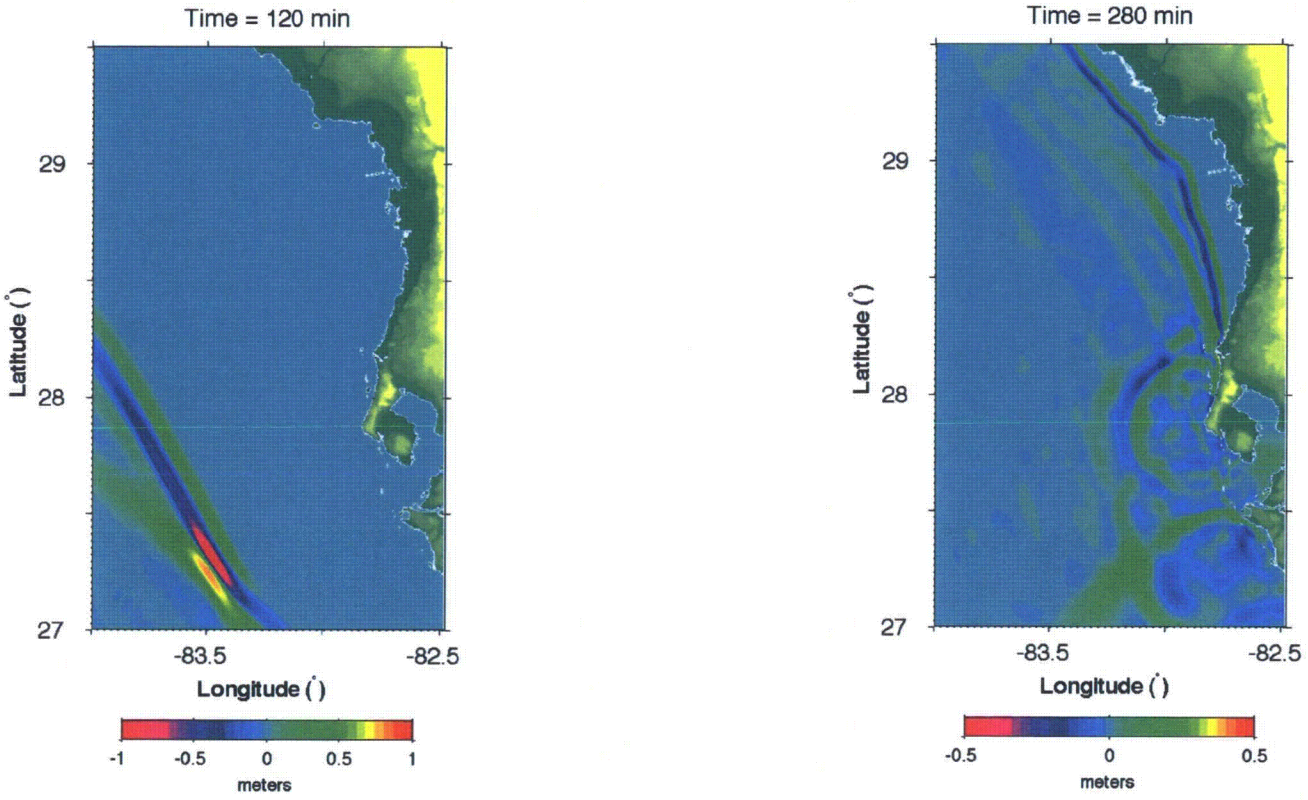

Progress Energy Florida
Levy Nuclear Plant
Units 1 and 2
Part 2, Final Safety Analysis Report

Florida Escarpment Landslide Event Simulation,
Static Source:
Instantaneous Surface Displacement (Grid *B*)
at T = 120 min and T = 280 min
FIGURE RAI 2.4.6-17-38 Rev 0

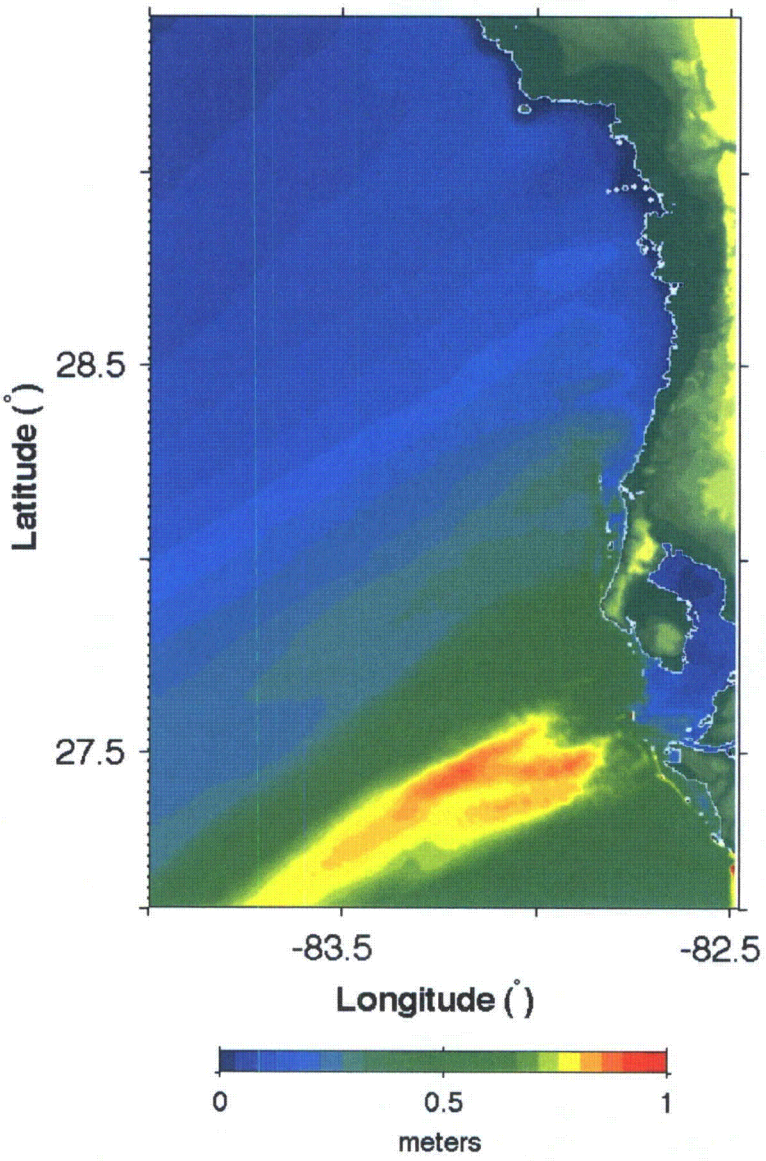

Progress Energy Florida
Levy Nuclear Plant
Units 1 and 2
Part 2, Final Safety Analysis Report

Florida Escarpment Landslide Event Simulation,
Static Source: Maximum Water Level
Generated During Simulation (Grid *B*)

FIGURE RAI 2.4.6-17-39 Rev 0

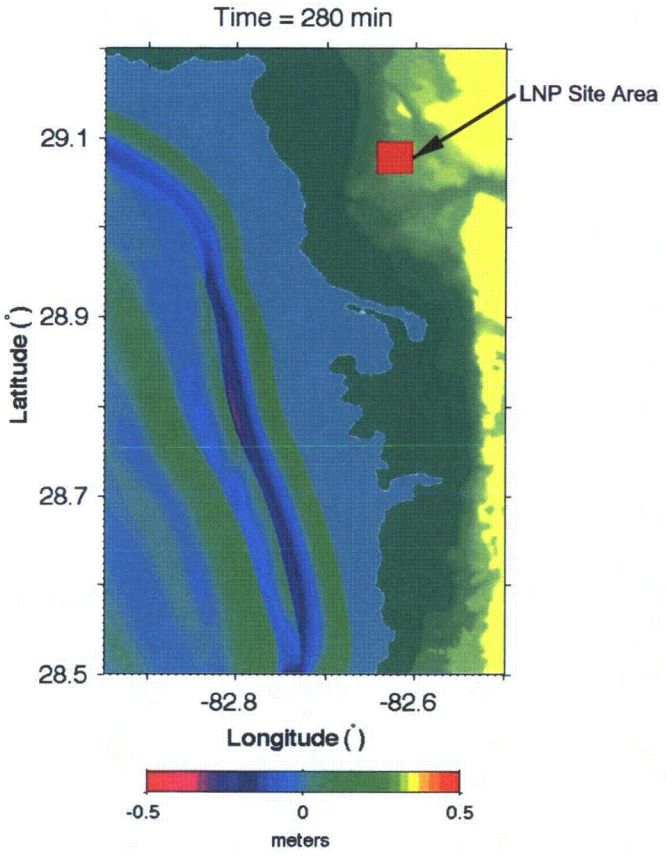

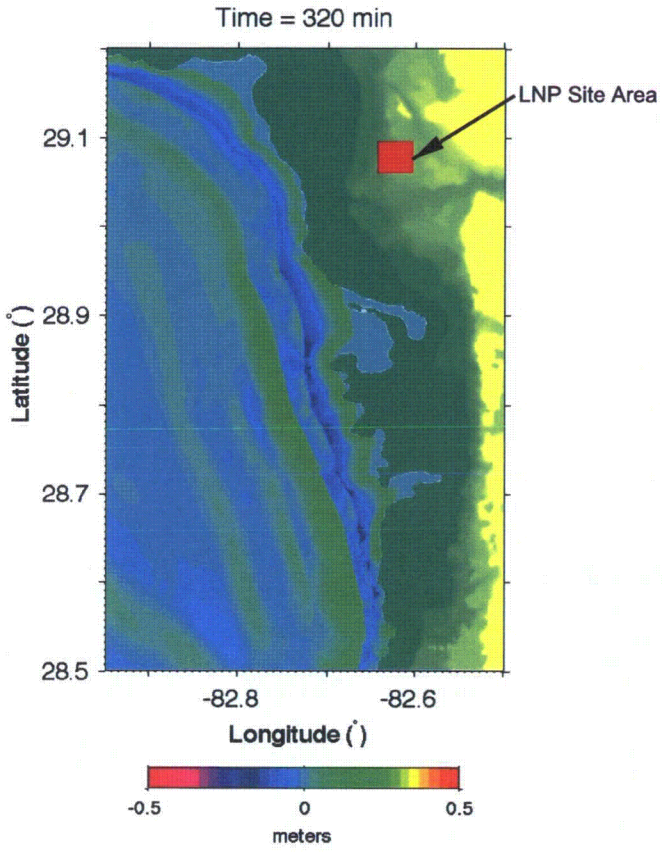

Progress Energy Florida
Levy Nuclear Plant
Units 1 and 2
Part 2, Final Safety Analysis Report

Florida Escarpment Landslide Event Simulation,
Static Source:
Instantaneous Surface Displacement (Grid C)
at T = 280 min and T = 320 min
FIGURE RAI 2.4.6-17-40 Rev 0

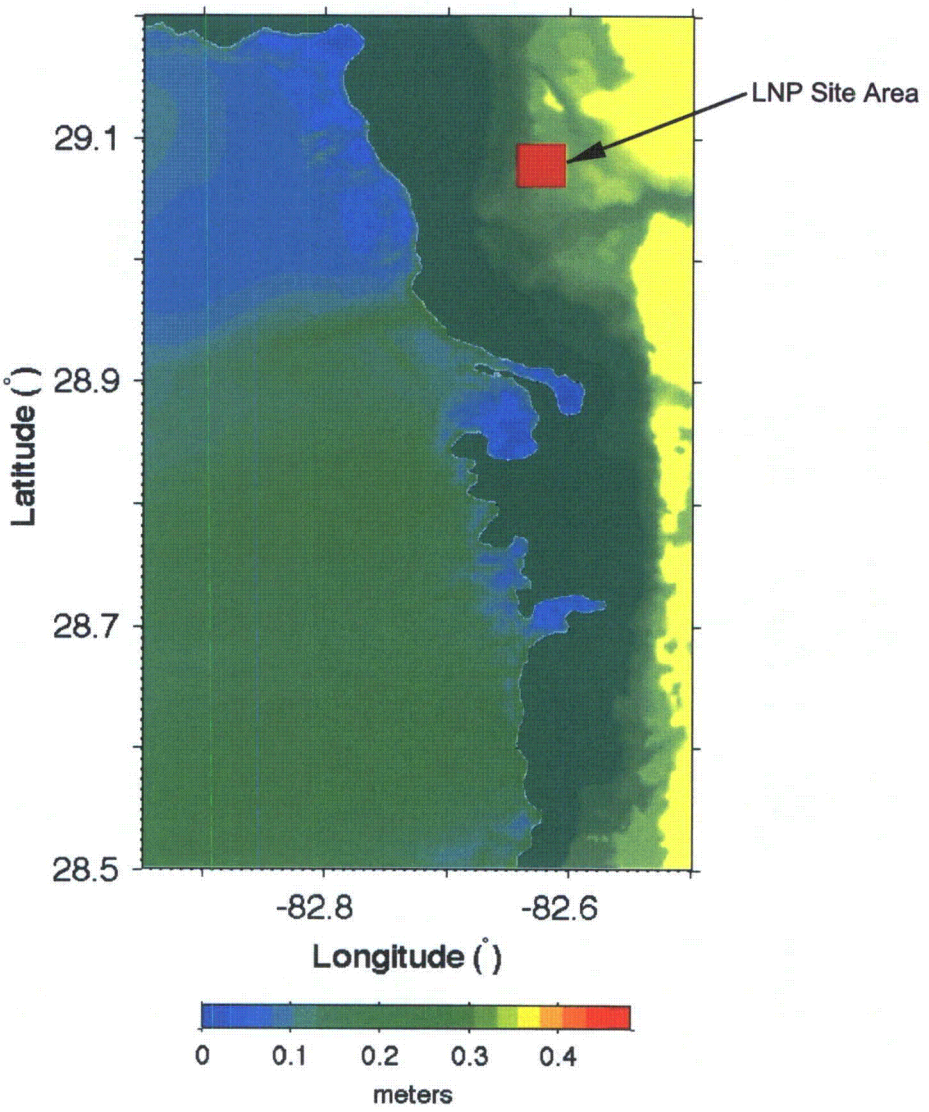

Progress Energy Florida
Levy Nuclear Plant
Units 1 and 2
Part 2, Final Safety Analysis Report

Florida Escarpment Landslide Event Simulation,
Static Source: Maximum Water Level
Generated During Simulation (Grid *C*)

FIGURE RAI 2.4.6-17-41 Rev 0

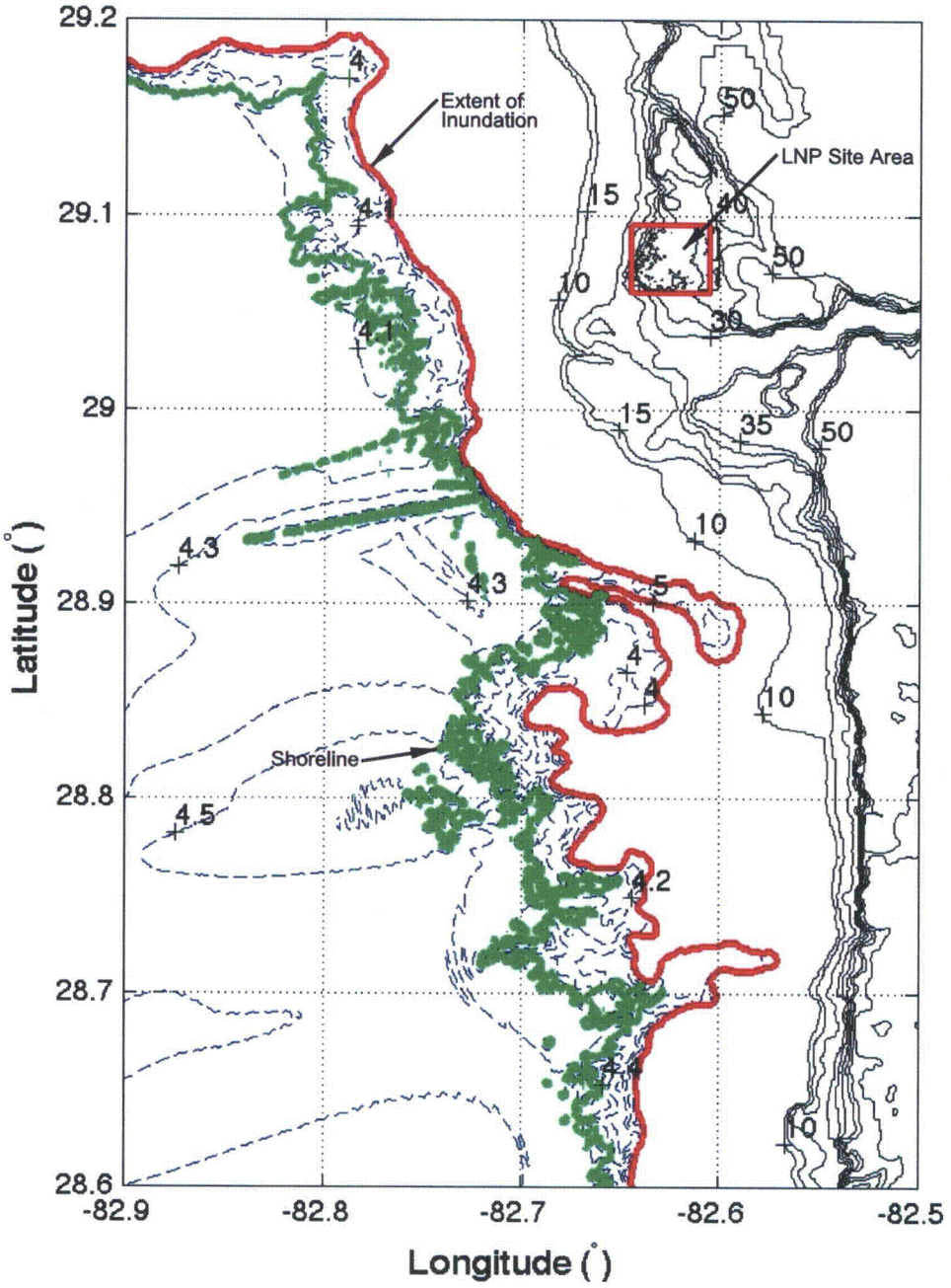

NOTE:
Contour elevations are given in feet NAVD 88.

Progress Energy Florida
Levy Nuclear Plant
Units 1 and 2
Part 2, Final Safety Analysis Report

Florida Escarpment Landslide Event Simulation,
Static Source:
Maximum Extent of Inundation

FIGURE RAI 2.4.6-17-42 Rev 0

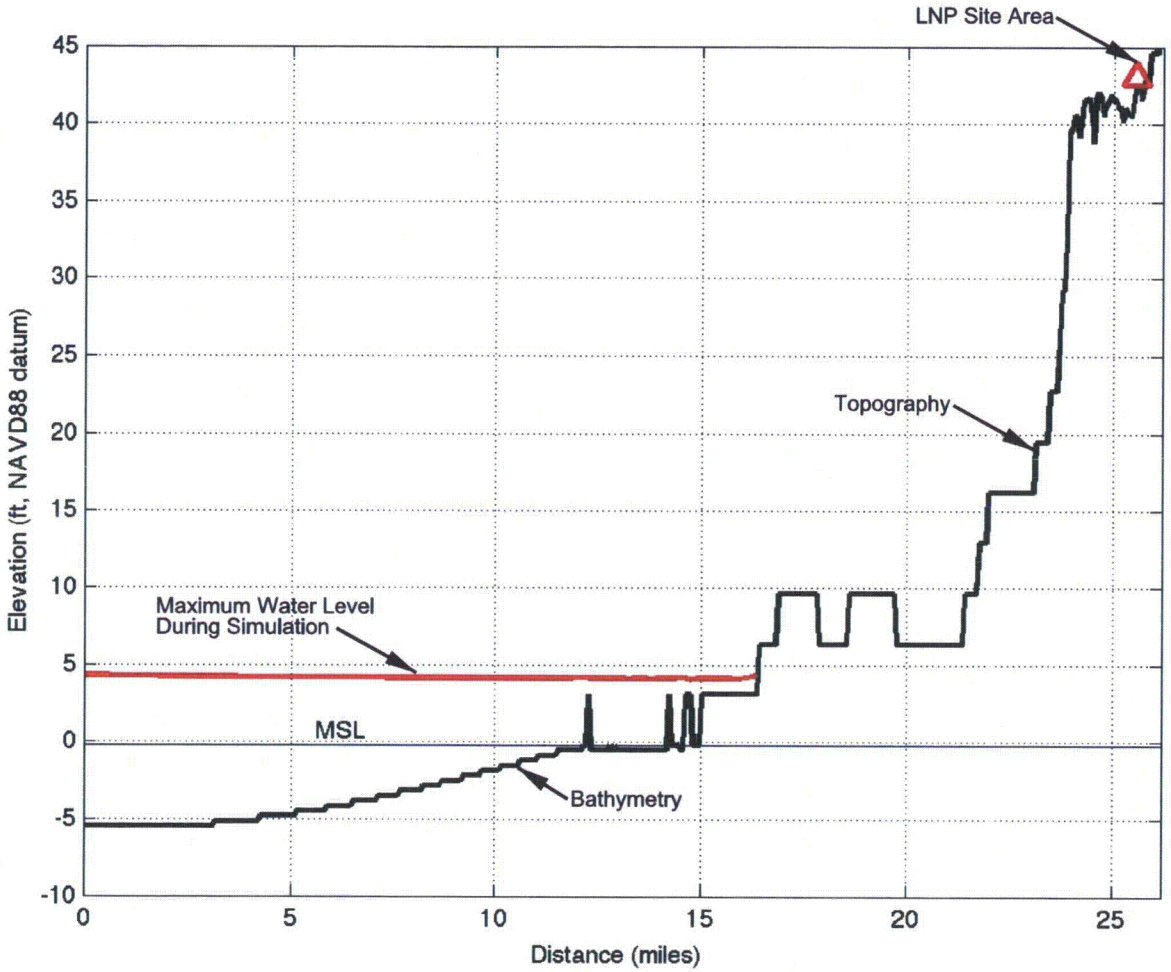

NOTE:
The existing grade elevation at the LNP site location is approximately 43 feet NAVD 88. The final grade elevation of LNP Units 1 & 2 will be raised to 50 feet NAVD 88.

Progress Energy Florida
Levy Nuclear Plant
Units 1 and 2
Part 2, Final Safety Analysis Report

Florida Escarpment Landslide Event Simulation,
Static Source:
Profile at Latitude = 29.075 N

FIGURE RAI 2.4.6-17-43 Rev 0

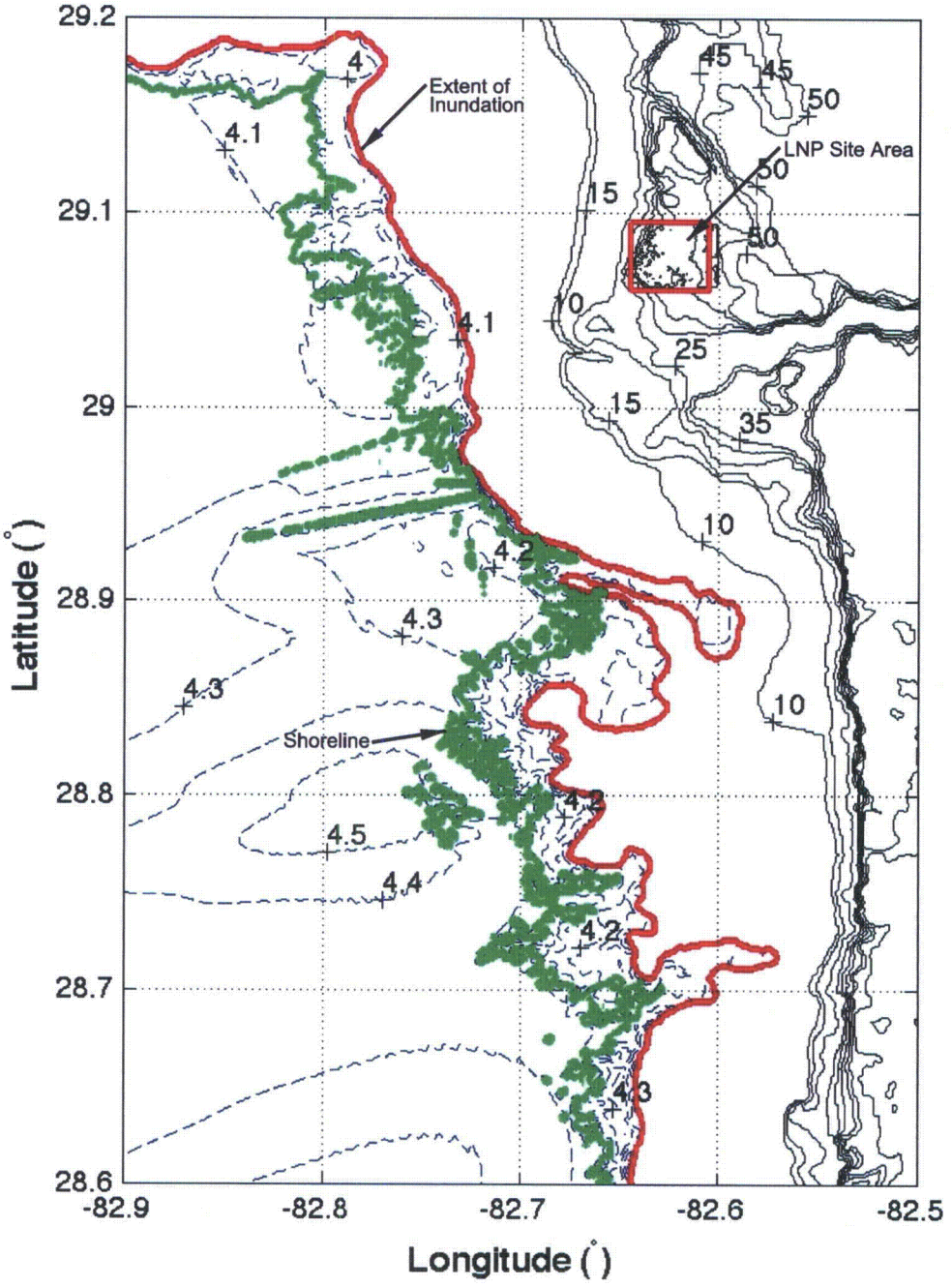

NOTE:
Contour elevations are given in feet NAVD 88.

Progress Energy Florida
Levy Nuclear Plant
Units 1 and 2
Part 2, Final Safety Analysis Report

Florida Escarpment Landslide Event Simulation, Dynamic (NHWAVE) Source: Maximum Extent of Inundation

FIGURE RAI 2.4.6-17-44 Rev 0

LNP FSAR Subsection 2.4.6.7 will be deleted in its entirety and replaced with the following text:

2.4.6.7 Probable Maximum Tsunami Analysis

Three different tsunami sources are considered for the PMT analysis: one seismic source and two landslide sources.

- Venezuela Seismic Source
- Mississippi Canyon Landslide Source
- Florida Escarpment Landslide Source

For the seismic source, the initial condition consists of a static surface displacement and a stationary water body. The initial static displacement is derived from earthquake source parameters using the method described by Okada (Reference 2.4.6-239).

For the two landslide sources, two approaches are considered. The first approach uses a static source based on the geometry of the initial and final positions of the slide mass. The second approach employs a dynamic source, which specifies both surface displacement and depth averaged horizontal velocity fields. This source is computed from the slide geometry using the model NHWAVE (Non-Hydrostatic Wave), Version 1.0, which is described in Reference 2.4.6-231. The computation of the initial source requires a value for slide velocity. This is computed using a methodology described by Enet and Grilli (Reference 2.4.6-229). For each of the landslides, a slide geometry equivalent to that in Reference 2.4.6-229 is employed with an adjustment to slide aspect ratio (width/length) to best fit the model slide to the measured shape of the excavated source region for the measured slide. This choice allows the use of the same geometric relationships between slide volume, area, thickness, length and width as utilized in Reference 2.4.6-229. The geometry of the slides is described below.

Parameters defining tsunami sources were obtained from ten Brink et al (Reference 2.4.6-238); a listing of parameters is provided in Table 2.4.6-206 and Table 2.4.6-207. The simulated tsunamis that are generated using source parameters for the different scenarios described herein are severe enough to be considered equivalent to the PMT for the LNP site.

The flood level near the LNP site due to PMT is estimated using the numerical wave model FUNWAVE-TVD (Fully Nonlinear Wave – Total Variation Diminishing Scheme), Version 1.0, described in References 2.4.6-230, 2.4.6-234, and 2.4.6-235. Benchmark testing of FUNWAVE-TVD is described in Reference 2.4.6-237. Inputs to FUNWAVE-TVD include depth grids, whose development is described herein, and information about the configuration of a tsunami source, used as the initial condition for the model run. Program documentation and users' manual for FUNWAVE-TVD is available in Reference 2.4.6-235.

Outputs generated by FUNWAVE-TVD include gridded surface displacement and horizontal velocities as a function of time during the model simulation. The model results are presented as snapshots of evolving surface displacement during each simulated case. The model accumulates information on the maximum runup water level occurring at each grid location during the simulation, and provides estimates of maximum

inundation and runup values near the LNP site based on these accumulated values. The results are used to estimate the maximum water level due to the PMT near the LNP site, and to determine if LNP Units 1 and 2 will be affected by the PMT maximum water level.

The verification and validation of the FUNWAVE-TVD and NHWAVE computer programs are described in the Verification and Validation document (Appendix 1). Computation grids are generated using Fortran programs and MATLAB scripts, for which detailed operation procedures and verification are also described in Appendix 1.

2.4.6.7.1 FUNWAVE-TVD Model Description

The propagation, shoreline runup and inundation caused by tsunamis are calculated using the Boussinesq wave model FUNWAVE-TVD. In the present application, FUNWAVE-TVD solves the spherical-polar form of the weakly-nonlinear, weakly-dispersive Boussinesq equations described by Kirby et al (Reference 2.4.6-230). Shi et al (Reference 2.4.6-235) describes the operation of both Cartesian and spherical-polar versions of the code. The model incorporates bottom friction and turbulent mixing effects. The model is available to the public as open source software.

The Cartesian coordinate version of FUNWAVE-TVD, described in Shi et al (Reference 2.4.6-234 and Reference 2.4.6-235), has been benchmarked for tsunami application using the PMEL-135 benchmarks provided in Synolakis et al (Reference 2.4.6-236), which are the presently accepted benchmarking standards adopted by the National Tsunami Hazard Mitigation Program (NTHMP) for judging model acceptance for use in development of coastal inundation maps and evacuation plans. Benchmark tests for the Cartesian FUNWAVE-TVD are described in Tehranirad et al (Reference 2.4.6-237). The spherical-polar version of the code used here is subjected to several of these benchmarks in order to document consistency and accuracy of the model.

The equations solved by FUNWAVE-TVD consist of a depth-integrated volume conservation equation together with depth-integrated horizontal momentum equations. The equations retain effects to second order in the ratio of water depth to wavelength, accounting for deviations from depth-uniform horizontal flow up to quadratic terms in the vertical coordinate. The resulting volume conservation equation is given by (Reference 2.4.6-230):

$$\frac{1}{\delta}H_t + \frac{1}{\cos\theta}\left\{\left(H\bar{u}\right)_{\phi^*} + \left(H\bar{v}\cos\theta\right)_{\theta^*}\right\} = 0 \qquad \text{Equation 2.4.6-2}$$

where H is the local total water depth, u is Easterly, depth-averaged horizontal velocity and v is depth-averaged Northerly horizontal velocity, θ is latitude in radians, δ is a dimensionless ratio of surface displacement scale to representative water depth, and subscripts t, ϕ^* and θ^* represent a time derivative and spatial derivatives with respect to scaled latitude and longitude (see Reference 2.4.6-230 for further details of the derivation).

The corresponding horizontal momentum equations for the Easterly (longitudinal) direction are given by (Reference 2.4.6-230):

$$\overline{u}_t - \mu^2 f\overline{v} + \delta\left\{\frac{\overline{u}}{\cos\theta}\overline{u}_{\phi^*} + \overline{vu}_{\theta^*}\right\} + \frac{1}{\cos\theta}\eta_{\phi^*}$$
$$+ \frac{\mu^2}{\cos^2\theta}\left\{\frac{h^2}{6}\left[\overline{u}_{\phi^*\theta^*t} + \left(\overline{v}\cos\theta\right)_{\phi^*\theta^*t}\right] - \frac{h}{2}\left[\left(h\overline{u}_t\right)_{\phi^*\phi^*} + \left(h\cos\theta\overline{v}_t\right)_{\phi^*\theta^*}\right]\right\} \qquad \text{Equation 2.4.6-3}$$
$$+ \frac{\mu^2}{\cos\theta}\left(BFT\right)_{\phi^*} - \tau_b^x = O\left(\delta^2, \delta\mu^2, \mu^4\right)$$

The corresponding horizontal momentum equations for the Northerly (latitudinal) direction are given by (Reference 2.4.6-230):

$$\overline{v}_t + \mu^2 f\overline{u} + \delta\left\{\frac{\overline{u}}{\cos\theta}\overline{v}_{\phi^*} + \overline{vv}_{\theta^*}\right\} + \eta_{\theta^*}$$
$$+ \mu^2\left\{\frac{h^2}{6}\left[\frac{1}{\cos\theta}\left\{\overline{u}_{\phi^*t} + \left(\overline{v}\cos\theta\right)_{\theta^*t}\right\}\right]_{\theta^*} - \frac{h}{2}\left[\frac{1}{\cos\theta}\left\{\left(h\overline{u}_t\right)_{\phi^*} + \left(h\cos\theta\overline{v}_t\right)_{\theta^*}\right\}\right]_{\theta^*}\right\}$$
$$+ \mu^2\left(BFT\right)_{\theta^*} - \tau_b^y = O\left(\delta^2, \delta\mu^2, \mu^4\right)$$

Equation 2.4.6-4

Here *f* represents the Coriolis parameter, η represents the water surface displacement from its initial position, *h* represents local still water depth, and μ is a dimensionless parameter characterizing the ratio of characteristic water depth to characteristic surface wave length. The term *BFT* contains the effect of continuous bottom motion in time, and is not utilized in the present study since bottom displacements are described either as static initial conditions, or are tied to initial surface displacement and velocity field in a separate model computation based on NHWAVE, described below. The term τ_b represents the effect of bottom friction and is given by (Reference 2.4.6-230):

$$\tau_b^{x,y} = \frac{1}{H}C_D\left|\mathbf{u}\right|(u,v) \qquad \text{Equation 2.4.6-5}$$

where C_D is the drag coefficient and **u** is the horizontal velocity vector. The value of the drag coefficient can range from 0.0008 to 0.0031 on continental shelf and slope environments (Reference 2.4.6-241) and can be as high as 0.005 during breaking and runup (Reference 2.4.6-240). Increased roughness of subaerial vegetation and other surface features can lead to higher apparent values of the drag coefficient. For this study, a lower end value of the drag coefficient of C_D = 0.001 is used and therefore will result in conservative estimates of runup water levels.

For tsunami applications here, FUNWAVE-TVD is run with closed boundaries and an initial hot start condition consisting of either a surface displacement alone (in the case of static initial conditions) or a surface displacement and initial velocity field (in the case of a dynamic initial condition based on NHWAVE calculations). The choice for each source will be described separately. The model is run from the initial start until past the time when significant wave activity has decayed at the target site.

2.4.6.7.2 NHWAVE Model Description

For several of the computations described below, the model NHWAVE is used to describe the early stages of surface displacement and velocity field development associated with an underwater landslide. NHWAVE solves fully non-hydrostatic Navier-Stokes equations in a surface and terrain following (sigma) coordinate system. The model is described in Ma et al (Reference 2.4.6-231). The model assumes a single valued water surface and represents turbulent stresses in terms of an eddy viscosity closure. Turbulent stresses are not modeled in the present study, and thus the model is basically solving Euler equations for incompressible flow with a moving surface and bottom.

The governing equations for NHWAVE in Cartesian tensor form are given by (Reference 2.4.6-231):

$$\frac{\partial u_i}{\partial x_i^*} = 0 \qquad \text{Equation 2.4.6-6}$$

and

$$\frac{\partial u_i}{\partial t^*} + u_j \frac{\partial u_i}{\partial x_j^*} = -\frac{1}{\rho}\frac{\partial p}{\partial x_i^*} + g_i + \frac{\partial \tau_{ij}}{\partial x_j^*} \qquad \text{Equation 2.4.6-7}$$

Here, g_i is the gravitational vector, p is fluid pressure, ρ is the fluid density, u_i is the velocity vector, and τ_{ij} is a tensor representing viscous and turbulent stresses which is not used in the current analysis. The σ coordinate version of the model is described in Ma et al (Reference 2.4.6-231). Surface boundary conditions for the model consist of a kinematic constraint on vertical velocity ω, and constraints on tangential and normal stresses (Reference 2.4.6-231).

$$\omega|_{z=\eta} = \frac{\partial \eta}{\partial t} + u\frac{\partial \eta}{\partial x} + \upsilon\frac{\partial \eta}{\partial y} \qquad \text{Equation 2.4.6-8}$$

In the absence of turbulent and viscous effects and with no atmospheric forcing, these reduce to the following for normal stress (Reference 2.4.6-231):

$$p|_{z=\eta} = 0 \qquad \text{Equation 2.4.6-9}$$

For tangential stress, these reduce to (Reference 2.4.6-231):

$$\frac{\partial u}{\partial \sigma}|_{z=\eta} = \frac{\partial \upsilon}{\partial \sigma}|_{z=\eta} = 0 \qquad \text{Equation 2.4.6-10}$$

where vertical stretched coordinate $\sigma = (\eta - z)/H$ and H is total depth defined after Equation 2.4.6-2.

At the bottom, zero tangential stress again gives (Reference 2.4.6-231):

$$\frac{\partial u}{\partial \sigma}|_{z=-h} = \frac{\partial \upsilon}{\partial \sigma}|_{z=-h} = 0 \qquad \text{Equation 2.4.6-11}$$

The kinematic constraint on vertical velocity at the bottom is given by (Reference 2.4.6-231):

$$\omega|_{z=-h} = -\frac{\partial h}{\partial t} - u\frac{\partial h}{\partial x} - \upsilon\frac{\partial h}{\partial y} \qquad \text{Equation 2.4.6-12}$$

The condition on normal stress on the moving bottom is derived from the vertical momentum equation and is given by (Reference 2.4.6-231):

$$\frac{\partial p}{\partial \sigma}|_{z=-h} = -\rho D\frac{d\omega}{dt}|_{z=-h} \qquad \text{Equation 2.4.6-13}$$

where *D* represents total water depth. In the current analysis, linearized forms of Equation 2.4.6-12 and Equation 2.4.6-13 are combined to obtain:

$$\frac{\partial p}{\partial \sigma}|_{z=-h} = \rho D\frac{\partial^2 h}{\partial t^2} \qquad \text{Equation 2.4.6-14}$$

This linearized boundary condition is the same as employed in the basic testing of the model against the laboratory data of Enet and Grilli (Reference 2.4.6-229) and described in Ma et al (Reference 2.4.6-231).

For the present cases, the modeled domain is set up so that the landslide event is centrally located and the generated motion does not reach lateral boundaries during the simulated time. Results from the model at the end of the model run are saved and used in FUNWAVE-TVD as initial conditions.

2.4.6.7.3 Model Grid Development and Description

Topographic data were obtained from high resolution LIDAR surveys around the LNP site converted into an ASCII file for use in the computer model. Bathymetric data for the model domains were obtained from the National Geophysical Data Center (NGDC) ETOPO 1 (Reference 2.4.6-228) and NGDC Coastal Relief Model (CRM) (Reference 2.4.6-232). The computational scheme is comprised of a nesting of three model grids which move the computation for a lower resolution large scale Grid *A* (A_l for landslide cases), through an intermediate resolution Grid *B*, to a high resolution Grid *C* encompassing the study site. All the grids are based on global (latitude-longitude) coordinates.

Grid *A* for the Venezuela seismic tsunami case was generated based on the ETOPO1 data set (Reference 2.4.6-228). The data were extracted using GEODAS, a standard tool described in Reference 2.4.6-228. ETOPO1 uses Mean Sea Level (MSL) as a vertical datum origin. The grid resolution for Grid *A* is 2 arc-minutes.

Grid A_l for the landslide cases was generated based on ETOPO1 in the same way as the Grid *A* was generated for the Venezuela seismic case. The grid resolution for Grid A_l is 1 arc-minute.

Grid *B*, which is nested within both Grid *A* and A_l, was generated based on Volume 3 of the CRM data set (Reference 2.4.6-232). GEODAS is used for data extraction. The CRM also uses MSL as the vertical datum origin. The grid resolution for Grid *B* is 15 arc-seconds.

Grid *C*, which is nested in Grid *B*, was developed from CRM data and the local LIDAR data at the study site. The LIDAR data was first converted into the global horizontal coordinates and the MSL vertical datum using standard tools. The data was merged into the computational grid. The grid resolution for Grid *C* is 3 arc-seconds, or about 90 m (295 ft.).

Grid *A* and A_l and nested Grids *B* and *C* are presented in Figures 2.4.6-228 through 2.4.6-231. One-way nesting between Grid *A* (for the Venezuela seismic case) or Grid A_l (for Gulf of Mexico landslide cases), Grid *B* and Grid *C* is performed through the one-way data transfer at nesting boundaries. The grid nesting scheme transfers surface elevation and velocity components calculated from a large domain to a nested small domain through host cells at nesting boundaries. A linear interpolation is performed between a large domain and small domain at nesting boundaries.

2.4.6.7.4 Vertical Datum and Initial Water Level for Model Runs

The vertical datum used to report maximum water level results near the LNP site is based on North American Vertical Datum 1988 (NAVD88). The vertical datum conversion between MSL and NAVD88 was obtained from National Oceanic and Atmospheric Administration (NOAA) data at Cedar Key, FL (Reference 2.4.6-242).

The initial water level used in all simulations is determined by adding the long-term sea level rise to the 10 percent exceedance high tide for this region.

The 10 percent exceedance predicted high tide is determined following the Regulatory Guide 1.59 (RG 1.59) (Reference 2.4.6-233). The 10 percent exceedance high tide value of 1.31 m (4.3 ft.) MLW for Crystal River is obtained from Table C1 of RG 1.59. This value from RG 1.59 is converted from MLW datum to NAVD88 datum using the datum conversion chart from Reference 2.4.6-242. The 10 percent exceedance high tide value is converted to 0.82 m (2.68 ft.) NAVD88. This 10 percent exceedance predicted high tide value of 0.82 m (2.68 ft.) NAVD88 is combined with initial rise of 0.18 m (0.6 ft.) from Table C1 of RG 1.59, to obtain the 10 percent exceedance high tide level of 1.00 m (3.28 ft.) NAVD88.

NOAA has evaluated sea level rise trends for each tide station. Reference 2.4.6-243 provides the data for the mean sea level trend at the Cedar Key tide gauge, station 8727520. From this reference the mean sea level rise of 0.2 m (0.59 ft.) in 100 years is obtained.

By adding the 10 percent exceedance high tide of 1.00 m (3.28 ft.) NAVD88 to the long-term sea level rise of 0.2 m (0.59 ft.), an initial water level of 1.18 m (3.87 ft.) NAVD88 was obtained.

2.4.6.7.5 Seismic Source: Venezuela

Source parameters for Venezuela seismic tsunami are based on ten Brink et al (Reference 2.4.6-238) and are presented in Table 2.4.6-206. There are two fault segments associated with the potential event. The first is the W. Southern Caribbean fault in the north Venezuela subduction zone. This fault is 550 km (342 miles) long and 50 km (31 miles) wide. The strike angle is N53E, the dip angle is 17S, and the rake angle is 90 degrees. The second fault is the E. Southern Caribbean in the north Venezuela subduction zone. It is 200 km (124 miles) long and 50 km (31 miles) wide. The strike, dip and rake angles are N95E, 17S and 90 degrees, respectively. The composite source was used with a slip of 23 m (75.5 ft.) for both of the segments, equivalent to magnitude $M_w = 9.0$. Figure 2.4.6-232 shows the initial source deformation calculated from the Okada formula. Results of the tsunami simulation for the Venezuela Seismic source are described in Subsection 2.4.6.7.9.

2.4.6.7.6 Landslide Source: Initial Conditions and Determination of Slide Velocities

Two initial conditions are considered for each landslide source in this analysis. The first is a static source configuration, which ten Brink et al (Reference 2.4.6-238) suggest is a conservative approach to conduct a simulated landslide event. For the static source configuration, the initial condition for the numerical simulation is a static surface displacement with a depression over the initial slide location and having the size and shape of the slide volume, and an elevation over the final slide position having the same size and shape. The second condition employs NHWAVE to generate a dynamic source, which specifies both surface displacement and depth averaged horizontal velocity fields. For the dynamic source configuration where initial conditions for landslide sources are determined from NHWAVE, it is necessary to determine a reasonable velocity for the sliding mass, as discussed below.

Slide velocities are estimated following the methods presented by Enet and Grilli (Reference 2.4.6-229). The slide shapes given in Reference 2.4.6-229 are utilized, with the thickness of the slide relative to a local origin (x,y) = (0,0) given by:

$$\zeta = \frac{T}{1-\varepsilon}\left[\operatorname{sech}\left(k_b x\right)\operatorname{sech}\left(k_w y\right) - \varepsilon\right] \qquad \text{Equation 2.4.6-15}$$

where ζ is the horizontal distribution of slide thickness, T is the maximum slide thickness at the center, $k_b = 2C/b$, $k_w = 2C/w$, b is landslide length in the forward (sliding) direction, w is landslide width in the transverse direction, $C = \operatorname{acosh}(1/\varepsilon)$, and truncation parameter $\varepsilon = 0.7$ as in Reference 2.4.6-229. This geometry gives a total slide volume V_b given by (Reference 2.4.6-229):

$$V_b = bwT\left(\frac{f^2-\varepsilon}{1-\varepsilon}\right) \quad \text{with} \quad f = \frac{2}{C}a\tan\sqrt{\frac{1-\varepsilon}{1+\varepsilon}} \qquad \text{Equation 2.4.6-16}$$

The motion of the landslide is estimated from a balance of inertia, gravity force, buoyancy, Coulomb friction and drag force, leading to the balance equation (Reference 2.4.6-229):

$$\left(M_b+\Delta M_b\right)\frac{d^2s}{dt^2}=\left(M_b-\rho_w V_b\right)\left(\sin\theta-C_n\cos\theta\right)g-\frac{1}{2}\rho_w\left(C_F A_w+C_D A_b\right)\left(\frac{ds}{dt}\right)^2 \quad \text{Equation 2.4.6-17}$$

where g is gravitational acceleration, M_b is slide mass, s is downslope slide displacement, ρ_w is water density, θ is bed slope angle, ΔM_b, A_w and A_b are slide added mass, wetted surface area and main cross-section perpendicular to the direction of motion, respectively. The remaining parameters are C_F, the skin friction coefficient, C_D, the form drag coefficient, and C_n, the basal Coulomb friction coefficient. Based on this model, a terminal velocity of the slide is calculated using the following equation with the assumption that the slide moves forward a distance equal to its initial width b in the slide direction (Reference 2.4.6-229):

$$u_t=\sqrt{gb\sin\theta\left(1-\frac{\tan\phi}{\tan\theta}\right)\left(\frac{\gamma-1}{C_d'}\right)\frac{2\left(f^2-\varepsilon\right)}{f-\varepsilon}} \quad \text{Equation 2.4.6-18}$$

The parameter $\gamma = \rho_s / \rho_w$ is the specific gravity of the sliding material, which is taken to be 2.65. Following Reference 2.4.6-229, the global drag coefficient $C'_d = 1.0$.

2.4.6.7.7 Landslide Source: Mississippi Canyon

The Mississippi Canyon landslide event was chosen as the largest credible event occurring in the Gulf of Mexico basin. The description of the Mississippi Canyon landslide source is based on the discussion in ten Brink et al (Reference 2.4.6-238). The bathymetric evidence for the event is illustrated in Figure 2.4.6-233, where the source region is outlined. Ten Brink et al (Reference 2.4.6-238) estimates that the initial slide has an area A = 3687 km^2 (1424 mi^2) and volume V_b = 425.5 km^3 (102.1 mi^3). From the outlined region in Figure 2.4.6-233, the slide source's length b is estimated to be 150 km (93.2 miles). Using the geometric description in the previous section, a slide width w is estimated to be 31.3 km (19.5 miles), and a maximum slide thickness T is estimated to be 0.306 km (0.19 miles), which corresponds well with the reported excavation depth of approximately 300 m (984 ft.) given in ten Brink et al (Reference 2.4.6-238). The source parameters for the Mississippi Canyon landslide event are presented in Table 2.4.6-207.

Two initial conditions are considered for the Mississippi Canyon landslide simulation. The first is a static source configuration, for which it is assumed that the initial slide volume described above translates downslope along its major axis a distance equal to its initial length, 150 km (93.2 miles). The initial and final positions of the slide are displayed in Figure 2.4.6-233. The water depths at the slides initial and final centroids are 1000 m (3281 ft.) and 2450 m (8038 ft.), respectively, giving an effective local slope (delta) h/b = 0.01. The runout distance of 150 km (93.2 miles) is less than the estimates based on measured bathymetry given in ten Brink et al (Reference 2.4.6-238), but the spreading and flattening of the sliding mass during the slide process is neglected in the present simulations. This gives a higher and narrower initial elevation hump at the final

slide location than would occur if the slide were allowed to deform, but the initial displaced water volume is equivalent in either case. The resulting initial surface displacement for input into FUNWAVE-TVD is shown in Figure 2.4.6-234.

The second initial condition employs the model NHWAVE to generate an initial surface displacement and horizontal velocity field based on direct modeling of the sliding mass described above. Input to NHWAVE includes bathymetric grid, initial slide position and orientation, total sliding distance, and down-slope translation velocity of the slide. Equation 2.4.6-18 is used to estimate a terminal velocity u_t = 151.4 m/s (496.7 ft/s). In the simulation, the slide is translated at this velocity for the entire slide event. The duration of the event is then (delta) $t = b/u_t = 990.7$ seconds. The model is run for this duration, and the final surface displacement field and horizontal velocity fields are saved for input into FUNWAVE-TVD. The resulting surface displacement at the end of the NHWAVE run is shown in Figure 2.4.6-235.

Using either the static or dynamic source as initial condition, FUNWAVE-TVD is run using one-way nesting using Grids A_l, B and C. Results of the tsunami simulation for the Mississippi Canyon source are described in Subsection 2.4.6.7.10.

2.4.6.7.8 Landslide Source: Florida Escarpment

The Florida Escarpment landslide event is the closest large event to LNP site, chosen since landslide tsunami impact is often most severe on adjacent shorelines. The Florida Escarpment landslide event is based on a collapse of the shelf break slope of the carbonate platform which forms the continental shelf on the western side of the Florida peninsula. The description of the Florida Escarpment landslide source is based on the discussion in ten Brink et al (Reference 2.4.6-238). The bathymetric evidence for the event is illustrated in Figure 2.4.6-236, where the source region is outlined, following on information presented in Figure 3-6 in ten Brink et al (Reference 2.4.6-238). Ten Brink et al (Reference 2.4.6-238) estimate that the initial slide has an area A = 647.47 km^2 (250 mi^2), width w = 42.94 km (26.68 miles) and volume V_b = 16.2 km^3 (6.26 mi^3). From the outlined region in Figure 2.4.6-236 the slide source's length b is estimated to be 19.2 km (11.9 miles), and a maximum slide thickness T is estimated to be 58 m (190 ft.), which differs from the estimate of 150 m (492 ft.) given in ten Brink et al (Reference 2.4.6-238), but results from the very uneven excavation pattern in the actual slide. The source parameters for the Florida Escarpment landslide event are presented in Table 2.4.6-207.

As in the Mississippi Canyon landslide event, two initial conditions are considered for the Florida Escarpment landslide simulation. For both, it is assumed that the initial source translated a downslope distance equal to its initial downslope length. Ten Brink et al (Reference 2.4.6-238) discuss this translation and point out that it is presently impossible to determine the configuration of the slide deposit from existing sonar data as the volume is buried under later deposits. The initial and final positions of the slide in the simulations are displayed in Figure 2.4.6-236. The water depths at the initial and final centroids of the slides are 1548 m (5079 ft.) and 3305 m (10,843 ft.), respectively, giving an effective local slope (delta) h/b = 0.09. For the dynamic source determination, Equation 2.4.6-18 is used to estimate a terminal velocity u_t = 175.3 m/s (575.2 ft/s). In the simulation, the slide is translated at this velocity for the entire slide event. The duration of the event is then (delta) $t = b/u_t = 109.5$ seconds. The model is run for this

duration, and the final surface displacement field and horizontal velocity fields are saved for input into FUNWAVE-TVD. Initial surface displacements for FUNWAVE-TVD for the static and dynamic sources are shown in Figure 2.4.6-237 and Figure 2.4.6-238, respectively.

Using either the static or dynamic sources as initial conditions, FUNWAVE-TVD is run using one-way nesting using Grids *A*, *B* and *C*. Results of the tsunami simulation for the Florida Escarpment source are described in Subsection 2.4.6.7.11.

2.4.6.7.9 Model Results: Venezuela Seismic Event Simulation

Figure 2.4.6-239 shows snapshots for the propagation of the tsunami in the Venezuela Grid *A* at 40 minutes and 80 minutes after the start of the model. Figure 2.4.6-240 shows a plot of the maximum water level occurring in Grid *A*, and shows that tsunami runup height on the west Florida shelf is on the order of 20 to 30 cm (7.9 to 11.8 in). Figure 2.4.6-241 shows snapshots, at 440 minutes and 520 minutes after the start of the model, of the tsunami wave crossing the shelf region (Grid *B*) and making landfall on the west coast of Florida. Maximum tsunami amplitudes are greatly reduced by frictional effects over the shelf, and are limited to values on the order of 15 cm (5.9 in) along the coast covered by Grid *B* (Figure 2.4.6-242). Figure 2.4.6-243 and Figure 2.4.6-244 show propagation and maximum water level in Grid *C*, respectively, and show that tsunami runup in the vicinity of the LNP site reaches levels on the order of 30 cm (11.8 in). Surface displacements in Figures 2.4.6-239 through 2.4.6-244 are with respect to model initial water level, which includes MSL plus 10 percent exceedence high tide plus the long-term sea level rise.

Figure 2.4.6-245 shows a plot of the initial MSL shoreline and maximum extent of tsunami inundation superimposed on a topographic contour map of the Grid C region. The extent of tsunami runup in the inundated region is illustrated in Figure 2.4.6-246, which shows a vertical section through Grid C at latitude 29.075N, representing an east-west line through the location of the LNP site, indicated on the figure. Results, including maximum water levels and inland distance of inundation, are summarized in Table 2.4.6-208. It should be noted that the elevations of the Levy site shown on Figures 2.4.6-245 and 2.4.6-246 and other topographical maps contained in following descriptions of model results represent the existing grade of approximately 12.5 to 14.9 m (41 to 49 ft.) NAVD88, as opposed to the plant grade elevation of 15.24 m (50 ft.) NAVD88.

2.4.6.7.10 Model Results: Mississippi Canyon Landslide Event Simulation

The Mississippi Canyon landslide source was run using two different source configurations: a static source following the procedure in Reference 2.4.6-238, and a dynamic source using the NHWAVE model and the determination of slide. Results of the tsunami simulation based on the static source are displayed in Figures 2.4.6-247 through 2.4.6-254, and results based on the dynamic source are displayed in Figures 2.4.6-255 through 2.4.6-262.

Although the methodology described in Reference 2.4.6-238 is aimed at giving the most conservative estimate of tsunami wave amplitude for a given source configuration, results of these simulations indicate that the geometry for the source also plays a role in determining the susceptibility of any segment of coastline to tsunami attack. For

example, a comparison of Figure 2.4.6-247 (for the static source) and Figure 2.4.6-255 (for the dynamic source) show a tendency for wave energy to be directed in a more southerly direction for the dynamic source. The resulting patterns of maximum wave amplitude for Grid A_I for the two sources, shown in Figure 2.4.6-248 and Figure 2.4.6-256, show that the tsunami wave height arriving at the west Florida shelf break is significantly larger for the dynamic source than for the static source.

The evolution of the landward propagating wave for either source is controlled by strong wave breaking dissipation over the shallow and broad extent of the shelf. A comparison of the maximum wave heights for the two sources over Grid *B*, presented in Figure 2.4.6-250 and Figure 2.4.6-258, show that the dynamic source produces higher waves over the inner shelf region, but that wave height is significantly reduced by the time waves reach the inner Grid *C* region. Results for the two sources over Grid *C* are very similar, as revealed by plot plans in Figure 2.4.6-253 and Figure 2.4.6-261 and transect plots in Figure 2.4.6-254 and Figure 2.4.6-262. Inundation depth offshore reaches about 4.6 m (15 ft.) NAVD88 in both cases, and there is significant inland flooding which reaches the base of the steeper terrain surrounding the LNP site. Details of the spatial distribution of maximum runup elevation differ for the two cases, although neither is likely to be strictly accurate due to the relatively inaccurate nature of the CRM bathymetry for the subaerial regions fronting the LNP site.

The maximum water level near the LNP site due to a tsunami caused by the simulated Mississippi Canyon landslide event is 3.94 m (12.94 ft.) NAVD88, considering both the static and dynamic source configurations. The inundation due to this tsunami reaches a location approximately 15.6 km (9.7 miles) inland and approximately 5.95 km (3.7 miles) from the LNP site. Tsunami simulation results are summarized in Table 2.4.6-208.

2.4.6.7.11 Model Results: Florida Escarpment Landslide Event Simulation

The tsunami simulation results for both static and dynamic source configurations for the Florida Escarpment landslide event are similar. Therefore, the time-wise simulation results for the static case only are presented in Figures 2.4.6-263 through 2.4.6-270. For comparison with the static source case, only the inland extent of inundation is provided for the dynamic case as presented in Figure 2.4.6-271.

The maximum water level near the LNP site due to a tsunami caused by the simulated Florida Escarpment landslide event is 1.32 m (4.33 ft.) NAVD88, considering both the static and dynamic source configurations. The inundation due to this tsunami reaches a location approximately 6.8 km (4.2 miles) inland and approximately 14.8 km (9.2 miles) from the LNP site. Results for all of the tsunami simulations are summarized in Table 2.4.6-208.

2.4.6.7.12 PMT Maximum Water Level near LNP 1 and 2 Site

The results of maximum water level and inundation distance for each of the simulated tsunami scenarios and source configurations are presented in Table 2.4.6-208. Based on the discussion of tsunami simulation results, the most severe PMT event is associated with the large scale Mississippi Canyon landslide event in the Gulf of Mexico. This event produced the highest runup and farthest extent of onshore inundation in the vicinity of the LNP site.

The maximum PMT runup elevation due to the Mississippi Canyon landslide was computed to be 3.94 m (12.94 ft.) NAVD88, which is the most conservative of all the simulation scenarios. The PMT runup includes the initial water level due to the 10 percent exceedance high tide and the long-term sea level rise. The maximum PMT runup elevation is below the plant grade elevation of 15.24 m (50 ft.) NAVD88. The extent of inundation due to the PMT closest to the LNP site is 5.95 km (3.7 miles) west of the LNP Units 1 and 2. Therefore, the safety-related systems and components of LNP Units 1 and 2 will not be affected by the PMT in the Gulf of Mexico.

LNP FSAR Subsection 2.4.16 will be updated to revise References 2.4.6-228 through 2.4.6-241 with the following References:

2.4.6-228 Amante, C. and B. W. Eakins, ETOPO1 1 Arc-Minute Global Relief Model: Procedures, Data Sources and Analysis. National Oceanic and Atmospheric Administration (NOAA) Technical Memorandum NESDIS NGDC-24, 19 pp, 2009, Available at: http://www.ngdc.noaa.gov/mgg/global/global.html.

2.4.6-229 Enet, F. and Grilli, S. T., "Experimental study of tsunami generation by three-dimensional rigid underwater landslides," *J. Waterway, Port, Coastal and Ocean Engineering*, 133, 442-454, 2007.

2.4.6-230 Kirby, J. T., Shi, F., Harris, J. C. and Grilli, S. T., "Sensitivity analysis of trans-oceanic tsunami propagation to dispersive and Coriolis effects," draft manuscript, 2011.

2.4.6-231 Ma, G., Shi, F. and Kirby, J. T., "Shock-capturing Non-hydrostatic Model for Fully Dispersive Surface Wave Processes," submitted to *Ocean Modelling*, June, 2011.

2.4.6-232 NOAA National Geophysical Data Center, U.S. Coastal Relief Model, Volume 3, Dates Retrieved: June 13 and June 17, 2011, http://www.ngdc.noaa.gov/mgg/coastal/crm.html.

2.4.6-233 U.S. Nuclear Regulatory Commission, Regulatory Guide 1.59, Design Basis Floods for Nuclear Power Plants, Revision 2, August 1977.

2.4.6-234 Shi, F., Kirby, J. T., Harris, J. C., Geiman, J. D. and Grilli, S. T., "A High-Order Adaptive Time-Stepping TVD Solver for Boussinesq Modeling of Breaking Waves and Coastal Inundation," Manuscript in preparation for *Ocean Modelling*, 2011.

2.4.6-235 Shi, F., Kirby, J. T., Tehranirad, B., Harris, J. C. and Grilli, S. T., "FUNWAVE-TVD Version 1.0, Fully Nonlinear Boussinesq Wave Model with TVD Solver, Documentation and User's Manual," Research Report No. CACR-11-04, Center for Applied Coastal Research, University of Delaware, Newark. (DRAFT), 2011.

2.4.6-236 Synolakis, C. E., Bernard, E. N., Titov, V. V., Kanoglu, U. and Gonzalez, F. I., Standards, Criteria, and Procedures for NOAA Evaluation of Tsunami Numerical Models, NOAA Technical Memorandum OAR PMEL-135, Pacific Marine Environmental Laboratory, Seattle, 2007.

2.4.6-237 Tehranirad, B., Shi, F., Kirby, J. T., Harris, J. C. and Grilli, S. T., "Tsunami Benchmark Results for Fully Nonlinear Boussinesq Wave Model FUNWAVE-TVD, Version 1.0," Research Report No. CACR-11-02, Center for Applied Coastal Research, University of Delaware, Newark. (DRAFT), 2011.

2.4.6-238 ten Brink, U., Twichell, D., Lynett, P., Geist, E., Chaytor, J., Lee, H., Buczkowski, B. and Flores, C., "Regional assessment of tsunami potential in the Gulf of Mexico," U. S. Geological Survey Administrative Report, 2009.

2.4.6-239 Okada, Y., "Surface Deformation Due to Shear and Tensile Faults in a Half-Space," Bulletin of the Seismological Society of America, Vol. 75, No. 4, pp. 1135-1154, August 1985.

2.4.6-240 Satake, K., "Linear and Nonlinear Computations of the 1992 Nicaragua Earthquake Tsunami," *Pure and Applied Geophysics*, 144, 455-470, 1995.

2.4.6-241 Soulsby, R. L., "The Bottom Boundary Layer of Shelf Seas," in B. Johns (ed), Physical Oceanography of Coastal and Shelf Seas, Elsevier, 189-266, 1983.

2.4.6-242 National Oceanic and Atmospheric Administration (NOAA), Tides and Currents, Datums, Cedar Key, Florida, Station ID: 8727520, Datums, Accessed in June 2010, http://tidesandcurrents.noaa.gov/data_menu.shtml?stn=8727520%20Cedar%20Key,%20FL&type=Datums.

2.4.6-243 National Oceanic and Atmospheric Administration (NOAA), Mean Sea Level Trend, 8727520 Cedar Key, Florida, Accessed in June 2010, http://tidesandcurrents.noaa.gov/sltrends/sltrends_station.shtml?stnid=8727520.

Levy Nuclear Plant Units 1 and 2
COL Application
Part 2, Final Safety Analysis Report

LNP COL 2.4-2

Table 2.4.6-206
Tsunami Source Parameters for the Venezuela Seismic Source

Seismic Source: Fault	Fault Length (km)	Fault Width (km)	Strike Angle	Dip Angle	Rake Angle (°)
Venezuela: W. Southern Caribbean	550	50	N53E	17S	90
Venezuela: E. Southern Caribbean	200	50	N95E	17W	90

Source: Reference 2.4.6-238

Levy Nuclear Plant Units 1 and 2
COL Application
Part 2, Final Safety Analysis Report

LNP COL 2.4-2

Table 2.4.6-207
Tsunami Source Parameters for the Landslide Sources

Landslide Source	Total Volume V_b (km^3)	Area A (km^2)	Excavation Depth (m)	Runout Distance (km from toe)
Mississippi Canyon	425.54	3687.26	~300	297
Florida Escarpment	16.2	647.57	~150	Uncertain

Source: Reference 2.4.6-238

Levy Nuclear Plant Units 1 and 2
COL Application
Part 2, Final Safety Analysis Report

LNP COL 2.4-2

Table 2.4.6-208
Probable Maximum Tsunami Simulation Results Using FUNWAVE

Scenario	Maximum Wave Amplitude at Five Miles Offshore (Feet) (1)	Maximum Wave Amplitude at Shoreline (Feet) (1)	Maximum Extent of Inundation Distance from Shoreline (Miles) (2)	Maximum Extent of Inundation Distance from LNP Site (Miles) (2)	Maximum Water Level Nearest the LNP Site (Feet NAVD88)	Grade Elevation / Floor Elevation of LNP Safety-Related Facilities (Feet NAVD88)
Venezuela Seismic Source	0.22	0.30	4.2	9.2	4.27	50.0 / 51.0
Mississippi Canyon Landslide – Static Source	9.93	9.11	9.7	3.7	12.94	50.0 / 51.0
Mississippi Canyon Landslide – Dynamic Source	10.05	8.93	9.6	3.8	11.66	50.0 / 51.0
Florida Escarpment Landslide – Static Source	0.27	0.29	4.2	9.2	4.33	50.0 / 51.0
Florida Escarpment Landslide – Dynamic Source	0.25	0.27	4.2	9.2	4.30	50.0 / 51.0

Notes:
(1) The tsunami wave amplitudes presented in the table are measured above the initial water level of 3.87 feet NAVD 88.
(2) The distances presented in the table are measured along latitude 29.075N. The LNP site is located approximately 13.4 miles from the shoreline.

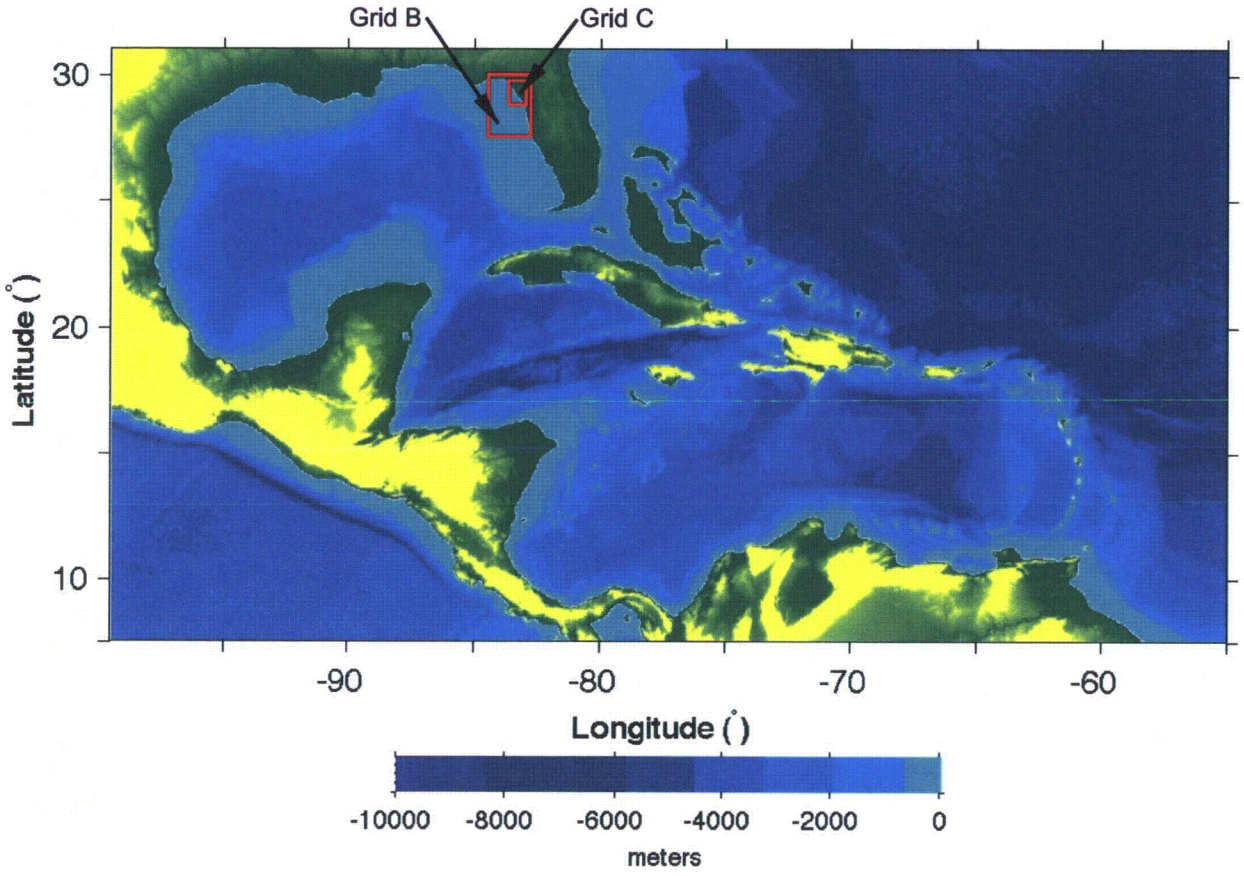

Progress Energy Florida
Levy Nuclear Plant
Units 1 and 2
Part 2, Final Safety Analysis Report

Venezuela Seismic Event Simulation:
Geometry of Grid *A*

FIGURE 2.4.6-228 Rev 3

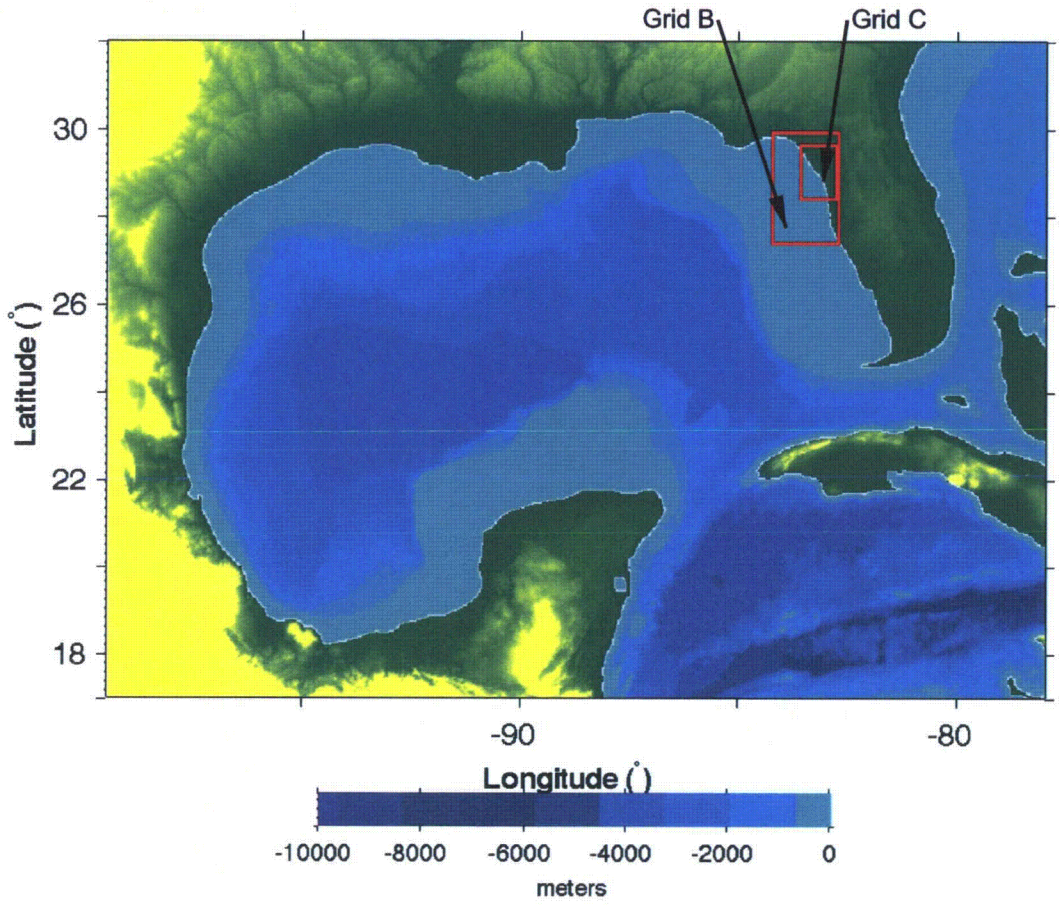

Progress Energy Florida
Levy Nuclear Plant
Units 1 and 2
Part 2, Final Safety Analysis Report

Mississippi Canyon and Florida Escarpment
Landslide Event Simulations:
Geometry of Grid A_l

FIGURE 2.4.6-229 Rev 3

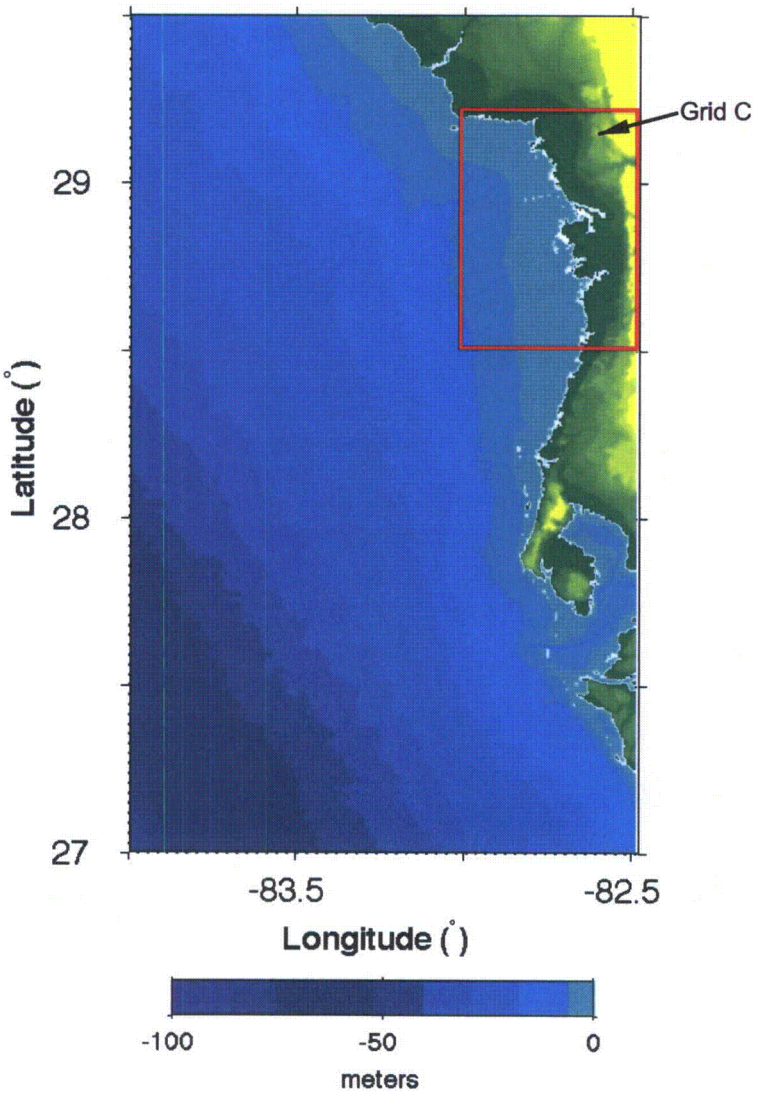

Progress Energy Florida
Levy Nuclear Plant
Units 1 and 2
Part 2, Final Safety Analysis Report

Geometry of Nested Grid *B*
for all Simulated Events

FIGURE 2.4.6-230 Rev 3

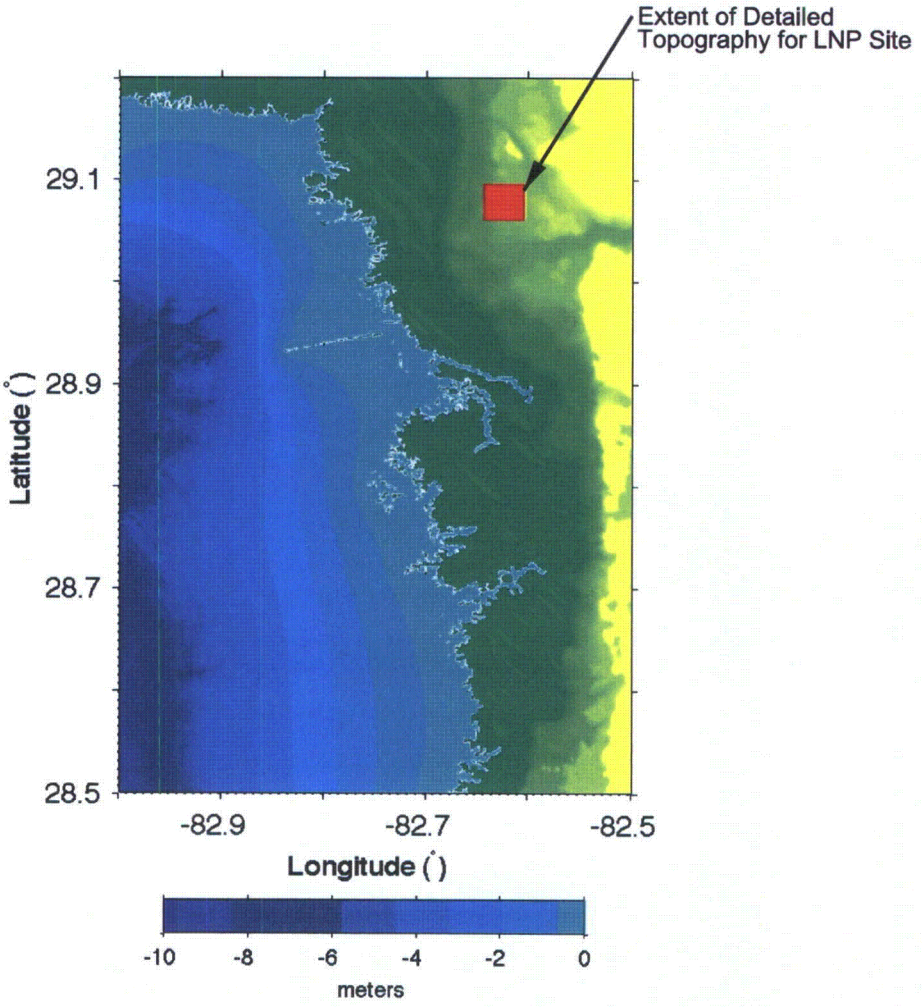

Progress Energy Florida
Levy Nuclear Plant
Units 1 and 2
Part 2, Final Safety Analysis Report

Geometry of Nested Grid *C*
for all Simulated Events

FIGURE 2.4.6-231 Rev 3

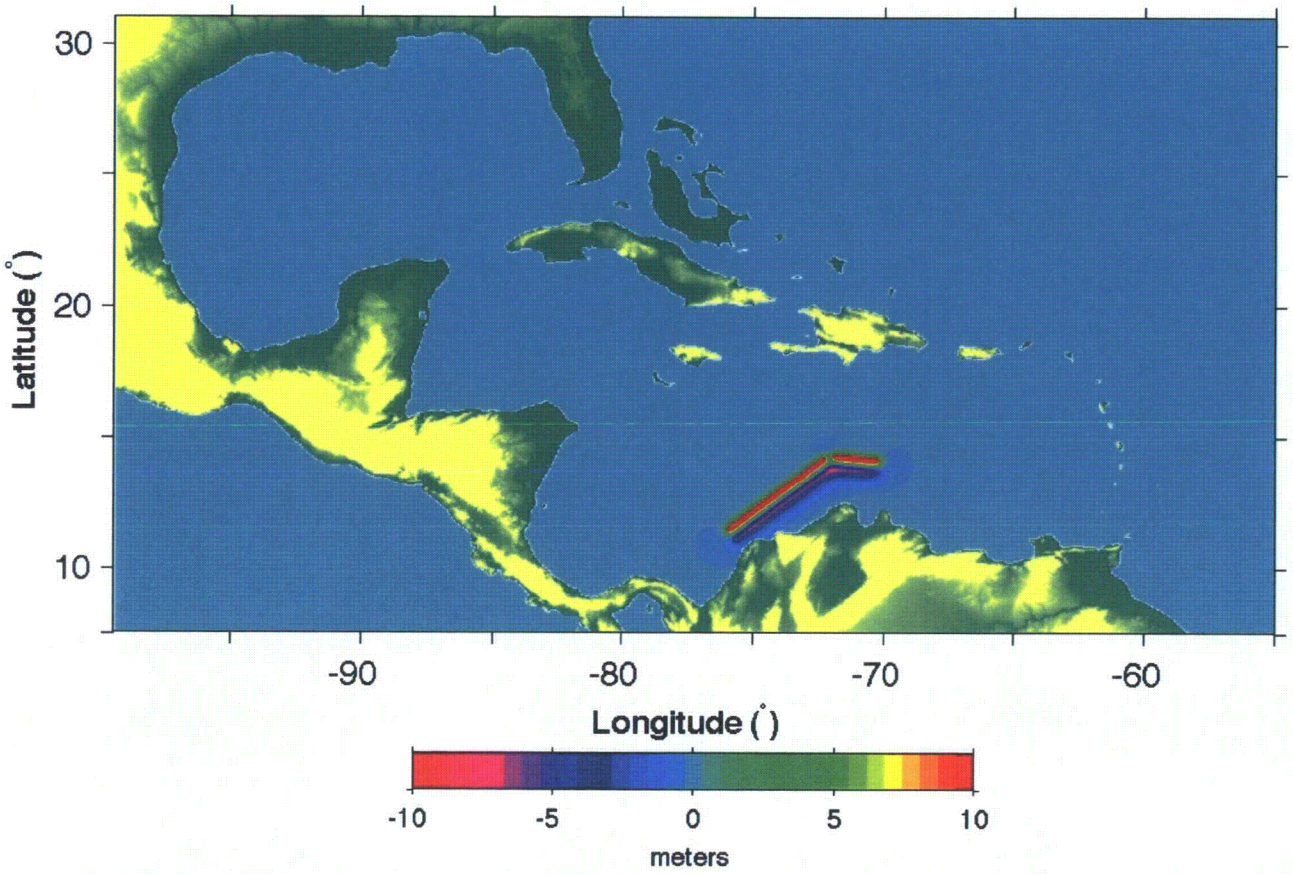

Progress Energy Florida
Levy Nuclear Plant
Units 1 and 2
Part 2, Final Safety Analysis Report

Venezuela Seismic Event Simulation:
Static Seismic Source,
Initial Bottom and Sea Surface Deformation

FIGURE 2.4.6-232 Rev 3

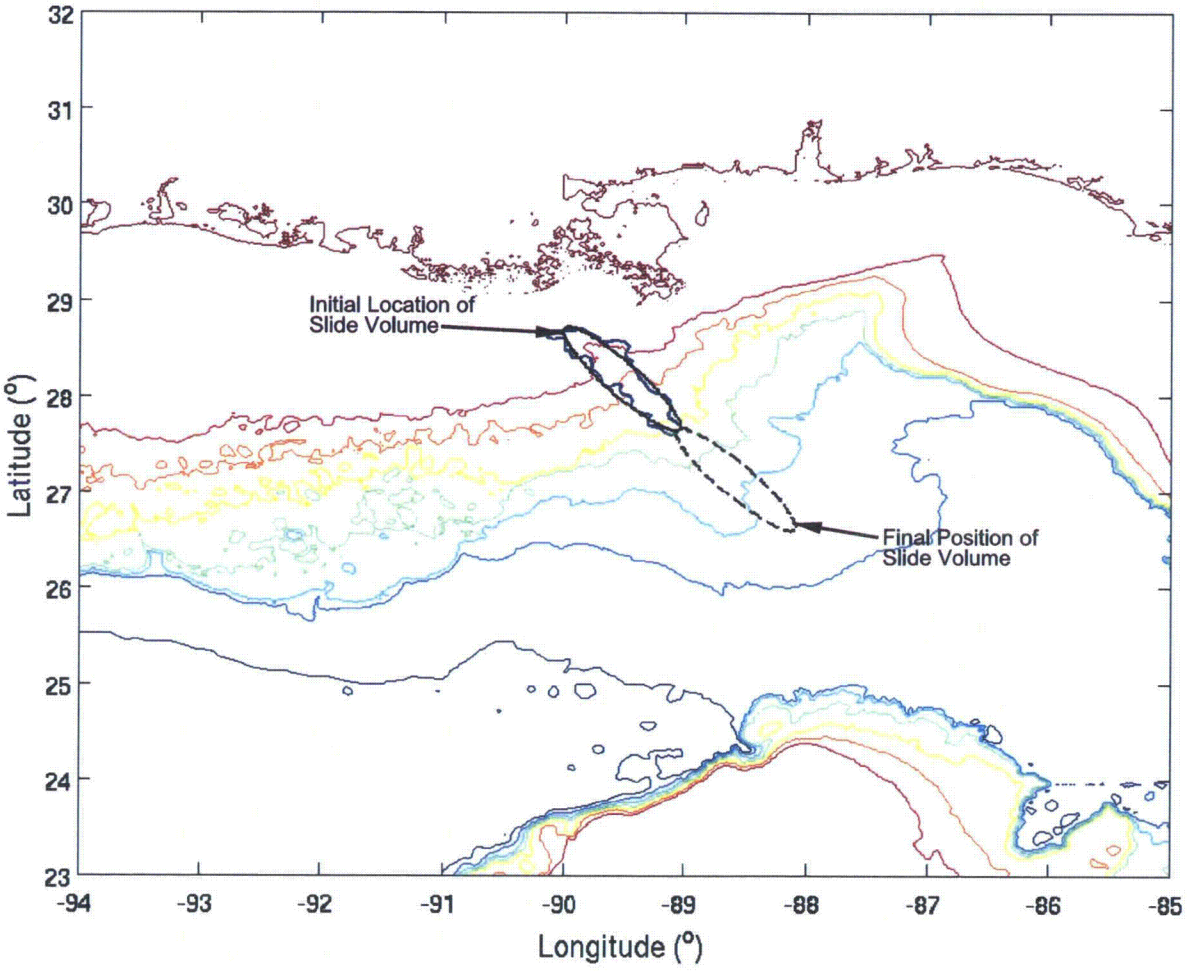

Progress Energy Florida
Levy Nuclear Plant
Units 1 and 2
Part 2, Final Safety Analysis Report

Mississippi Canyon Landslide Event Simulation:
Geometry of Slide Area Superimposed on
ETOPO1 Bathymetry

FIGURE 2.4.6-233 Rev 3

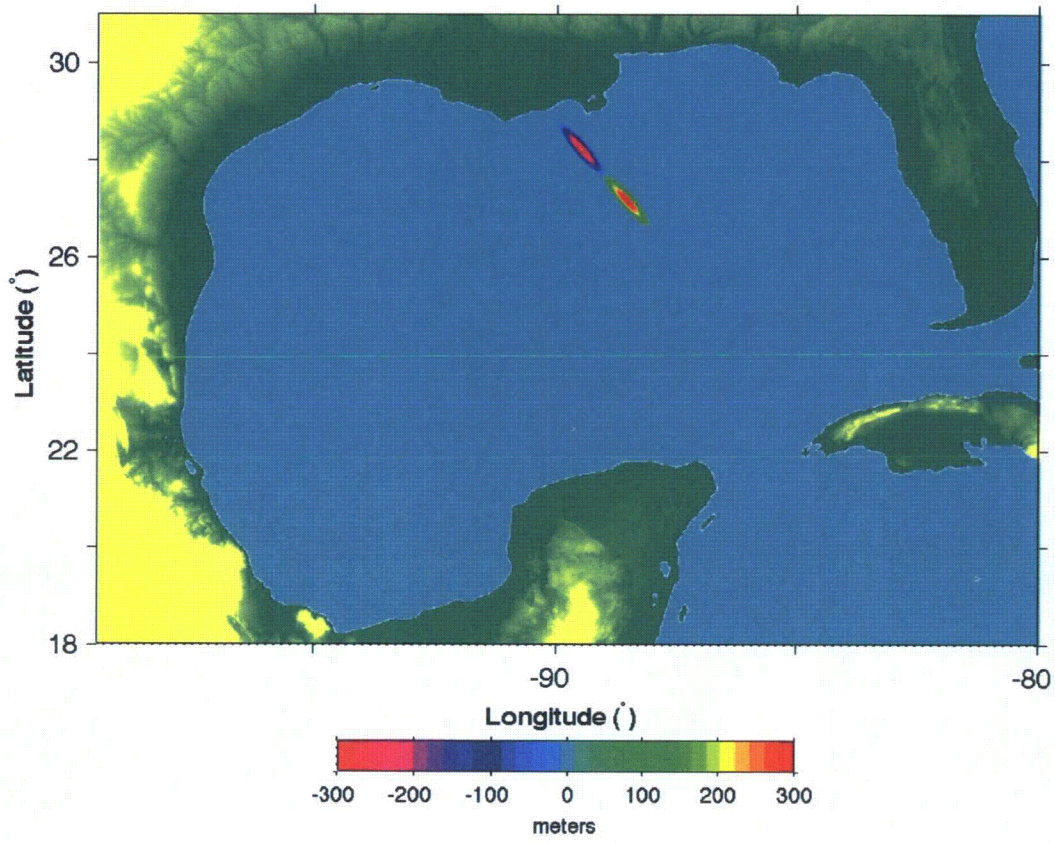

Progress Energy Florida
Levy Nuclear Plant
Units 1 and 2
Part 2, Final Safety Analysis Report

Mississippi Canyon Landslide Event Simulation:
Initial Static Source,
Initial Sea Surface Displacement (Grid A_I)

FIGURE 2.4.6-234 Rev 3

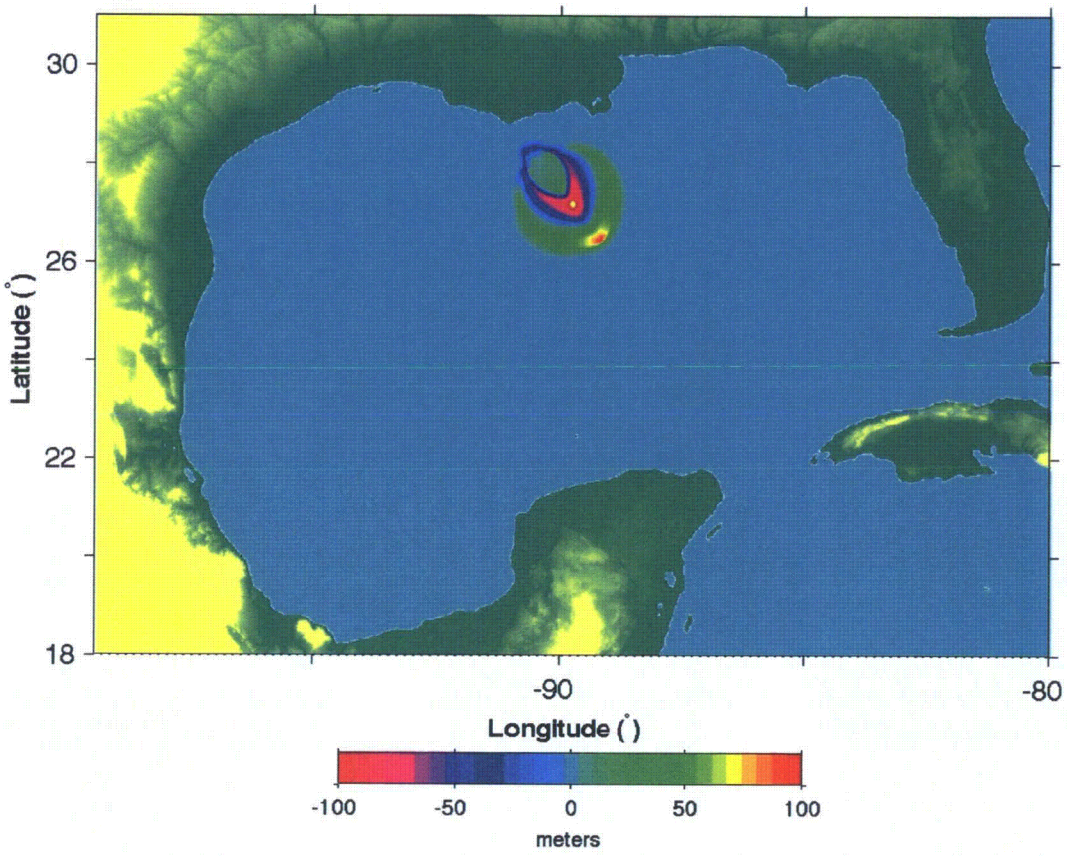

Progress Energy Florida
Levy Nuclear Plant
Units 1 and 2
Part 2, Final Safety Analysis Report

Mississippi Canyon Landslide Event Simulation:
Initial Dynamic Source, Sea Surface Displacement
at the end of NHWAVE Run (Grid A_I)

FIGURE 2.4.6-235 Rev 3

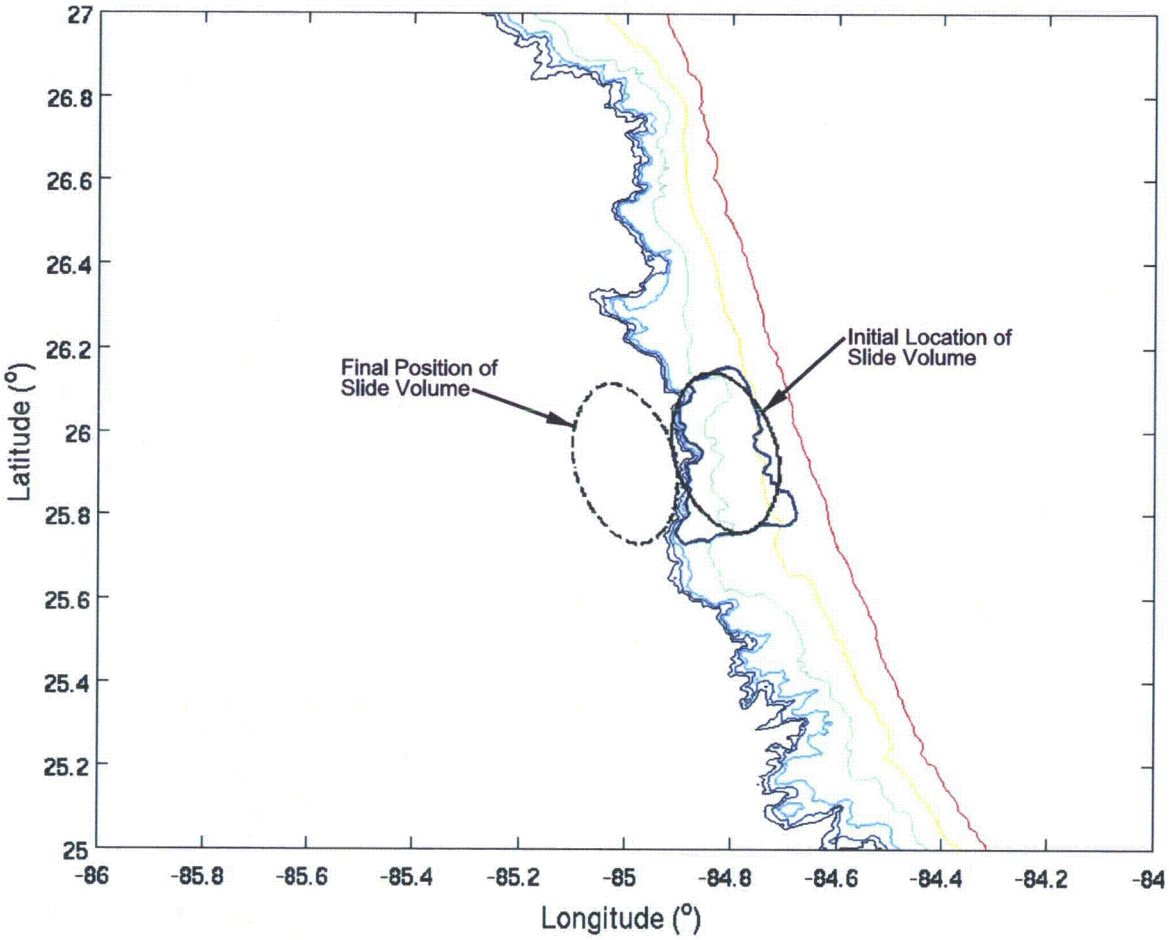

Progress Energy Florida
Levy Nuclear Plant
Units 1 and 2
Part 2, Final Safety Analysis Report

Florida Escarpment Landslide Event Simulation:
Geometry of Slide Configuration
Superimposed on CRM Bathymetry

FIGURE 2.4.6-236 Rev 3

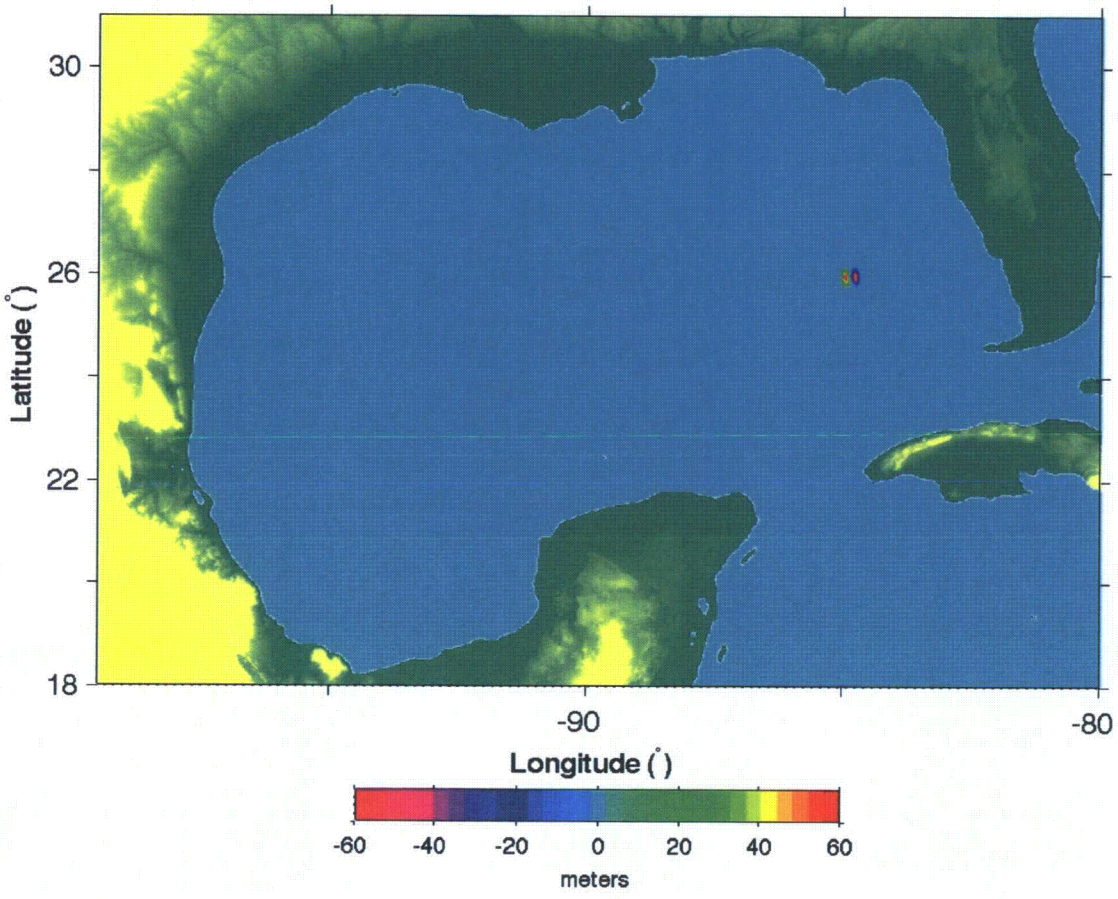

Progress Energy Florida
Levy Nuclear Plant
Units 1 and 2
Part 2, Final Safety Analysis Report

Florida Escarpment Landslide Event Simulation:
Initial Static Source,
Initial Sea Surface Displacement (Grid A_i)

FIGURE 2.4.6-237 Rev 3

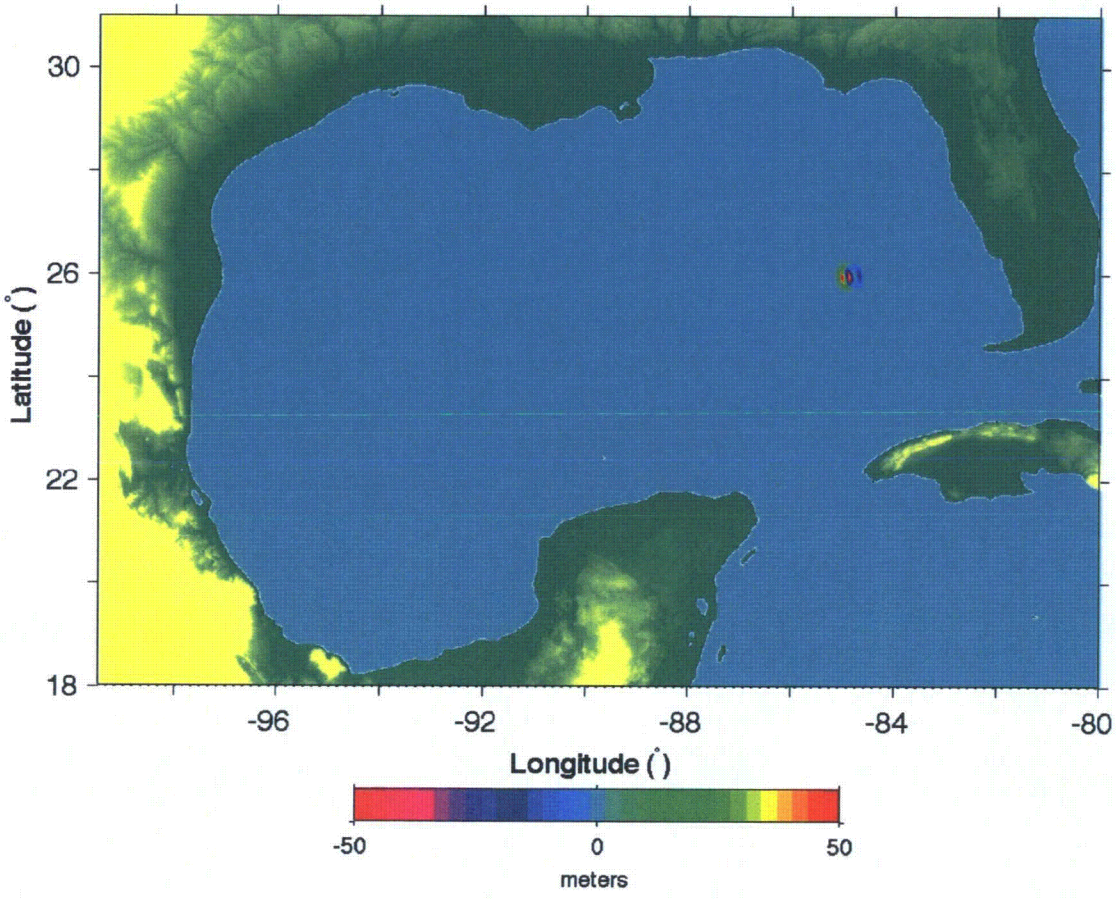

Progress Energy Florida
Levy Nuclear Plant
Units 1 and 2
Part 2, Final Safety Analysis Report

Florida Escarpment Landslide Event Simulation:
Initial Dynamic Source, Sea Surface Displacement
at the end of NHWAVE Run (Grid A_I)

FIGURE 2.4.6-238 Rev 3

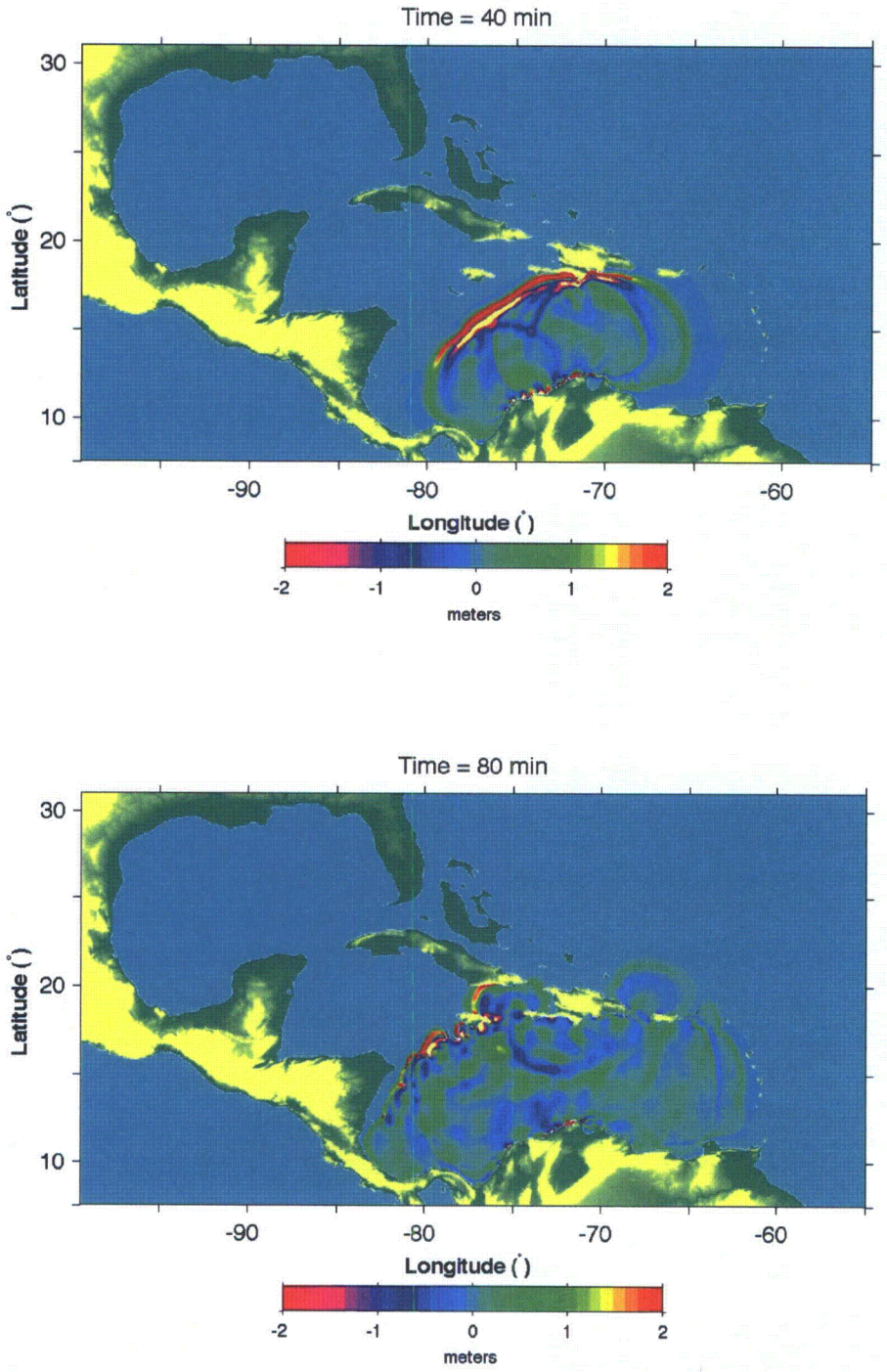

Progress Energy Florida
Levy Nuclear Plant
Units 1 and 2
Part 2, Final Safety Analysis Report

Venezuela Seismic Event Simulation:
Instantaneous Surface Displacement (Grid *A*)
at T = 40 min and T = 80 min

FIGURE 2.4.6-239 Rev 3

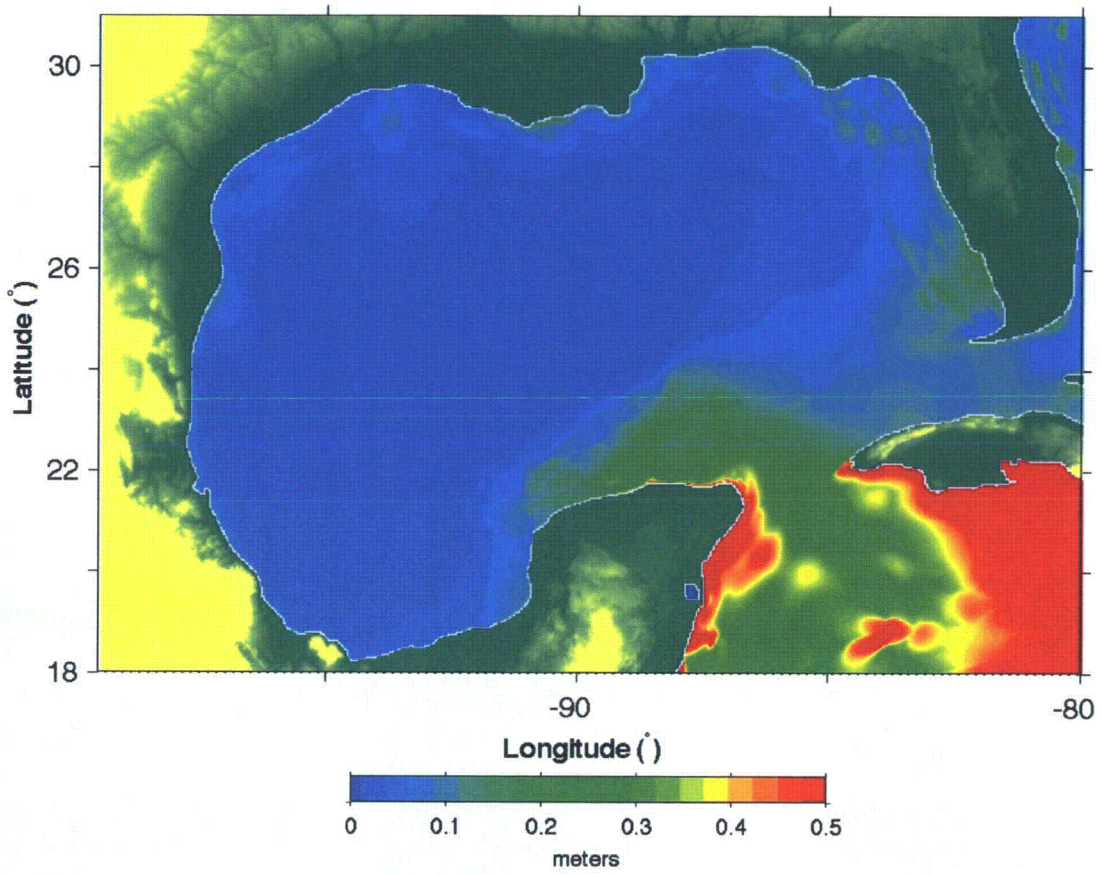

Progress Energy Florida
Levy Nuclear Plant
Units 1 and 2
Part 2, Final Safety Analysis Report

Venezuela Seismic Event Simulation:
Maximum Water Level
Generated During Simulation (Grid *A*)

FIGURE 2.4.6-240 Rev 3

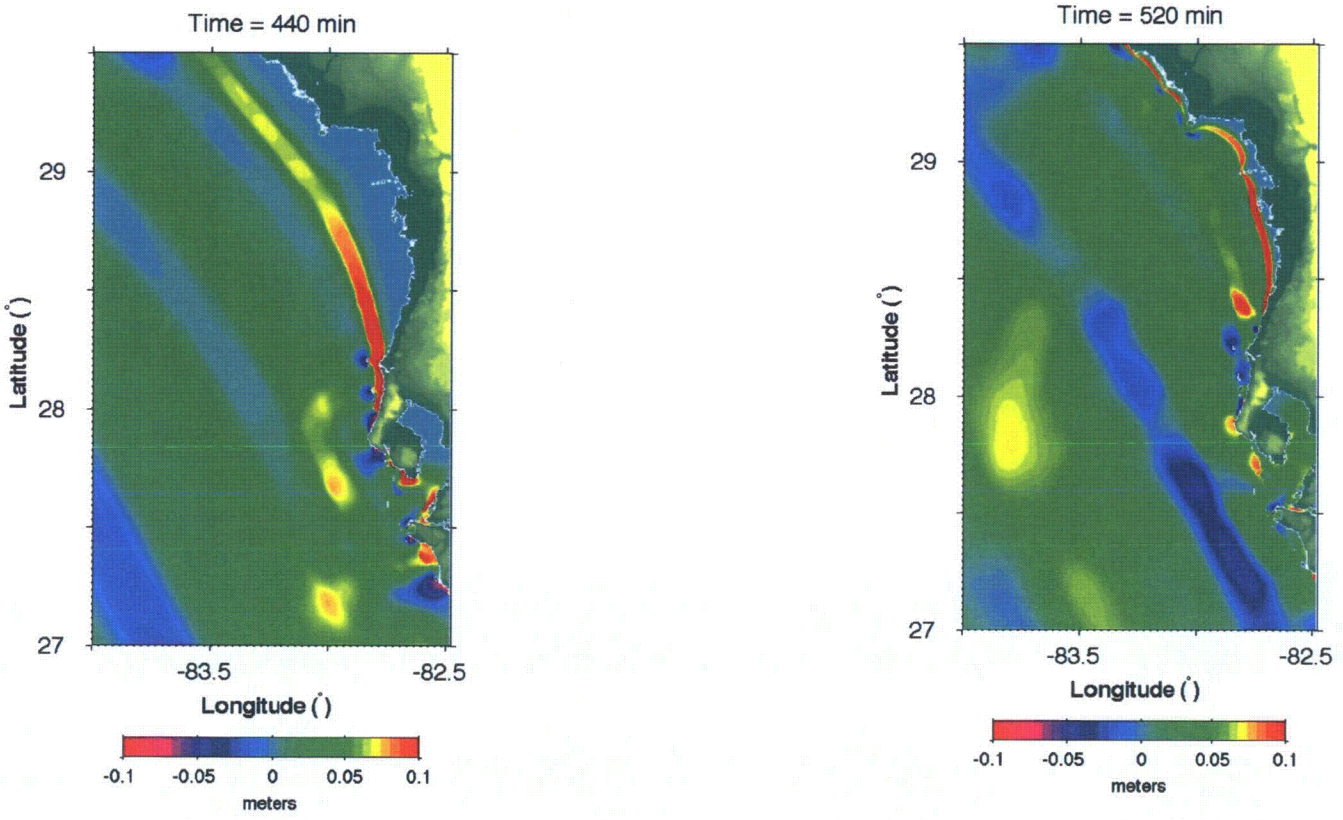

Progress Energy Florida
Levy Nuclear Plant
Units 1 and 2
Part 2, Final Safety Analysis Report

Venezuela Seismic Event Simulation:
Instantaneous Surface Displacement (Grid *B*)
at T = 440 min and T = 520 min

FIGURE 2.4.6-241 Rev 3

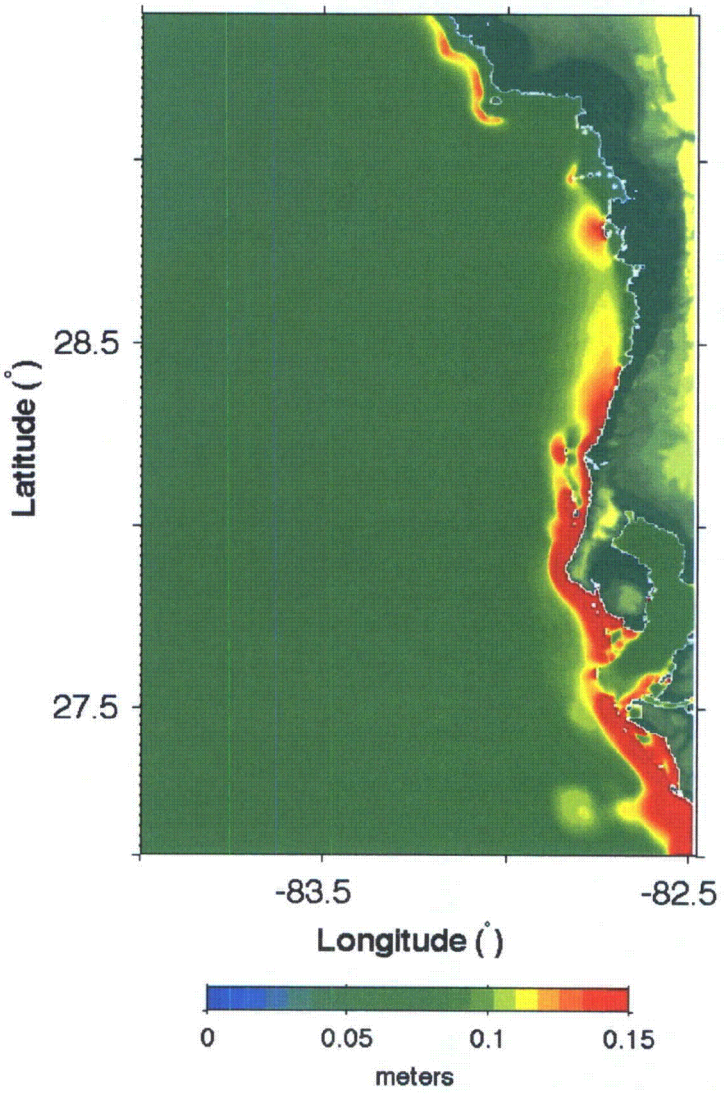

Progress Energy Florida
Levy Nuclear Plant
Units 1 and 2
Part 2, Final Safety Analysis Report

Venezuela Seismic Event Simulation:
Maximum Water Level
Generated During Simulation (Grid *B*)

FIGURE 2.4.6-242 Rev 3

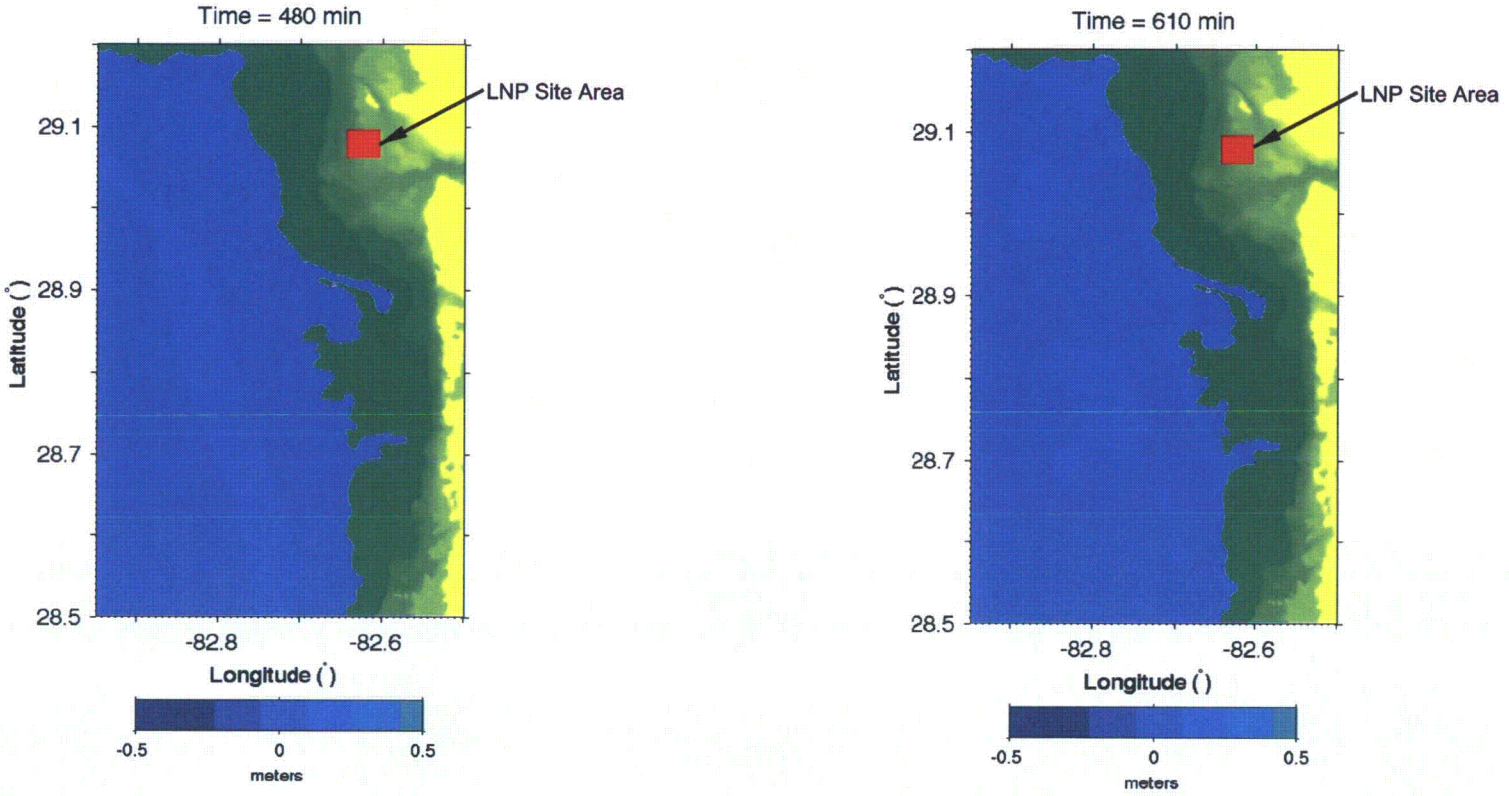

Progress Energy Florida
Levy Nuclear Plant
Units 1 and 2
Part 2, Final Safety Analysis Report

Venezuela Seismic Event Simulation:
Instantaneous Surface Displacement (Grid *C*)
at T = 480 min and T = 610 min

FIGURE 2.4.6-243 Rev 3

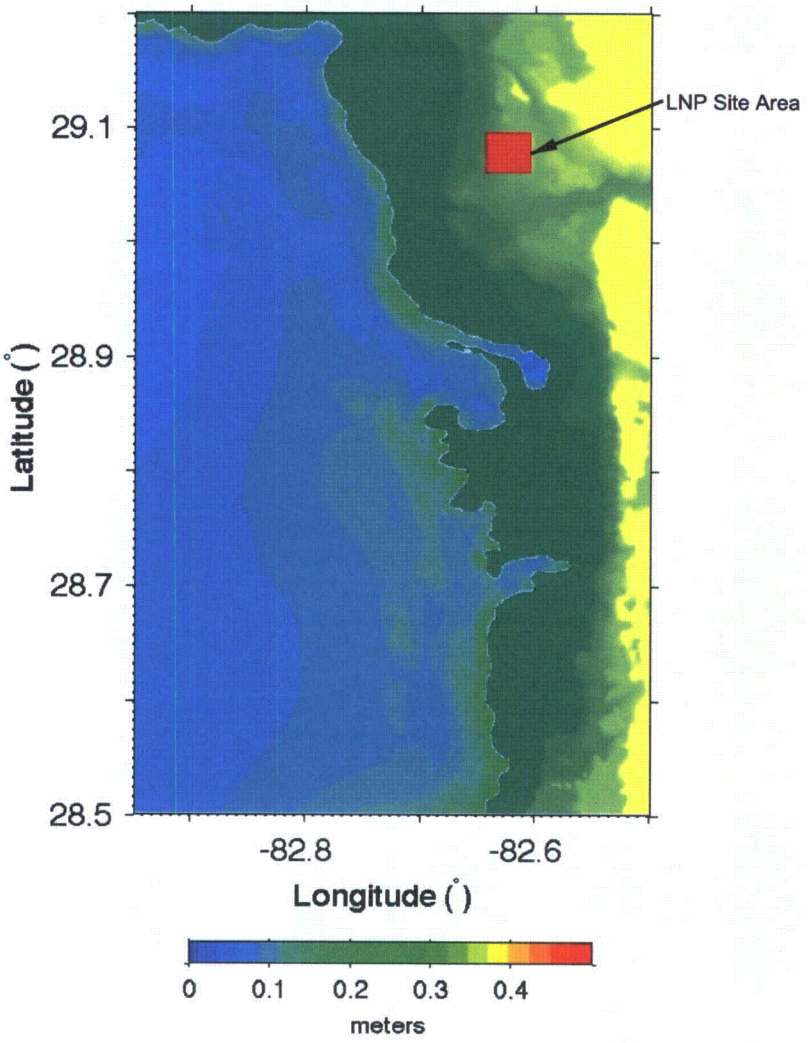

Progress Energy Florida
Levy Nuclear Plant
Units 1 and 2
Part 2, Final Safety Analysis Report

Venezuela Seismic Event Simulation:
Maximum Water Level
Generated During Simulation (Grid *C*)

FIGURE 2.4.6-244 Rev 3

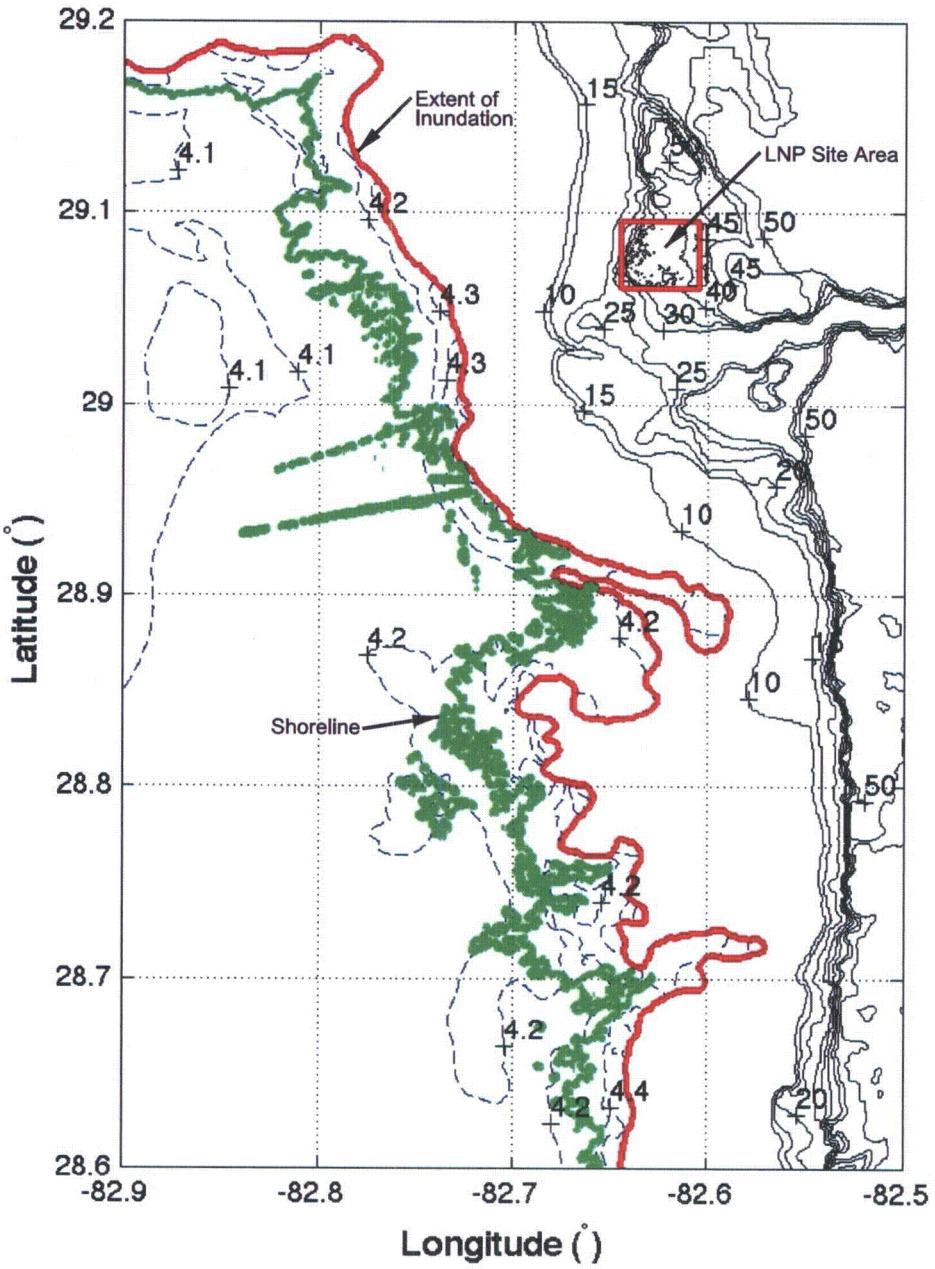

NOTE:
Contour elevations are given in feet NAVD 88.

Progress Energy Florida
Levy Nuclear Plant
Units 1 and 2
Part 2, Final Safety Analysis Report

Venezuela Seismic Event Simulation:
Maximum Extent of Inundation

FIGURE 2.4.6-245 Rev 3

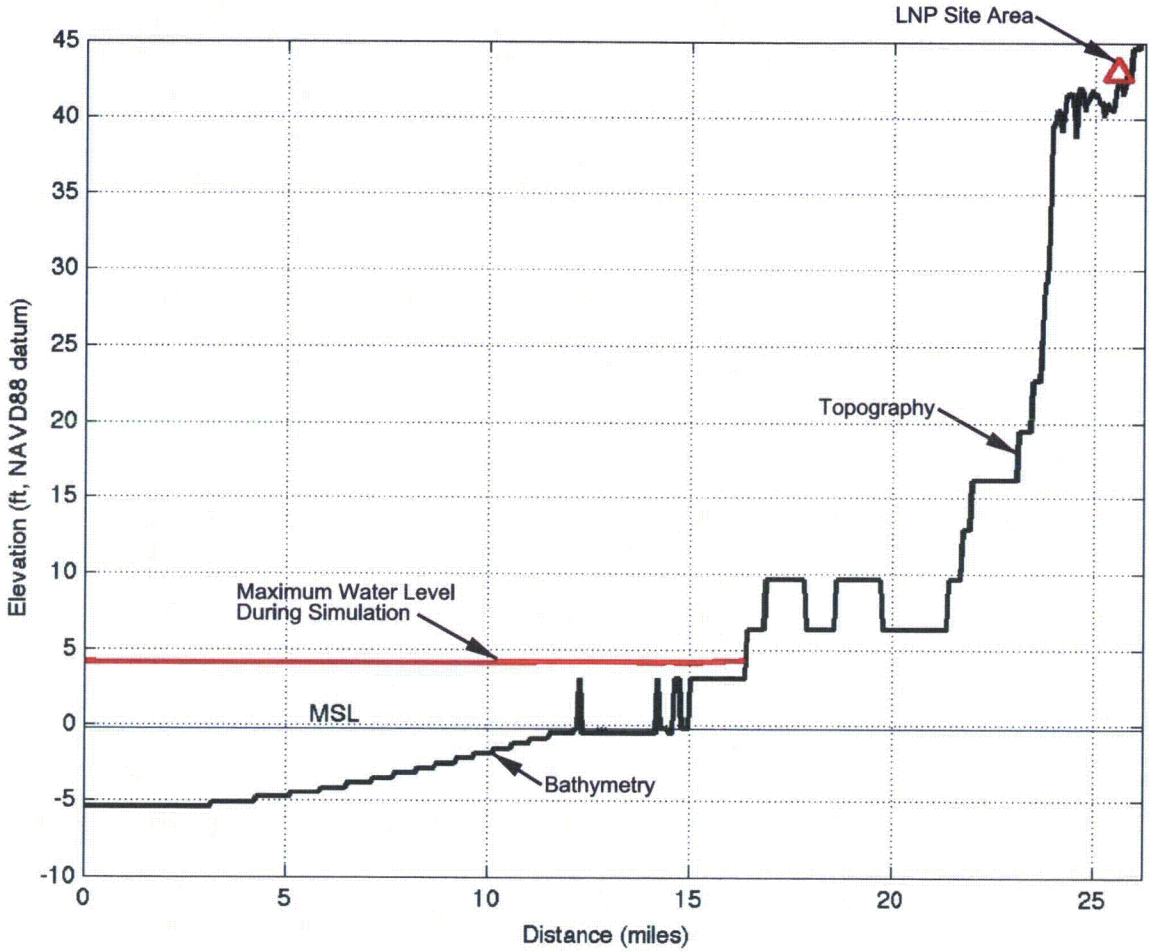

NOTE:
The existing grade elevation at the LNP site location is approximately 43 feet NAVD 88. The final grade elevation of LNP Units 1 & 2 will be raised to 50 feet NAVD 88.

Progress Energy Florida
Levy Nuclear Plant
Units 1 and 2
Part 2, Final Safety Analysis Report

Venezuela Seismic Event Simulation:
Profile at Latitude = 29.075 N

FIGURE 2.4.6-246 Rev 3

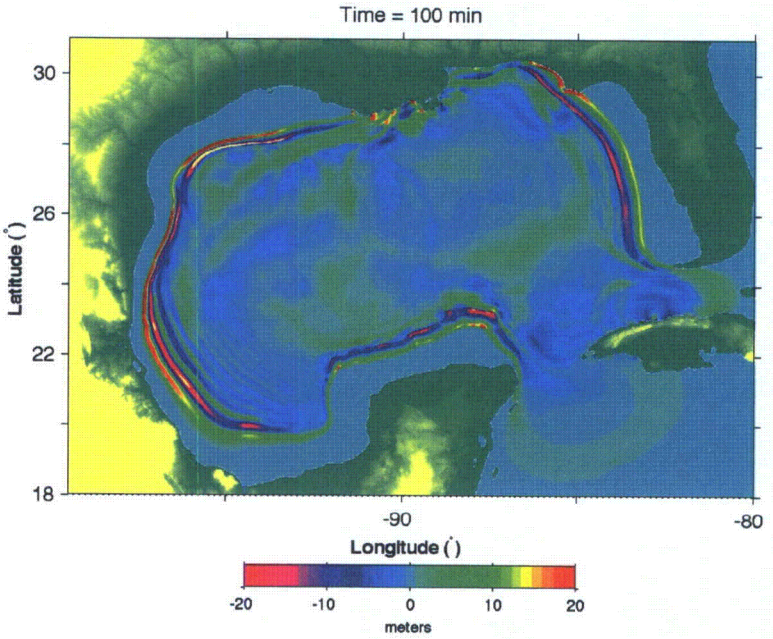

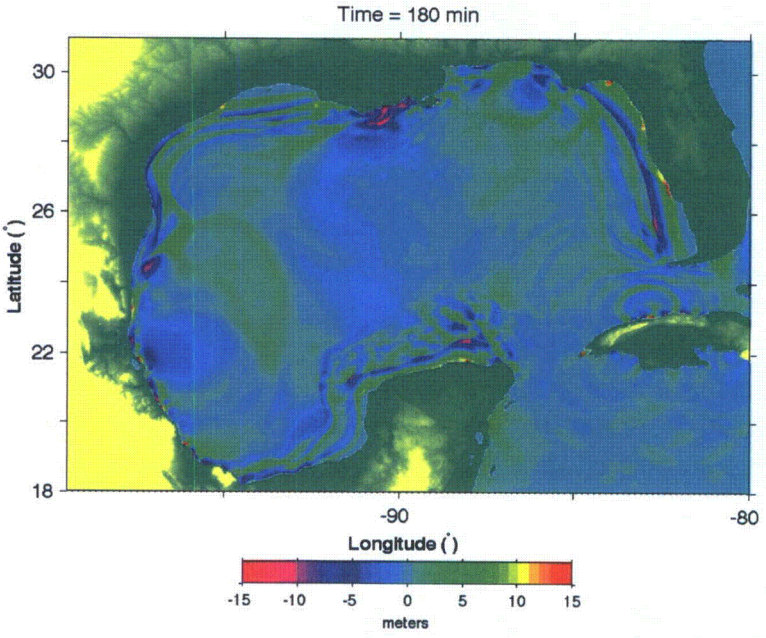

Progress Energy Florida
Levy Nuclear Plant
Units 1 and 2
Part 2, Final Safety Analysis Report

Mississippi Canyon Landslide Event Simulation,
Static Source:
Instantaneous Surface Displacement (Grid A_I)
at T = 100 min and T = 180 min
FIGURE 2.4.6-247 Rev 3

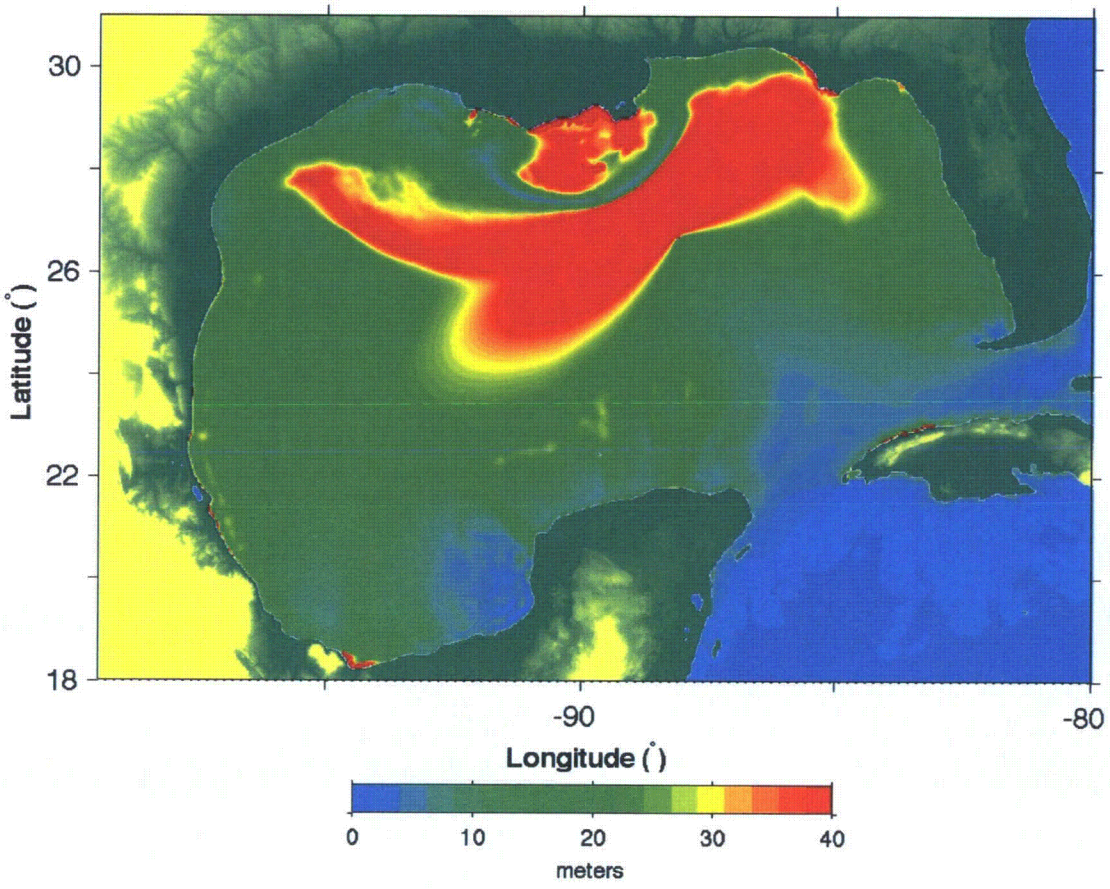

Progress Energy Florida
Levy Nuclear Plant
Units 1 and 2
Part 2, Final Safety Analysis Report

Mississippi Canyon Landslide Event Simulation, Static Source: Maximum Water Level Generated During Simulation (Grid A_l)

FIGURE 2.4.6-248 Rev 3

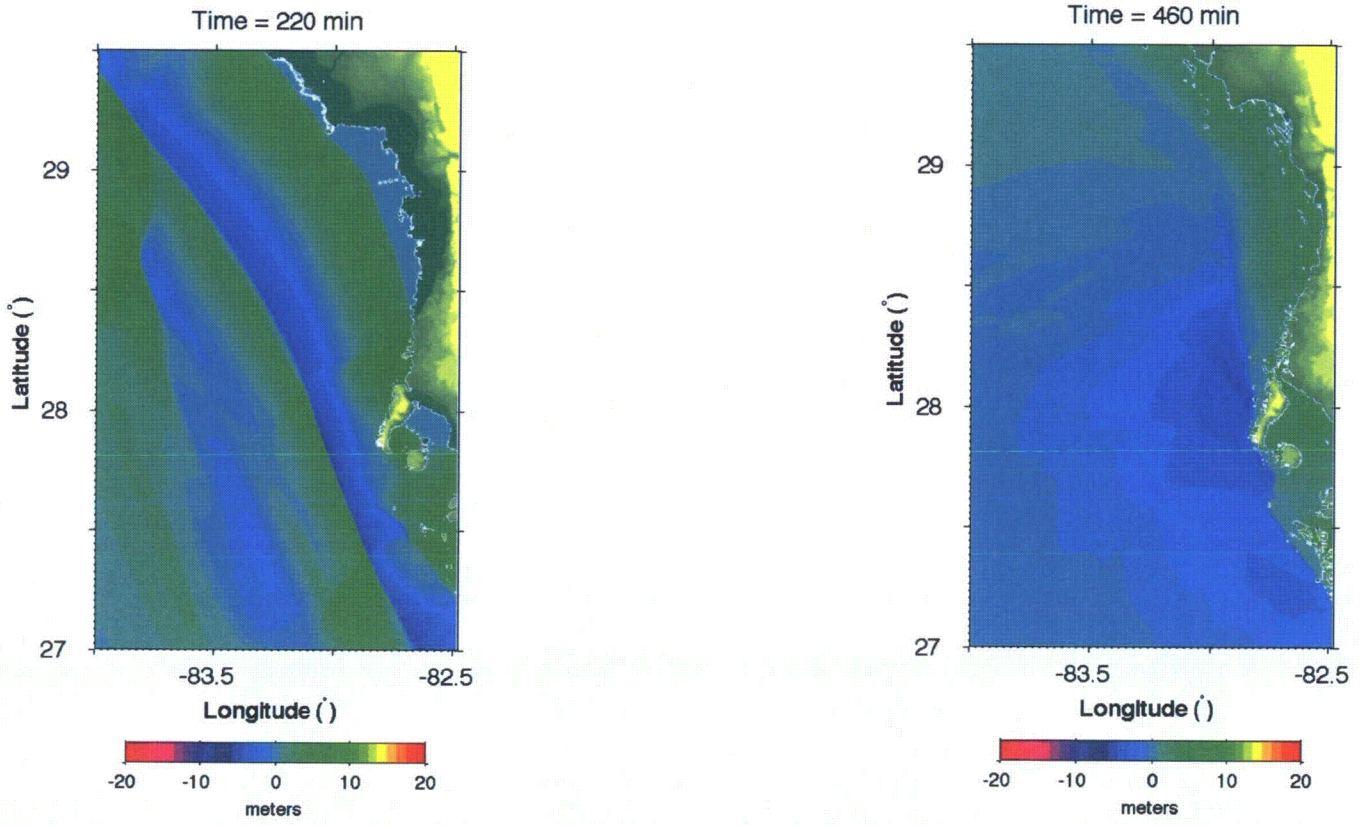

Progress Energy Florida
Levy Nuclear Plant
Units 1 and 2
Part 2, Final Safety Analysis Report

Mississippi Canyon Landslide Event Simulation,
Static Source:
Instantaneous Surface Displacement (Grid *B*)
at T = 220 min and T = 460 min
FIGURE 2.4.6-249 Rev 3

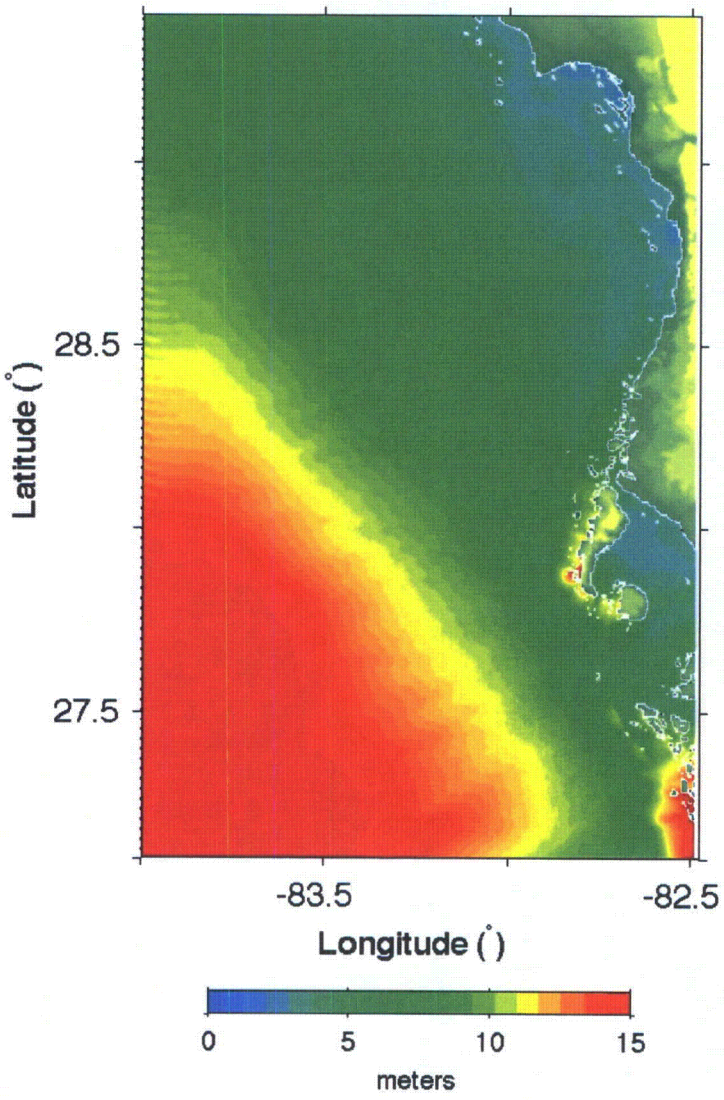

Progress Energy Florida
Levy Nuclear Plant
Units 1 and 2
Part 2, Final Safety Analysis Report

Mississippi Canyon Landslide Event Simulation,
Static Source: Maximum Water Level
Generated During Simulation (Grid *B*)

FIGURE 2.4.6-250 Rev 3

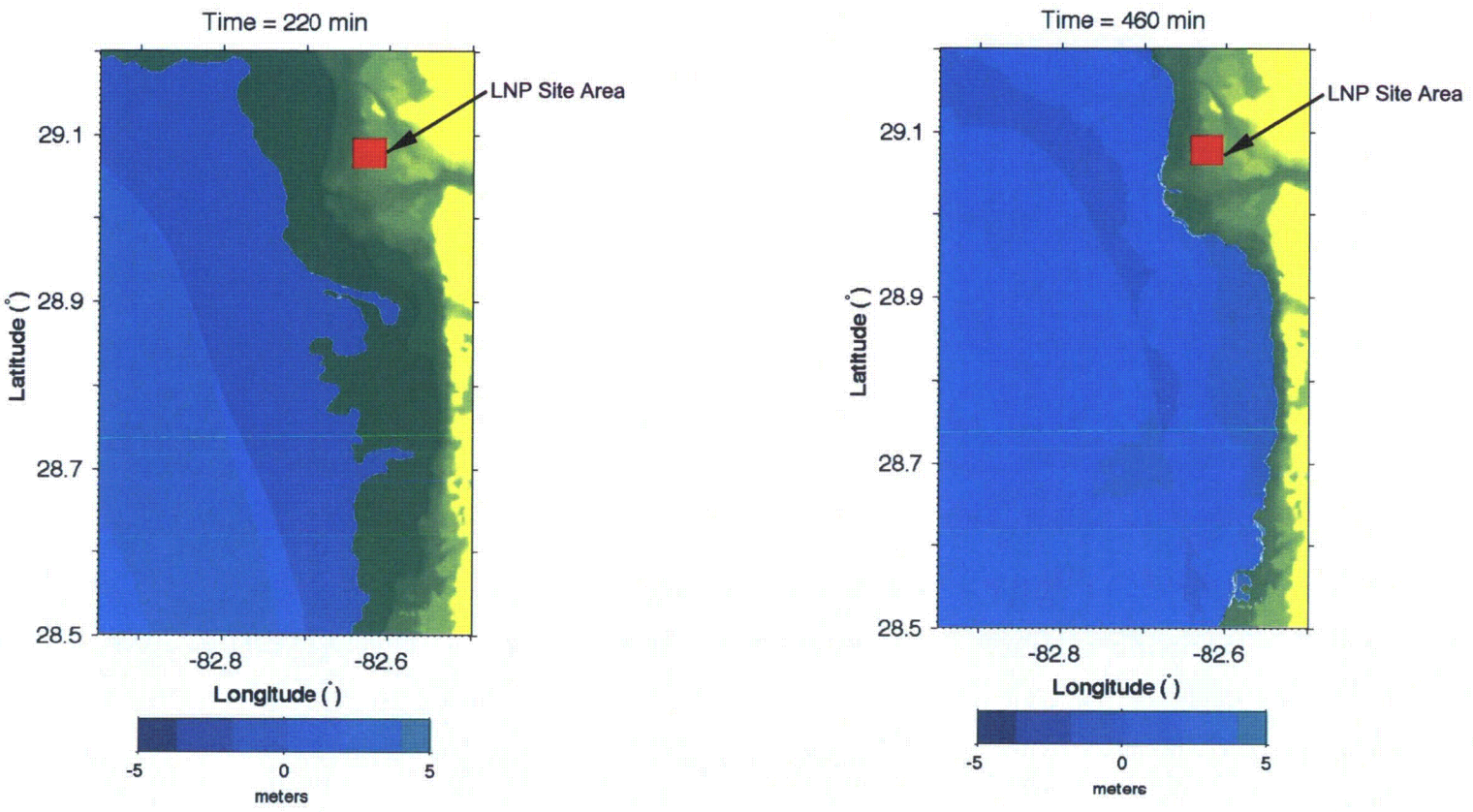

Progress Energy Florida
Levy Nuclear Plant
Units 1 and 2
Part 2, Final Safety Analysis Report

Mississippi Canyon Landslide Event Simulation,
Static Source:
Instantaneous Surface Displacement (Grid *C*)
at T = 220 min and T = 460 min
FIGURE 2.4.6-251 Rev 3

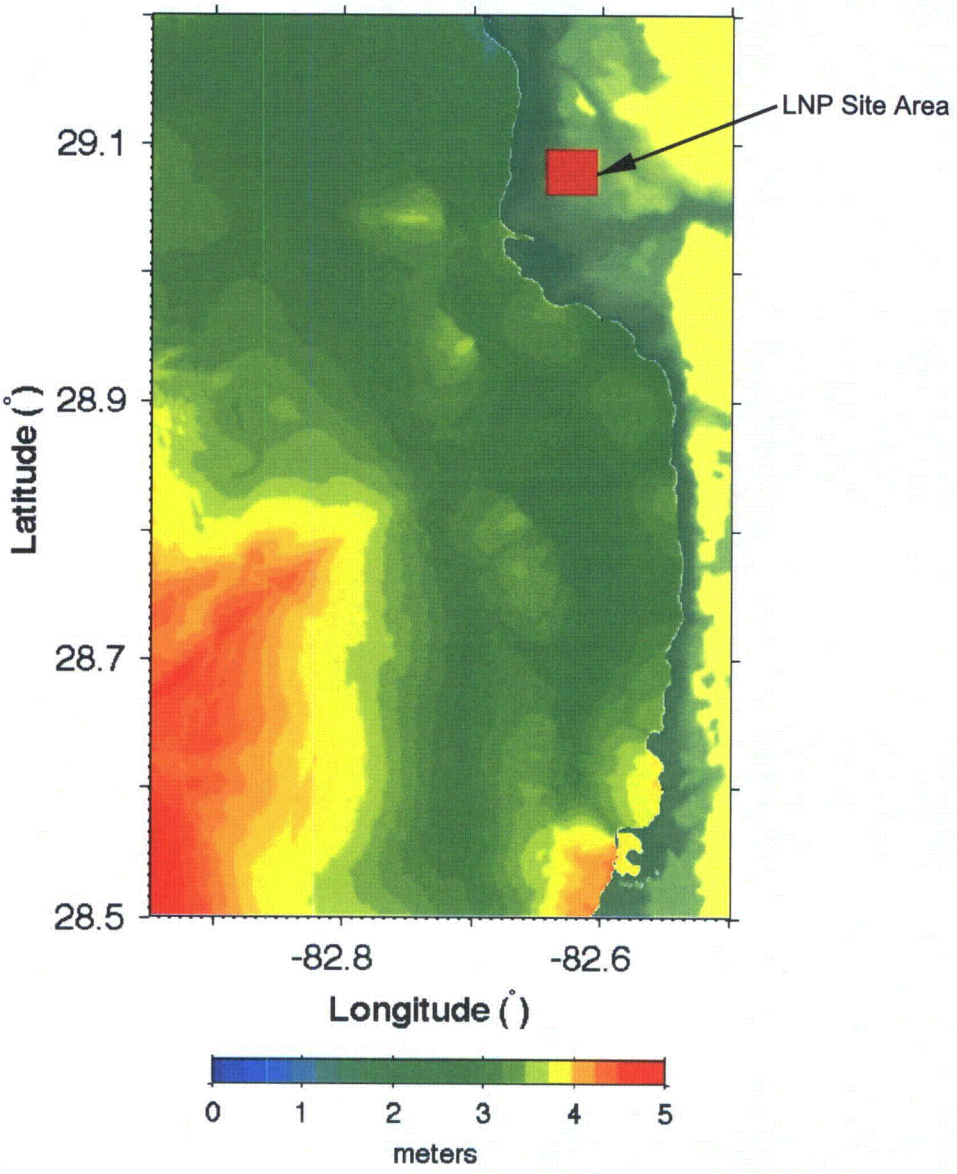

Progress Energy Florida
Levy Nuclear Plant
Units 1 and 2
Part 2, Final Safety Analysis Report

Mississippi Canyon Landslide Event Simulation,
Static Source: Maximum Water Level
Generated During Simulation (Grid *C*)

FIGURE 2.4.6-252 Rev 3

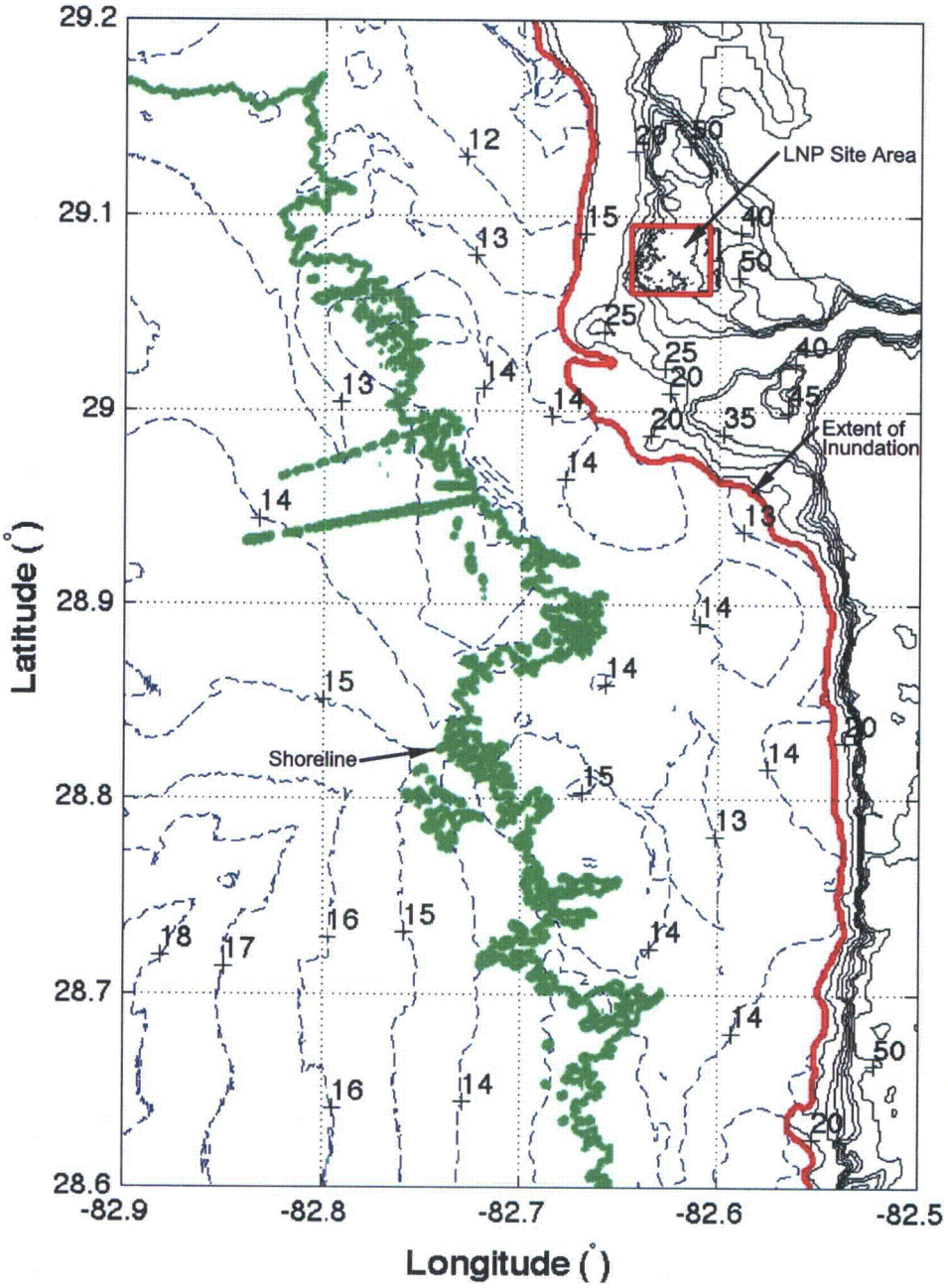

NOTE:
Contour elevations are given in feet NAVD 88.

Progress Energy Florida
Levy Nuclear Plant
Units 1 and 2
Part 2, Final Safety Analysis Report

Mississippi Canyon Landslide Event Simulation,
Static Source:
Maximum Extent of Inundation

FIGURE 2.4.6-253 Rev 3

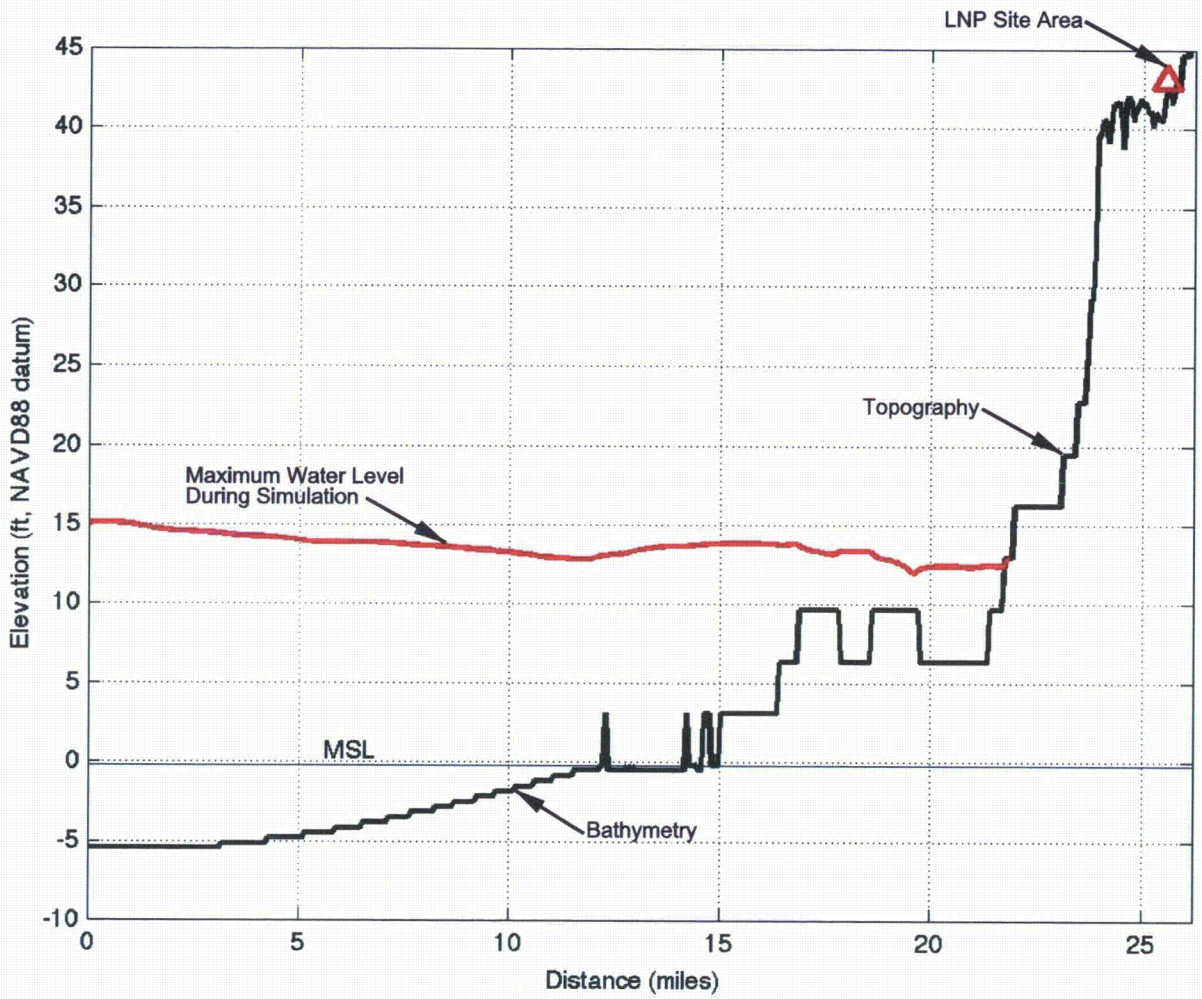

NOTE:
The existing grade elevation at the LNP site location is approximately 43 feet NAVD 88. The final grade elevation of LNP Units 1 & 2 will be raised to 50 feet NAVD 88.

Progress Energy Florida
Levy Nuclear Plant
Units 1 and 2
Part 2, Final Safety Analysis Report

Mississippi Canyon Landslide Event Simulation,
Static Source:
Profile at Latitude = 29.075 N

FIGURE 2.4.6-254 Rev 3

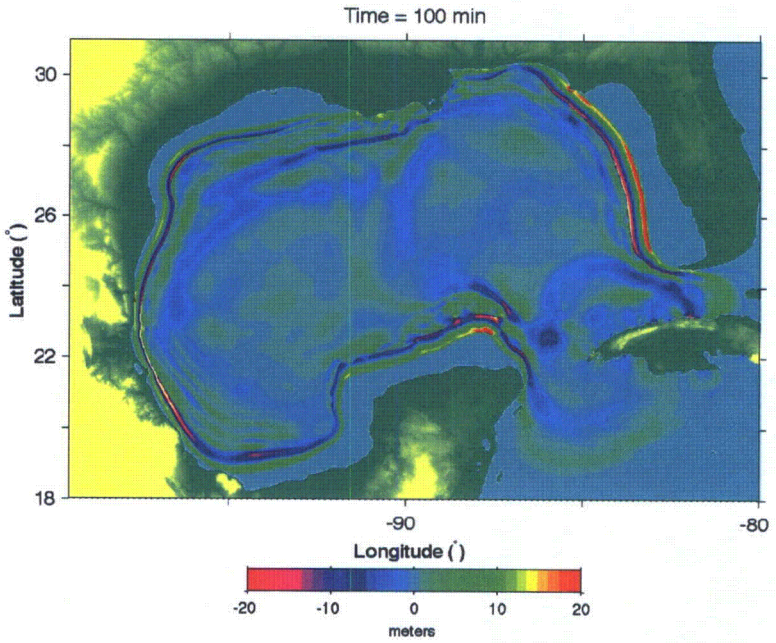

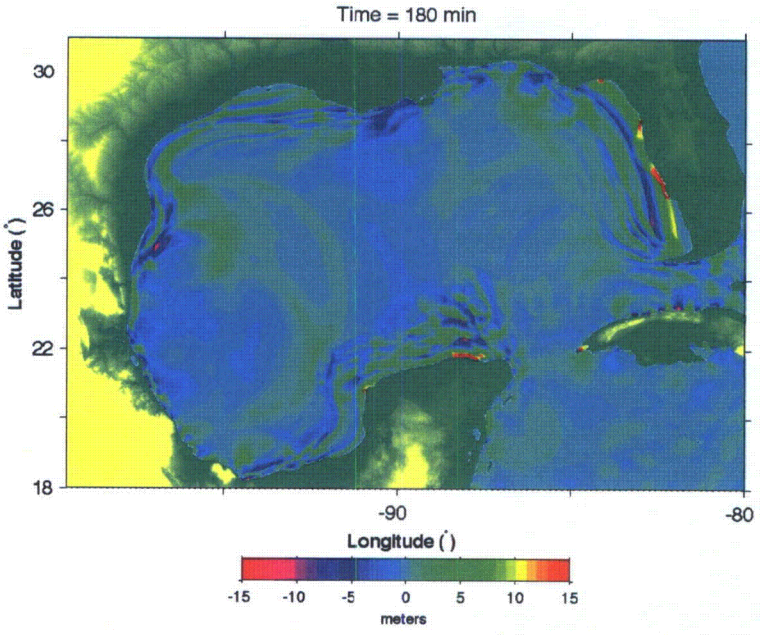

Progress Energy Florida
Levy Nuclear Plant
Units 1 and 2
Part 2, Final Safety Analysis Report

Mississippi Canyon Landslide Event Simulation,
Dynamic (NHWAVE) Source:
Instantaneous Surface Displacement (Grid A_l)
at T = 100 min and T = 180 min
FIGURE 2.4.6-255 Rev 3

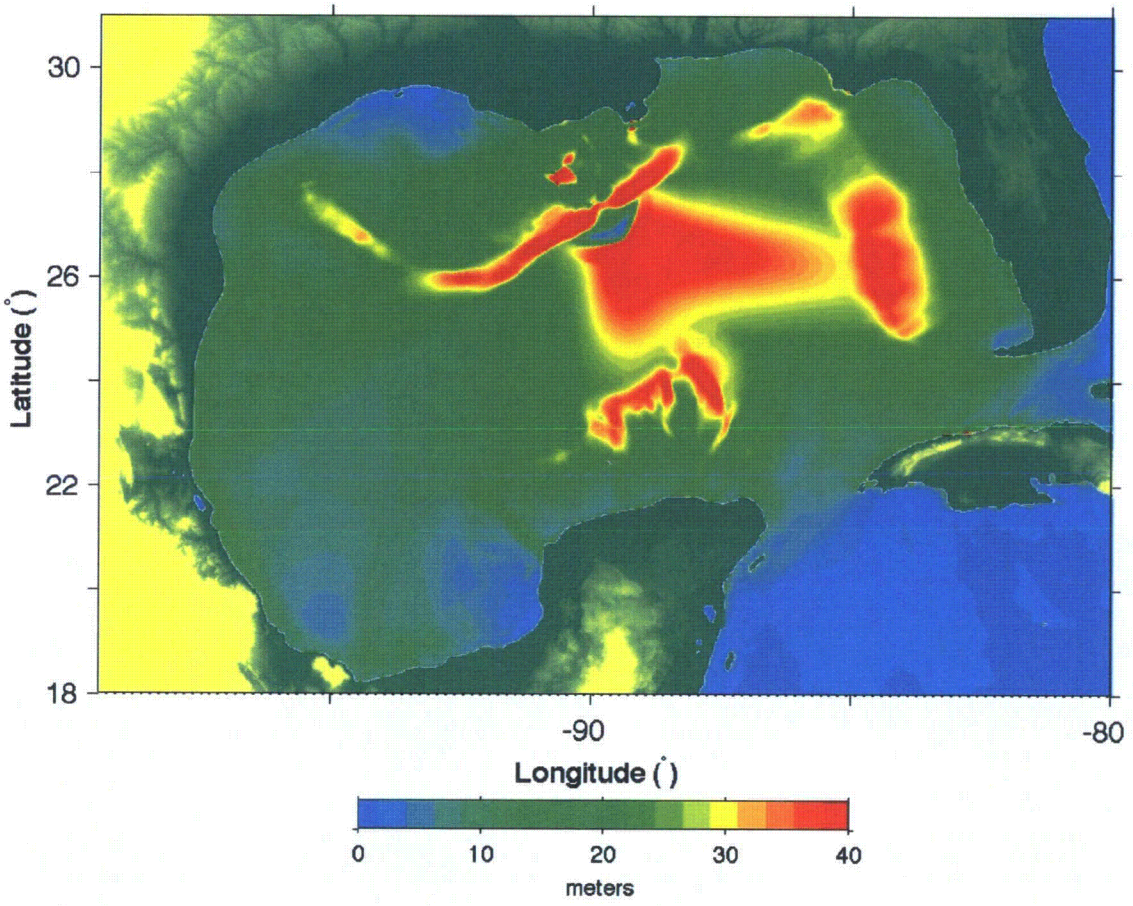

Progress Energy Florida
Levy Nuclear Plant
Units 1 and 2
Part 2, Final Safety Analysis Report

Mississippi Canyon Landslide Event Simulation,
Dynamic (NHWAVE) Source:
Maximum Water Level
Generated During Simulation (Grid A_I)
FIGURE 2.4.6-256 Rev 3

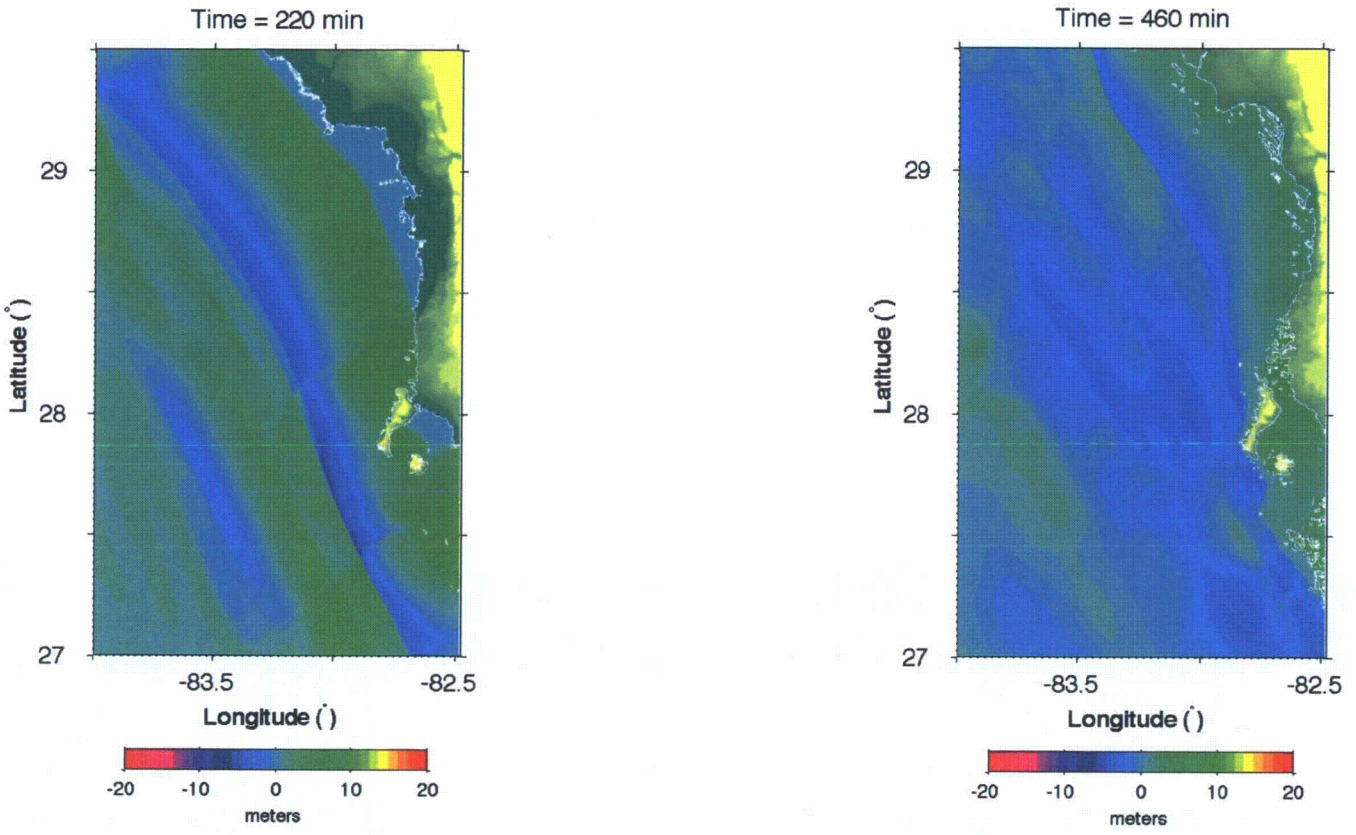

Progress Energy Florida
Levy Nuclear Plant
Units 1 and 2
Part 2, Final Safety Analysis Report

Mississippi Canyon Landslide Event Simulation,
Dynamic (NHWAVE) Source:
Instantaneous Surface Displacement (Grid *B*)
at T = 220 min and T = 460 min
FIGURE 2.4.6-257 Rev 3

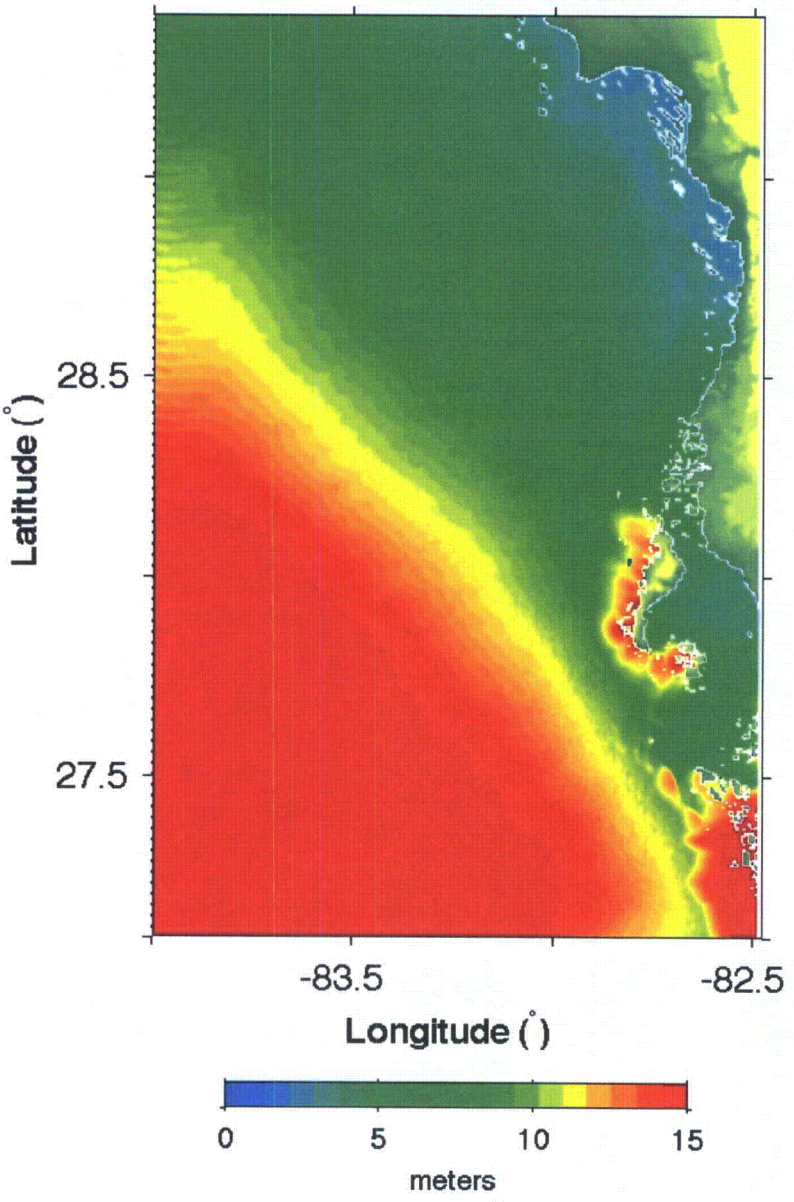

Progress Energy Florida
Levy Nuclear Plant
Units 1 and 2
Part 2, Final Safety Analysis Report

Mississippi Canyon Landslide Event Simulation,
Dynamic (NHWAVE) Source:
Maximum Water Level
Generated During Simulation (Grid *B*)
FIGURE 2.4.6-258 Rev 3

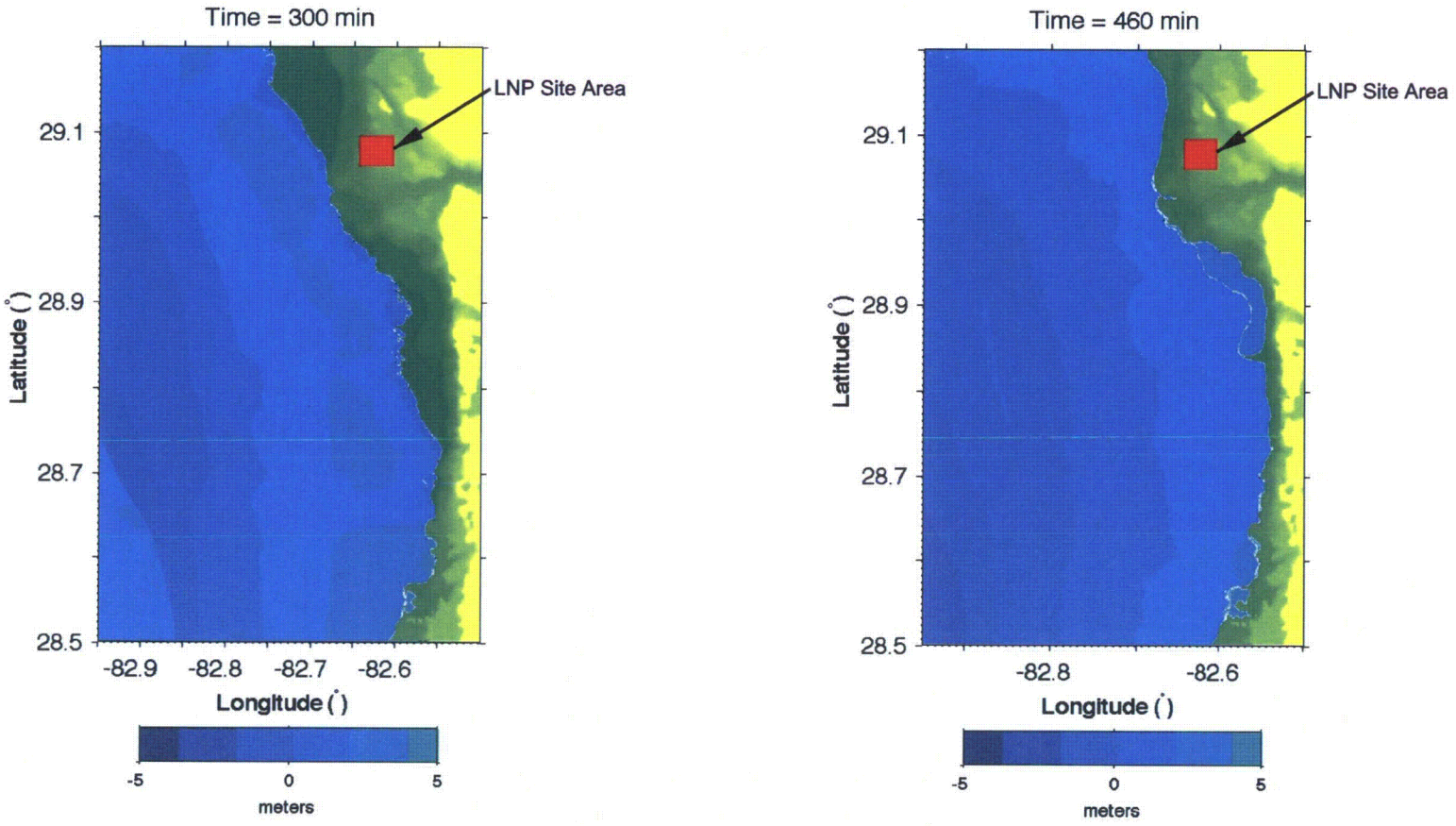

Progress Energy Florida
Levy Nuclear Plant
Units 1 and 2
Part 2, Final Safety Analysis Report

Mississippi Canyon Landslide Event Simulation,
Dynamic (NHWAVE) Source:
Instantaneous Surface Displacement (Grid C)
at T = 300 min and T = 460 min
FIGURE 2.4.6-259 Rev 3

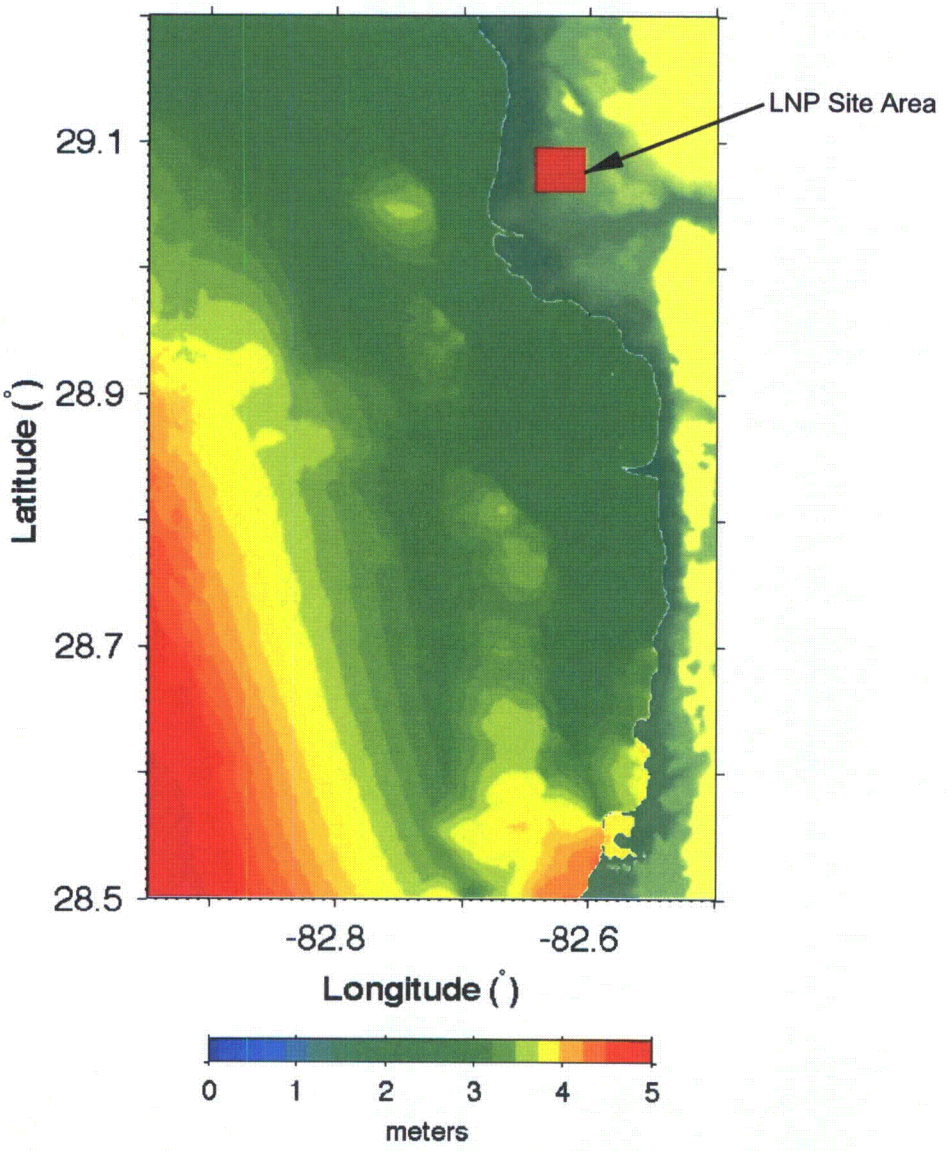

Progress Energy Florida
Levy Nuclear Plant
Units 1 and 2
Part 2, Final Safety Analysis Report

Mississippi Canyon Landslide Event Simulation,
Dynamic (NHWAVE) Source:
Maximum Water Level
Generated During Simulation (Grid C)
FIGURE 2.4.6-260 Rev 3

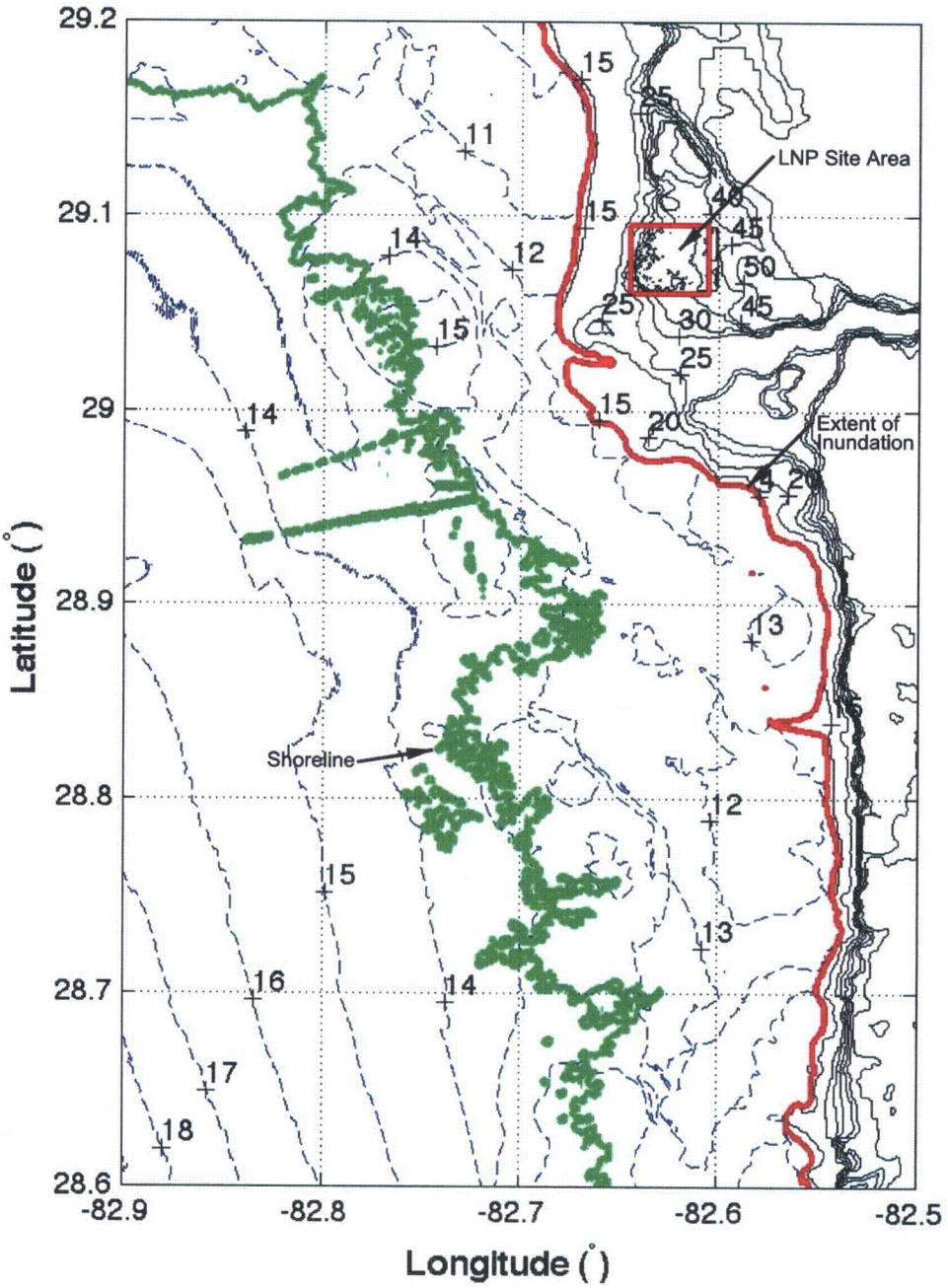

NOTE:
Contour elevations are given in feet NAVD 88.

Progress Energy Florida
Levy Nuclear Plant
Units 1 and 2
Part 2, Final Safety Analysis Report

Mississippi Canyon Landslide Event Simulation, Dynamic (NHWAVE) Source: Maximum Extent of Inundation

FIGURE 2.4.6-261 Rev 3

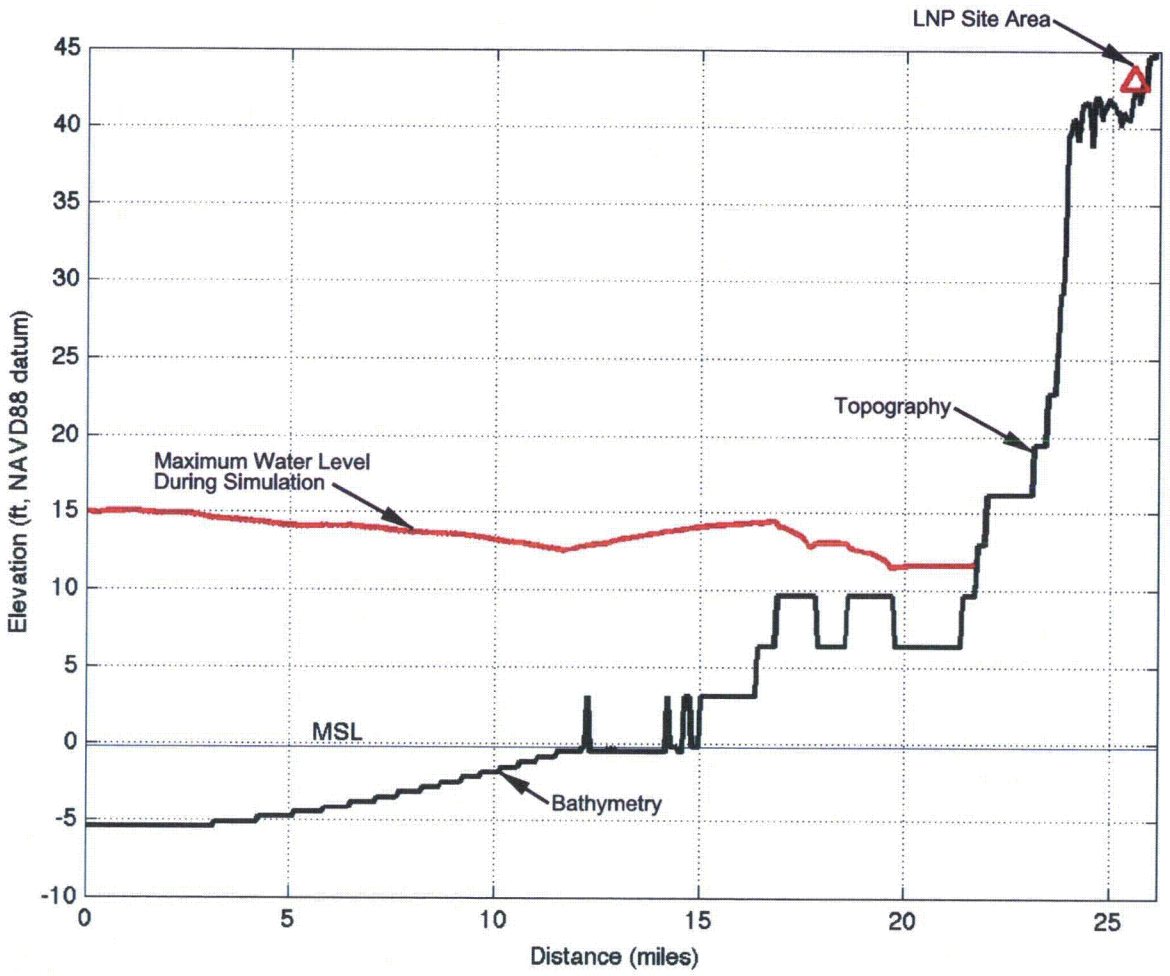

NOTE:
The existing grade elevation at the LNP site location is approximately 43 feet NAVD 88. The final grade elevation of LNP Units 1 & 2 will be raised to 50 feet NAVD 88.

Progress Energy Florida
Levy Nuclear Plant
Units 1 and 2
Part 2, Final Safety Analysis Report

Mississippi Canyon Landslide Event Simulation,
Dynamic (NHWAVE) Source:
Profile at Latitude = 29.075 N

FIGURE 2.4.6-262 Rev 3

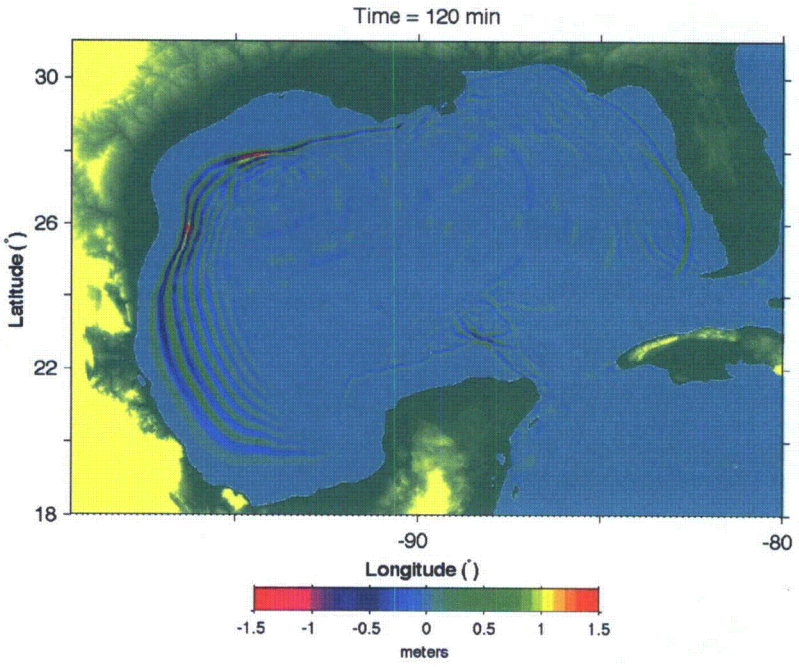

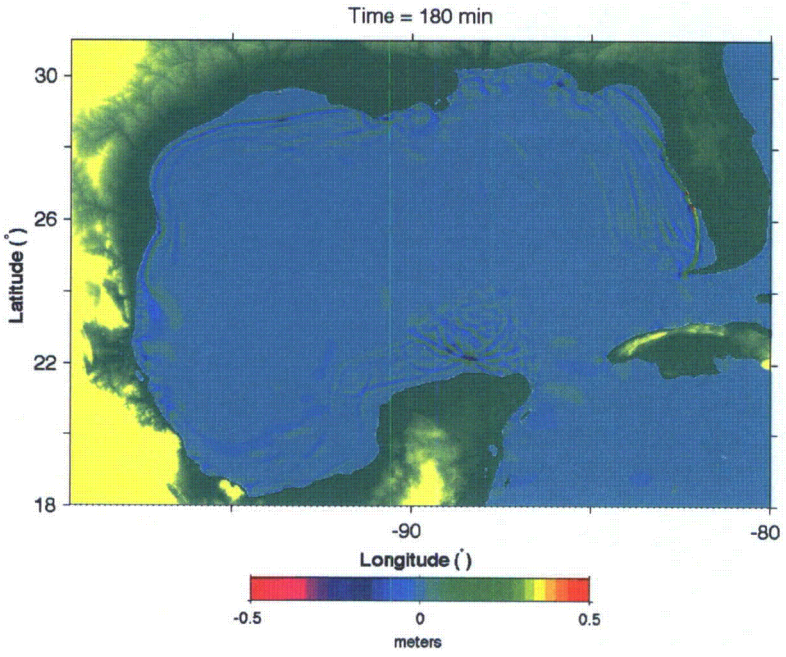

Progress Energy Florida
Levy Nuclear Plant
Units 1 and 2
Part 2, Final Safety Analysis Report

Florida Escarpment Landslide Event Simulation,
Static Source:
Instantaneous Surface Displacement (Grid A_i)
at T = 120 min and T = 180 min
FIGURE 2.4.6-263 Rev 3

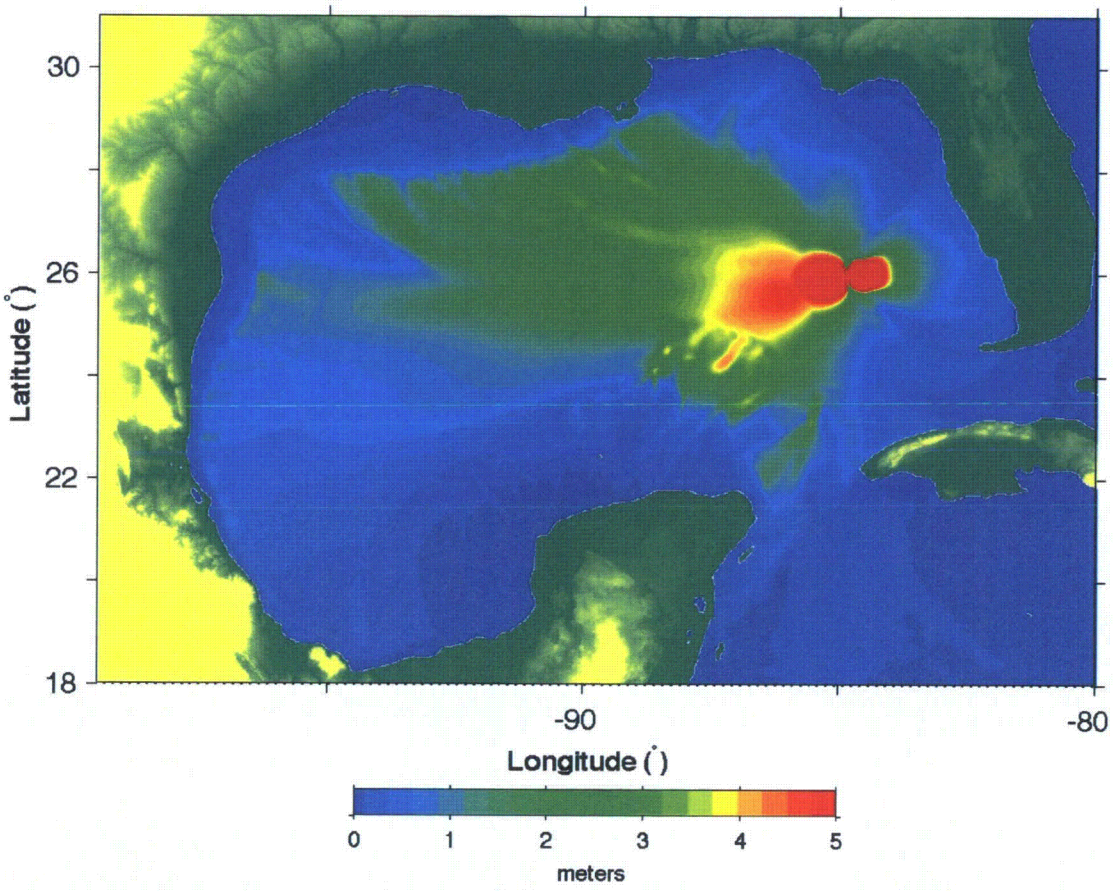

Progress Energy Florida
Levy Nuclear Plant
Units 1 and 2
Part 2, Final Safety Analysis Report

Florida Escarpment Landslide Event Simulation,
Static Source: Maximum Water Level
Generated During Simulation (Grid A_l)

FIGURE 2.4.6-264 Rev 3

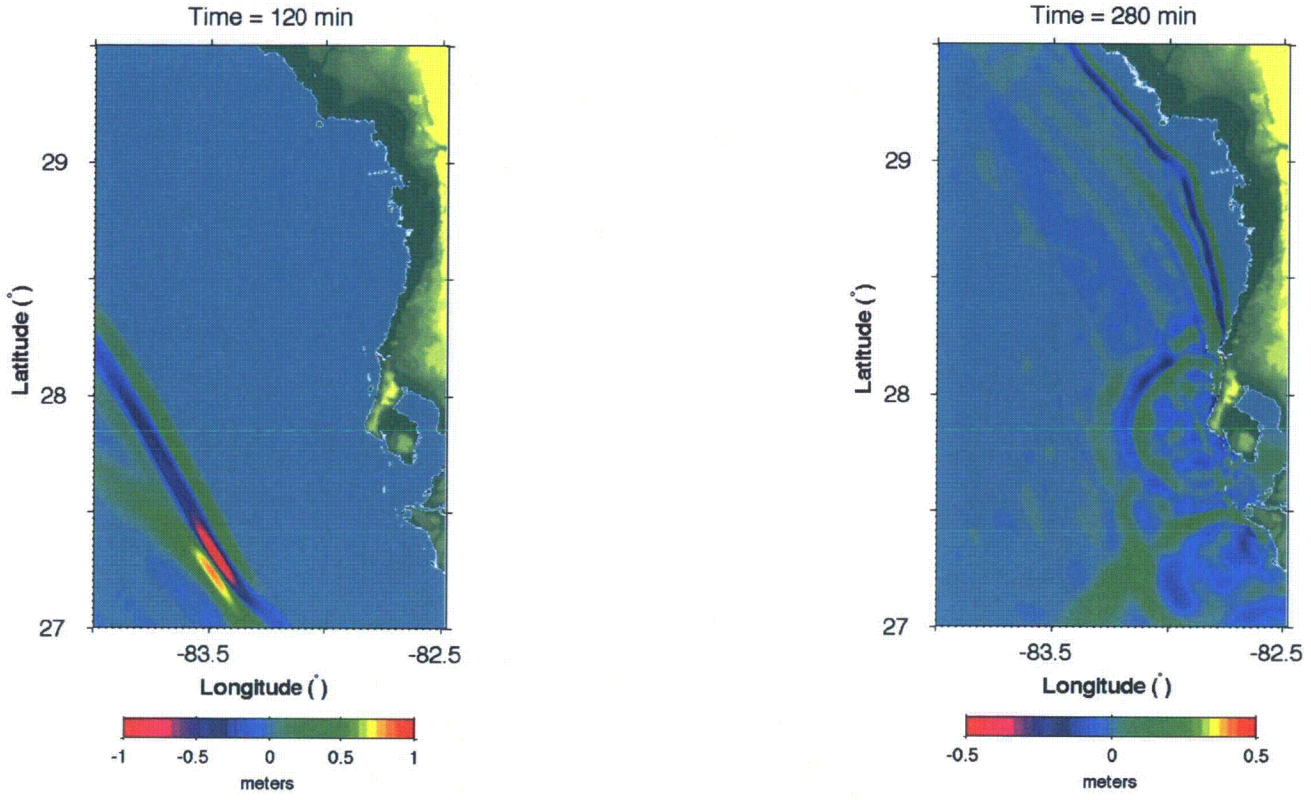

Progress Energy Florida
Levy Nuclear Plant
Units 1 and 2
Part 2, Final Safety Analysis Report

Florida Escarpment Landslide Event Simulation,
Static Source:
Instantaneous Surface Displacement (Grid *B*)
at T = 120 min and T = 280 min
FIGURE 2.4.6-265 Rev 3

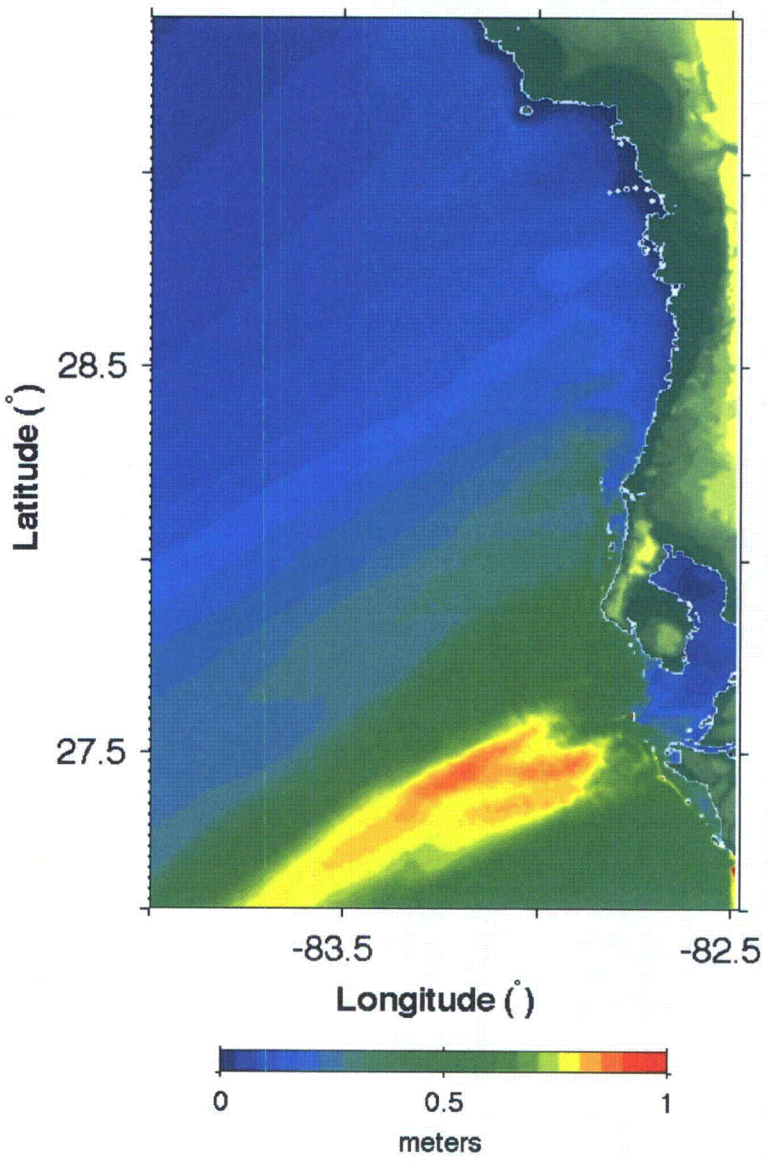

Progress Energy Florida
Levy Nuclear Plant
Units 1 and 2
Part 2, Final Safety Analysis Report

Florida Escarpment Landslide Event Simulation,
Static Source: Maximum Water Level
Generated During Simulation (Grid *B*)

FIGURE 2.4.6-266 Rev 3

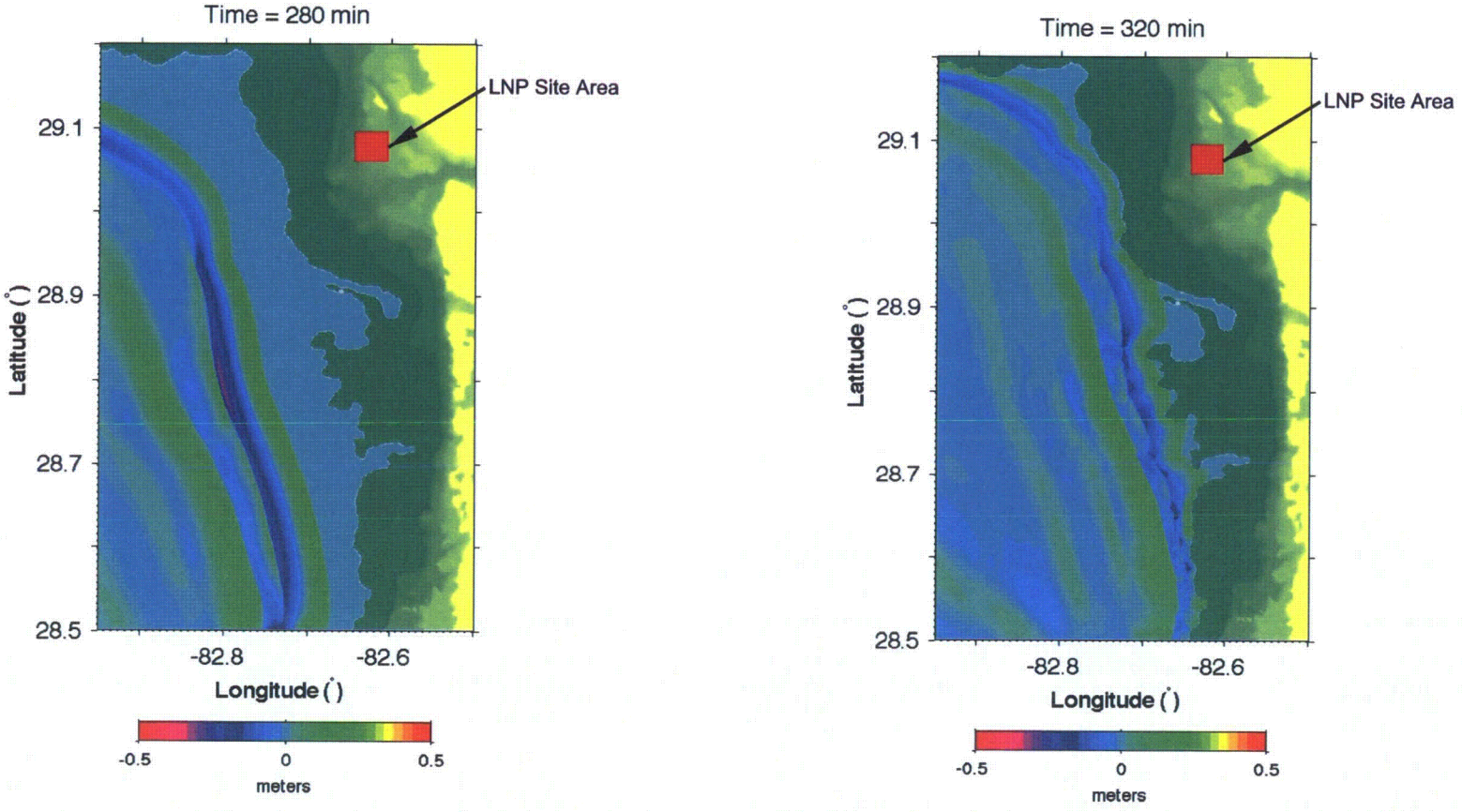

Progress Energy Florida
Levy Nuclear Plant
Units 1 and 2
Part 2, Final Safety Analysis Report

Florida Escarpment Landslide Event Simulation,
Static Source:
Instantaneous Surface Displacement (Grid *C*)
at T = 280 min and T = 320 min
FIGURE 2.4.6-267 Rev 3

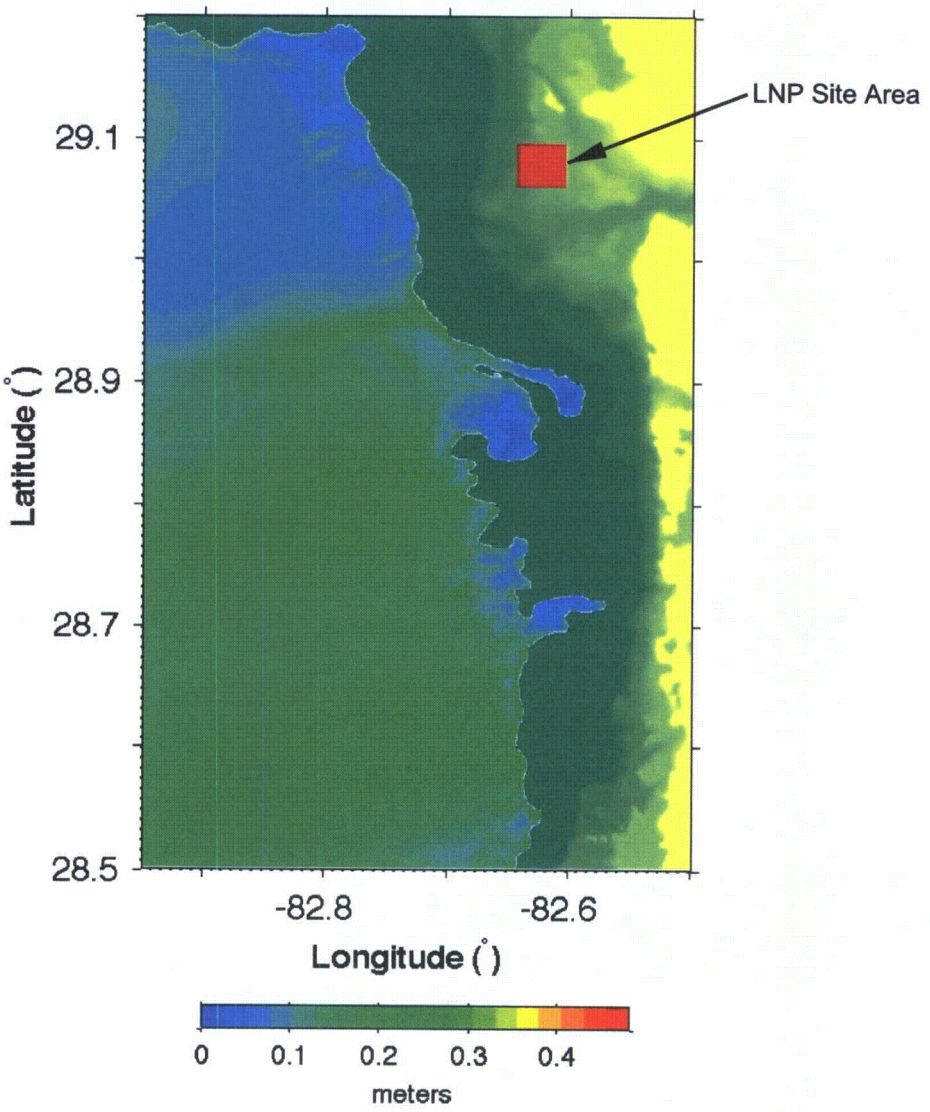

Progress Energy Florida
Levy Nuclear Plant
Units 1 and 2
Part 2, Final Safety Analysis Report

Florida Escarpment Landslide Event Simulation,
Static Source: Maximum Water Level
Generated During Simulation (Grid *C*)

FIGURE 2.4.6-268 Rev 3

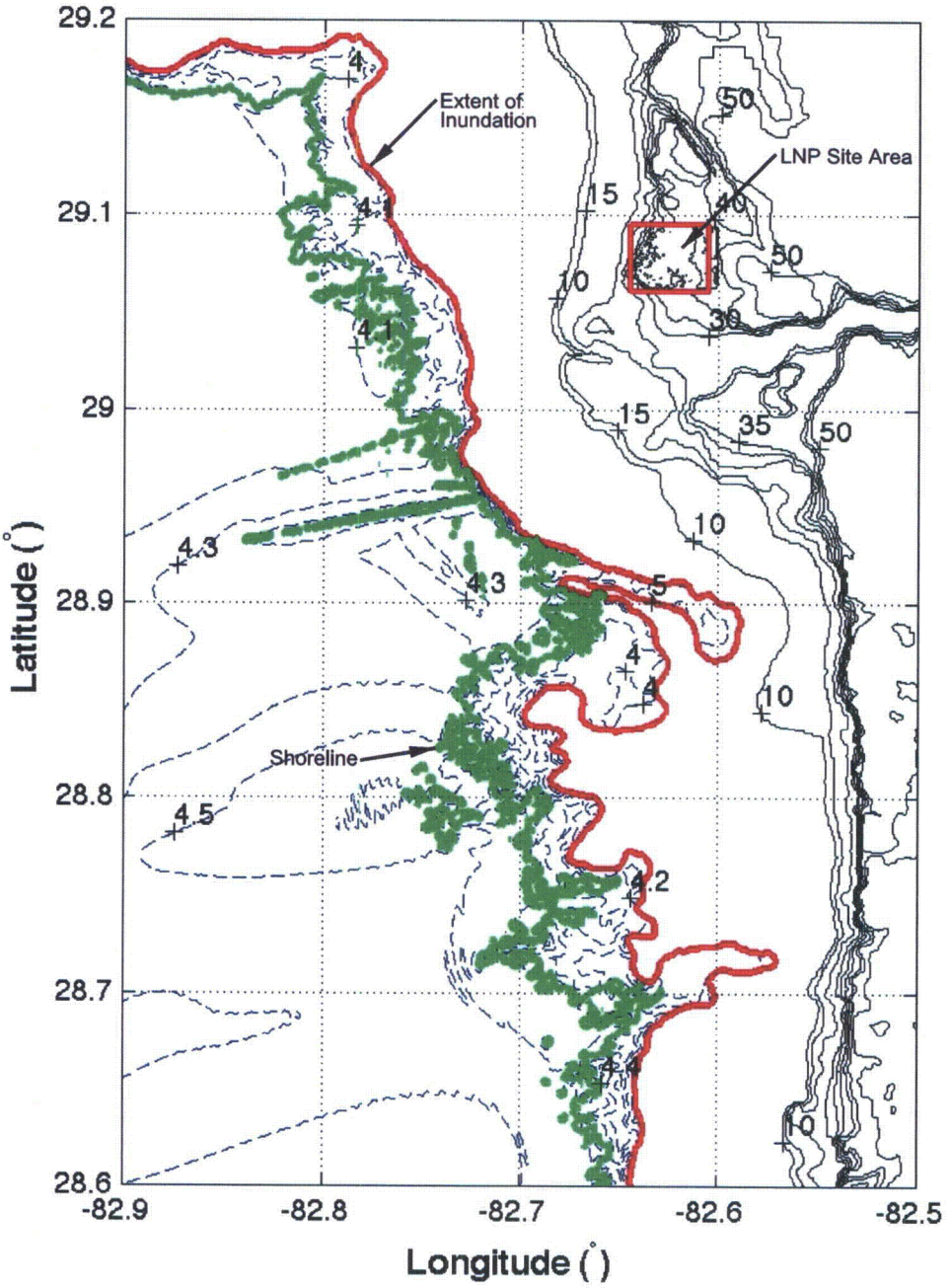

NOTE:
Contour elevations are given in feet NAVD 88.

Progress Energy Florida
Levy Nuclear Plant
Units 1 and 2
Part 2, Final Safety Analysis Report

Florida Escarpment Landslide Event Simulation,
Static Source:
Maximum Extent of Inundation

FIGURE 2.4.6-269 Rev 3

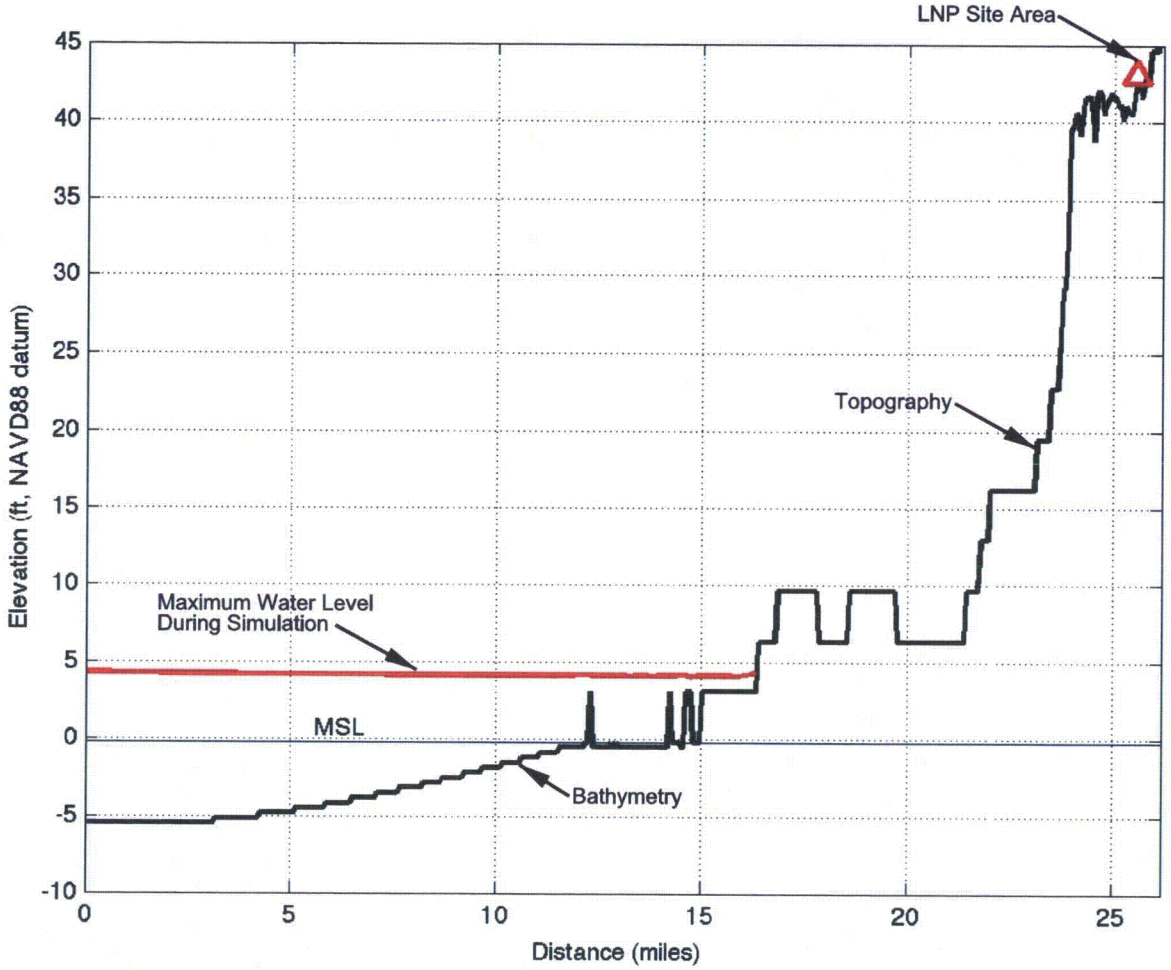

NOTE:
The existing grade elevation at the LNP site location is approximately 43 feet NAVD 88. The final grade elevation of LNP Units 1 & 2 will be raised to 50 feet NAVD 88.

Progress Energy Florida
Levy Nuclear Plant
Units 1 and 2
Part 2, Final Safety Analysis Report

Florida Escarpment Landslide Event Simulation,
Static Source:
Profile at Latitude = 29.075 N

FIGURE 2.4.6-270 Rev 3

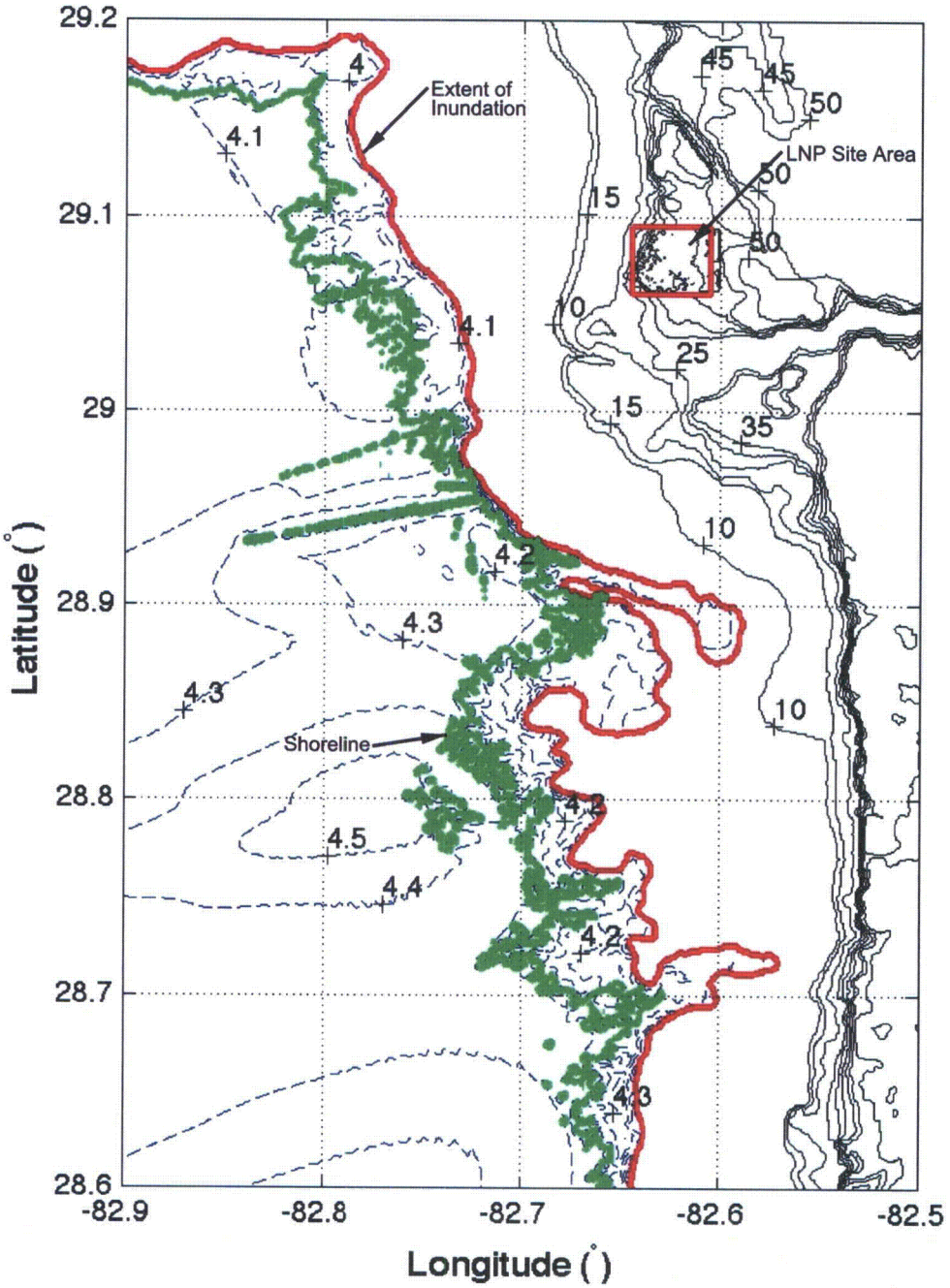

NOTE:
Contour elevations are given in feet NAVD 88.

Progress Energy Florida
Levy Nuclear Plant
Units 1 and 2
Part 2, Final Safety Analysis Report

Florida Escarpment Landslide Event Simulation, Dynamic (NHWAVE) Source: Maximum Extent of Inundation

FIGURE 2.4.6-271 Rev 3

Appendix 1

Verification and Validation Document

1. **FUNWAVE-TVD Version 1.0**
2. **NHWAVE Version 1.0**
3. **Bathymetry/Topography**
4. **NHWAVE Output and FUNWAVE-TVD Input**
5. **Datum Conversion**
6. **FUNWAVE-TVD Operation Structure and Result Backup Directory Listing**
7. **NHWAVE Operation Structure and Result Backup Directory Listing**
8. **Calculation of Earthquake Magnitude**
9. **Post Processing of the Results**

Table of Contents

#	Section	Page No.
1	Purpose and Scope	3
2	Assumptions	4
3	Methodology	4
4	Results	6
5	Conclusions	12
6	References	12
	Attachments	No of Pages
A	Results of FUNWAVE-TVD verification (Purpose A)	4
B	Results of NHWAVE verification (Purpose B)	2
C	Results of verification of bathymetry/topography files (Purpose C)	6
D	Results from verification of FUNWAVE-TVD input files from NHWAVE outputs (Purpose D)	2
E	Results from verification of datum conversions (Purpose E)	2
F	Backup of FUNWAVE-TVD Directory Listing (Purpose F)	1
G	Backup of NHWAVE Directory Listing (Purpose G)	1
H	Program for Calculation of Earthquake Magnitude (Purpose H)	1
I	Verification of Post Processing of FUNWAVE-TVD and NHWAVE (Purpose I)	1
J	DVD for Files (READ ME file Attached) :	5 and DVD
	-FUNWAVE Version 1.0	
	-NHWAVE Version 1.0	
	-Bathymetric, and Topographic Data files	
	- Grid Generation Programs	
	-Post processing MATLAB programs	
K	Reference 5	55
L	Reference 6	58
M	Reference 7	56
N	Reference 8	59
O	Reference 9	41
P	Reference 4	27
	Total Pages	334

1. Purpose and Scope

Purpose of this document is to present Verification & Validation (V&V) of computer programs and input data used for calculation of Probable Maximum Tsunami (PMT) Flood Level at LNP Site. Verification & Validation was performed for followings:

- **Purpose A:** Verify that the Boussinesq wave model FUNWAVE-TVD Version 1.0, developed by Shi et al (Reference 6 and 7) and Kirby et al (Reference 4) at the Center for Applied Coastal Research, University of Delaware and used for the present study, has been validated as an accurate predictor of tsunami runup.
- **Purpose B:** Verify that the surface and terrain following, 3-D Navier-Stokes solver NHWAVE Version 1.0, developed by Ma et al (Reference 5) at the Center for Applied Coastal Research, University of Delaware and used for the present study, has been validated for basic performance and as a means for computing initial surface displacement and velocity field generated by a submarine mass displacement (SMD).
- **Purpose C:** Verify the bathymetry/topography files used as input in FUNWAVE-TVD/NHWAVE.
- **Purpose D:** Verify FUNWAVE-TVD input files of surface displacement and velocity field calculated by NHWAVE.
- **Purpose E:** Verify the conversion between NAD 83 and Longitude/Latitude, and NAVD 88 and MSL.
- **Purpose F:** Backup of FUNWAVE-TVD simulations on the Linux cluster DARKSTAR – Directory Listing
- **Purpose G:** Backup of NHWAVE simulations on the Linux cluster DARKSTAR – Directory Listing
- **Purpose H**: Verify the calculation of earthquake magnitude in the Venezuela
- **Purpose I**: Verify Post-processing of the Results

The scope of this document is to describe the methodology used to accomplish each of the nine purposes and describe the corresponding results and conclusions. The tools required to achieve the seven purposes are:

- **FUNWAVE-TVD v1.0:** FUNWAVE-TVD Version 1.0 is developed by Shi et al (Reference 6 and 7) and Kirby et al (Reference 4) at the Center for Applied Coastal Research, University of Delaware. Version 1.0 is under version control (file://birdsong.coastal.udel.edu/usr/local/funwave_tvd/version1.0) and has been validated against NTHMP-approved benchmarks (Reference 8). All benchmarks were performed using the Linux cluster called DARKSTAR located in the University of Delaware. DARKSTAR is used for the present study (http://darkstar.coastal.udel.edu/gridengine.php).

- **NHWAVE v1.0:** NHWAVE Version 1.0 is developed by Ma et al (Reference 5) at the Center for Applied Coastal Research, University of Delaware. It has been benchmarked against NTHMP-approved benchmark (Reference 8). The benchmark test was performed using the Linux cluster DARKSTAR, the same computer as used by FUNWAVE-TVD. No data transfer is needed between different machines during the present study.
- **MATLAB 7.11.0.584 (R2010b):** Matlab R2010b is provided by University of Delaware. The MATLAB program was performed on **DARKSTAR.** MATLAB (matrix laboratory) is a numerical computing environment and fourth-generation programming language. Developed by MathWorks, MATLAB allows matrix manipulations, plotting of functions and data, implementation of algorithms, creation of user interfaces.

2. Assumptions

No assumptions were made.

3. Methodology

All validation benchmarking discussed in this document were performed using the Linux cluster called DARKSTAR located in the University of Delaware. DARKSTAR is used for the present study (http://darkstar.coastal.udel.edu/ganglia). Description of hardware and operating system is provided in the main calculation document.

3.1 Purpose A: FUNWAVE-TVD Validation

FUNWAVE-TVD code may be run in either Cartesian coordinates (for use in small geographic areas) or spherical polar (latitude-longitude) coordinates (for use in large geographic area), or use at ocean basin scales down to smaller scales. The Cartesian version of FUNWAVE-TVD has been fully benchmarked against National Tsunami Hazard Mitigation Program (NTHMP)-approved benchmarks (Reference 8) and results are available in (Reference 9). A similar benchmark result for the spherical polar coordinates form of the code, which is used for computation of PMT flood level at LNP Site, is presented in the results section.

FUNWAVE-TVD as utilized here implements one feature not described in the manual for Version 1.0 (Reference 7): one-way nesting of grids to obtain higher resolution at landfall in the vicinity of the target site of interest. The procedure for doing the nested calculation is described in the Main Calculation Document (section 5.2). This appendix provides an example calculation indicating that a solitary wave of permanent form is undistorted as it moves from larger down to smaller scale grids.

3.2 Purpose B: NHWAVE Validation

NHWAVE model uses terrain following coordinates and can simulate an underwater landslide using a time-varying bottom boundary condition. The model validation against the underwater landslide experiments performed by Enet and Grilli (Reference 3) in a 3.7 m wide, 1.8 m deep and 30 m long wave tank with a plane underwater slope with 15 degrees angle is demonstrated in this document. The laboratory experiments by Enet and Grilli (Reference 3) have been included in NTHMP standard benchmark tests for submarine landslides.

3.3 Purpose C: Verify the bathymetry/topography files

Direct comparisons between bathymetry data in model grid files and the data downloaded from ETOPO 1 (Reference 1), CRM (Reference 2) and site measurement data. Direct comparison was performed using MATLAB R2010B tool.

3.4 Purpose D: Verify FUNWAVE-TVD input files from NHWAVE outputs

Direct comparisons between output file of NHWAVE and input file of FUNWAVE-TVD. The comparisons were performed using the MATLAB program are described in the result section and Attachment D.

3.5 Purpose E: Verify datum conversions

Datum conversions are performed using available information and data.

Horizontal datum conversion from Florida State Plane Coordinates, West Zone, NAD 83 to global Latitude/Longitude coordinates was performed using the Earth Point tool available on the Web site www.earthpoint.us. (Reference11). The vertical datum conversion was performed using the elevation of Cedar Key, FL, Station ID 8727520 based on different datum obtained from National Oceanic and Atmospheric Administration (NOAA)'s web site (Reference 12)

3.6 Purpose F: Backup of FUNWAVE-TVD on the Linux cluster DARKSTAR

Create a backup of the FUNWAVE-TVD program and results. Complete directory listing including sub directories is provided in Attachment F

3.7 Purpose G: Backup of NHWAVE on the Linux cluster DARKSTAR

Create a backup of the NHWAVE program and results. Complete directory listing including sub directories is provided in Attachment G

3.8 Purpose H: Verify calculation of earthquake magnitude

Use source parameters in the Reference 13 to validate the calculation of earthquake magnitude.

3.9 Purpose I: Post processing of the Results

Use approximate comparisons between output values and values scaled in plotted figures to verify that programs used for post-processing produce plots reflecting computational results.

4. Results

4.1 Purpose A: FUNWAVE-TVD Validation

A benchmark test of solitary wave a composite beach was carried out using the spherical version of FUNWAVE-TVD. The physical experiment of this benchmark was conducted at the Coastal Engineering Laboratory of U.S. Army Corps of Engineering, Vicksburg, Mississippi facility. Details of the benchmark are described in Section 3.2 of Appendix A of Reference 8. The laboratory prototype was scaled up 100 times in order to avoid computational truncation errors due to small grid spacing in the spherical coordinates. The coordinate origin was specified at (0.0E, 0.0 N). Figure A-1 (Attachment A) shows model/data comparisons of surface elevation time series at 7 measurement gauges in which red lines represent numerical results and blue lines are measured data. Figure A-2 (Attachment A) shows the same comparison from the Cartesian version of FUNWAVE-TVD (Figure 13 in Reference 9). The comparison between Figure A-1 and A-2 indicates that the spherical version of FUNWAVE-TVD can predict wave propagation and breaking as accurately as the Cartesian version. A benchmark test of solitary wave on a simple beach was also conducted using the spherical FUNWAVE-TVD. The model setup was based on the NTHMP requirement (Reference 8). A sloping beach of 1:20 attached to the constant depth of 100 m was used in the test. Numerical result was compared to the theoretical solution in Reference 8 as required by NTHMP. The relative computational error of maximum runup is 0.9%, which meets the NTHMP requirement (5% or less is required for simple beach cases). As shown in the Figures -A1 and A-2, FUNWAVE-TVD spherical version model results matches well with the experimental results obtained from the laboratory and with the results for Cartesian version of FUNWAVE-TVD. Reference 8 and Reference 9 of this Appendix are presented in Attachments N and Attachment O respectively to document the V&V of FUNWAVE-TVD.

Model nesting was verified by a test of solitary wave propagation in a two-grid nested domain. The large computational domain is 3,000 m long and 100 m deep with grid spacing of 4 m. The nested small domain starts at 1000 m of the large domain and ends at 3,000m with grid spacing of 1 m. A solitary wave with an amplitude of 1 m was initialized at 300 m of the large domain. Figure A-3 (Attachment A) shows the solitary wave in the large domain at Time = 25s, 50s, 75s, 100s, 125s, 150s, 175s, and 200s. Figure A-4 (Attachment A) shows the solitary wave in the nested small domain at Time = 50s, 75s, 100s, 125s, 150s, 175s, and 200s. The test indicates that a solitary wave of permanent form is undistorted as it moves from larger down to smaller scale grids.

Users Manual and other input and output files used for FUNWAVE-TVD program are provided in Attachment J of this Appendix.

4.2 Purpose B: NHWAVE Validation

NHWAVE model setup exactly followed the laboratory experiment configuration by Enet and Grilli (Reference 3). Figure B-1 (Attachment B) demonstrates the vertical cross section and the landslide. The horizontal domain is discretized by a uniform grid with grid spacing of 0.02 m. Three vertical layers are employed. Figure B-2 (Attachment B) shows the comparisons of numerical and experimental surface elevations at three wave gauges for a case with submergence depth of 61 mm, landslide of terminal velocity of 1.70 m/s and initial acceleration of 1.12 m/s^2. Figure B-3 shows the same comparisons for a case with submergence depth of 120 mm, landslide of terminal velocity of 2.03 m/s and initial acceleration of 1.17 m/s^2. The results indicate that the model predicted well evolution of surface elevation generated by the landslide. The model can serve as a landslide tsunami generator for computing initial surface displacement and velocity field generated by a submarine mass displacement (SMD).

The model documentation and other input and output files used for NHWAVE program are provided in Attachment J of this Appendix.

4.3 Purpose C: Verify the bathymetry/topography files

The bathymetry/topography data for constructions of Grids A, B and C were downloaded from ETOPO 1 (Reference 1) website at http://www.ngdc.noaa.gov/mgg/global/global.html, CRM (Reference 2) website at http://www.ngdc.noaa.gov/mgg/coastal/startcrm.htm.

The downloaded data were saved in
/levy/bathy_data/grid_a/fyshi0001-4652.txt
/levy/bathy_data/gulf_grid/fyshi0001-1718.txt
/levy/bathy_data/grid_b/fyshi0001-9328.txt
/levy/bathy_data/site/fyshi0001-4161.txt

Grid A for Venezuela case was constructed using mkbathy_a_2m.f (Program C-1 in attachment C) and saved as large_grid.txt. A direct comparison between the model input file large_grid.txt and fyshi0001-4652.txt was performed using MATLAB as shown in Figure C-1 (Attachment C). Note that the data downloaded from ETOPO 1 have opposite sign compared to the bathymetry used in the model. (1,1) point in ETOPO 1 is the northeast corner while (1,1) point in the model

bathymetry is the southeast point corner. The direct comparison indicates that the two files are consistent.

Grid A_l for landslide cases was constructed using mkbathy_a_1m.f (Program C-2 in Attachment C) and saved as gulf_grid. A direct comparison between the model input file gulf_grid and fyshi0001-1718.txt was performed using MATLAB as shown in Figure C-2 (Attachment C). The direct comparison indicates that the two files are consistent.

Grid B was constructed using mkbathy_b_15s.f (Program C-3 in Attachment C) and saved as grid_b. A direct comparison between the model input file grid_b and fyshi0001-9328.txt was performed using MATLAB as shown in Figure C-3 (Attachment C). The direct comparison indicates that the two files are consistent.

Grid C was constructed using mksite_3s.f (Program C-4 in Attachment C) and saved as site_grid.txt. The lidar topography data at the site was first formatted as 30mx30m arrays using intp.m (Program C-5 in Attachment C) and saved as z30m.txt,x30m.txt and y30m.txt. Then they were converted into 1-arc sec Lon/Lat data using nav_convert.m (Program C-6 in Attachment C) and saved as Xg30m.txt, Yg30m.txt and Zg30m.txt. The matlab program process_site.m (Program C-7 in Attachment C) was used to merge the site data at site into the grid. The grid was saved as Xsmall.txt, Ysmall.txt and Zsmall_MSL.txt. A direct comparison between Zsmall_MSL.txt, fyshi0001-4161.txt and the site data was performed using MATLAB as shown in Figure C-4 (Attachment C). The direct comparison indicates that the converted files are consistent.
The files for Grids A, B and C files are provided in Attachment J of this Appendix.

4.4 Purpose D: Verify FUNWAVE-TVD input files from NHWAVE outputs

Output files of surface elevation and velocity field from NHWAVE were saved in
/levy/nhwave_result/landslide_msc/u_0016
/levy/nhwave_result/landslide_msc/v_0016
/levy/nhwave_result/landslide_msc/z_0016
for the Mississippi Canyon case. nhwave_funwave.f was used to get depth-averaged velocity by three-layer averaging. The FUNWAVE-TVD input files were saved as defu_ma.txt, defv_ma_txt and defz_ma.txt. Consistency between NHWAVE output and FUNWAVE-TVD input can be obtained using direct comparisons in matlab as show in Figure D-1 (Attachment D).

For the Florida escarpment case, output files of surface elevation and velocity field from NHWAVE were saved in

/levy/nhwave_result/landslide_florida/eta_0048
/levy/nhwave_result/landslide_florida/u_0048
/levy/nhwave_result/landslide_florida/v_0048
interpolation2global.m (Program D-1 in Attachment D) was used to convert those data based on a rectangular grid into spherical grid: ma_defz.txt, ma_defu.txt and ma_defv.txt. Figure D-2 (Attachment D) shows a plot of comparison between data on the rectangular grid and data on the spherical grid. The plot confirms that the data after the interpolation is consistent with the original data.

4.5 Purpose E: Verify datum conversions

The measured topography data are based on Florida State Plane Coordinates, West Zone, NAD 83, and North American Vertical Datum 1988 (NAVD 88). ETOPO-1 and CRM from NOAA are based on global Longitude/Latitude coordinates and MSL. The horizontal datum conversion was performed using www.earthpoint.us (Reference 11) as shown in Figure E-1 (Attachment E). The vertical datum conversion used NOAA data at Cedar Key, FL, Station ID: 8727520 (Reference 12) as shown in Figure E-2 (Attachment E).

4.6 Purpose F: Directory Listing of FUNWAVE-TVD

The complete listing of directory structure including sub directories of FUNWAVE-TVD program and results is demonstrated in Figure F-1 (Attachment F). Usages of all folders are listed below.
/src/ funwave-tvd source without coupling function
/src_coupling/ funwave-tvd source with coupling function
/work_large/ work folder for Venezuela seismic tsunami case, Grid A
/work_msc_ma/ work folder for MC case, Grid A_I with NHWAVE source
/work_msc_conserv/ work folder for MC case, Grid A_I with static source
/work_flo/ work folder for FE case, Grid A_I with NHWAVE source
/work_flo_st/ / work folder for FE case, Grid A_I with statice source
/work_b_cari/ work folder for Venezuela seismic tsunami case, Grid B
/work_b_msc_ma/ work folder for MC case, Grid B with NHWAVE source
/work_b_msc_st/ work folder for MC case, Grid B with static source
/work_b_flo/ / work folder for FE case, Grid B with NHWAVE source
/work_b_flo_st/ work folder for FE case, Grid B with static source
/work_c_cari_10/ work folder for Venezuela seismic tsunami case, Grid C
/work_c_msc_ma_10/ work folder for MC case, Grid C with NHWAVE source
/work_c_msc_st_10/ work folder for MC case, Grid C with static source

/work_c_flo_ma/ work folder for FE case, Grid C with NHWAVE source

/work_c_flo_st/ work folder for FE case, Grid C with static source

4.7 Purpose G: Directory Listing of NHWAVE

The complete listing of directory structure including sub directories of NHWAVE program and results is demonstrated in Figure G-1 (Attachment G). Usages of all folders are listed below.

/LandSlide_MIS NHWAVE source for Mississippi Canyon

/LandSlide_FLO NHWAVE source for Florida Escarpment

4.8 Purpose H: Verify the calculation of earthquake magnitude in the Venezuela seismic tsunami case

The calculation of the earthquake magnitude for the Venezuela seismic tsunami case was based on Reference 10. Calculation of the earthquake's seismic moment uses the following equation:

$M_0=\mu u_0 LW$

where the earth's rigidity, μ, is assumed to be 4.0×10^{10} Pa, u_0 is slip, L and W represent the length and width of a fault, respectively. The moment was then converted to M_w using

$M_w=(\log M_0-9)/\log 32$

The earthquake parameters for the Venezuela case are L = 750km (two segments), W = 50km, $u_0 = 23$ m. The result is M_w = 9.0. The calculation program is attached in Program H-1 in Attachment H.

4.9 Purpose I: Post-processing of FUNWAVE-TVD and NHWAVE

Post-processing was performed in the directory /levy/post processing. Figures shown in the calculation package and this document are plotted by the following MATLAB programs:

cari_eta.m: plot surface elevation for the Venezuela case, Grid A

cari_gulf_eta.m: plot surface elevation for the Venezuela case, Grid A, gulf scale

cari_gulf_hmax.m: plot maximum magnitude for the Venezuela case, Grid A

gulf_eta_conserv.m: plot surface elevation for MC case, static source, Grid A

gulf_eta_flo.m: plot surface elevation for FE case, NHWAVE source, Grid A

gulf_eta_flo_st.m: plot surface elevation for FE case, static source, Grid A

gulf_eta_ma.m: plot surface elevation for MC case, NHWAVE source, Grid A

gulf_hmax.m: plot maximum magnitude for MC case, NHWAVE source, Grid A

gulf_hmax_conserv.m: plot maximum magnitude for MC case, static source, Grid A

gulf_hmax_flo.m: plot maximum magnitude for FE case, NHWAVE source, Grid A

gulf_hmax_flo_st.m: plot maximum magnitude for FE case, static source, Grid A

gulf_hmax_ma.m: plot maximum magnitude for MC case, NHWAVE source, Grid A

gulf_b_eta_cari.m: plot surface elevation for Venezuela case, Grid B
gulf_b_eta_flo_ma.m: plot surface elevation for FE case, NHWAVE source, Grid B
gulf_b_eta_flo_st.m: plot surface elevation for FE case, static source, Grid B
gulf_b_eta_ma.m: plot surface elevation for MC case, NHWAVE source, Grid B
gulf_b_eta_st.m: plot surface elevation for MC case, static source, Grid B
gulf_b_hmax_cari.m: plot maximum magnitude for Venezuela case, Grid B
gulf_b_hmax_flo_ma.m: plot maximum magnitude for FE case, NHWAVE source, Grid B
gulf_b_hmax_flo_st.m: plot maximum magnitude for FE case, static source, Grid B
gulf_b_hmax_ma.m: plot maximum magnitude for MC case, NHWAVE source, Grid B
gulf_b_hmax_st.m: plot maximum magnitude for MC case, static source, Grid B
flood_cari.m: plot surface elevation for Venezuela case, Grid C
flood_cari_hmax.m: plot maximum magnitude for Venezuela case, Grid C
flood_flo_hmax.m: plot maximum magnitude for FE case, NHWAVE source, Grid C
flood_flo_hmax_st.m: plot maximum magnitude for FE case, static source, Grid C
flood_flo_ma.m: plot surface elevation for FE case, NHWAVE source, Grid C
flood_flo_st.m: flood_flo_ma.m: plot surface elevation for FE case, static source, Grid C
flood_msc_hmax.m: plot maximum magnitude for MC case, NHWAVE source, Grid C
flood_msc_hmax_st.m: plot maximum magnitude for MC case, static source, Grid C
flood_msc_ma.m: plot surface elevation for MC case, NHWAVE source, Grid C
flood_msc_st.m: plot surface elevation for MC case, static source, Grid C
max_runup_1d_cari_miles.m: plot 1D wave runup for Venezuela case
max_runup_1d_flo_miles.m: plot 1D wave runup for FE case, NHWAVE source
max_runup_1d_flo_st_miles.m: plot 1D wave runup for FE case, static source
max_runup_1d_msc_miles.m: plot 1D wave runup for MC case, NHWAVE source
max_runup_1d_msc_st_miles.m: plot 1D wave runup for MC case, static source
max_runup_contour_cari.m: plot contours of wave runup, Venezuela case
max_runup_contour_flo.m: plot contours of wave runup, FE case, NHWAVE source
max_runup_contour_flo_st.m: plot contours of wave runup, FE case, static source
max_runup_contour_msc.m: plot contours of wave runup, MC case, NHWAVE source
max_runup_contour_msc_st.m: plot contours of wave runup, MC case, static source

Validation for the post processing is presented in Figure I-1 (Attachment I)

All programs above are provided in Attachment J.

References 5, 6, 7, 8, 9 and 4 which are used for Verification and Validation (V&V) of FUNWAVE-TVD and NHWAVE are provided in Attachments K, L, M, N, O and P respectively.

5. Conclusions

As discussed in the Results section, the spherical version of FUNWAVE-TVD is verified and validated using benchmark tests required by NTHMP. Model nesting scheme is accurate in modeling waves from larger down to smaller scale grids. FUNWAVE-TVD can serve as an appropriate tool for estimating the Probable Maximum Tsunami (PMT) flood level at the LNP site.

NHWAVE is verified and validated against the laboratory experimental data of Enet and Grilli (Reference 3). It can serve as an appropriate tool for computing initial surface displacement and velocity field generated by a submarine displacement which can be used as input to FUNWAVE-TVD model.

Bathymetry/topography files are verified for all computational grids. Output files from NHWAVE for FUNWAVE-TVD input files are verified. Conversions between different data are validated.

6. References

1. Amante, C. and Eakins, B. W., 2008, "ETOPO 1 Arc-Minute Global Relief Model: Procedures, Data Sources and Analysis," National Geophysical Data Center, NESDIS, NOAA, U.S. Department of Commerce, Boulder, CO, August, 2008.

2. Divins, D.L., and Metzger, D., "National Geophysical Data Center (NGDC) Coastal Relief Model", Volume 2, http://www.ngdc.noaa.gov/mgg/coastal/coastal.html.

3. Enet, F. and Grilli, S. T., 2007, "Experimental study of tsunami generation by three-dimensional rigid underwater landslides," J. Waterway, Port, Coastal and Ocean Engineering, 133, 442-454.

4. Kirby, J. T., Shi, F., Harris, J. C. and Grilli, S. T., 2011, "Sensitivity analysis of trans-oceanic tsunami propagation to dispersive and Coriolis effects", draft manuscript.

5. Ma, G., Shi, F. and Kirby, J. T., 2011, "Shock-capturing non-hydrostatic model for fully dispersive surface wave processes," submitted to Ocean Modelling, June, 2011.

6. Shi, F., Kirby, J. T., Harris, J. C., Geiman, J. D. and Grilli, S. T., 2011a, "A high-order adaptive time-stepping TVD solver for Boussinesq modeling of breaking waves and shoreline inundation", draft manuscript in preparation for Ocean Modelling,

7. Shi, F., Kirby, J. T., Tehranirad, B., Harris, J. C. and Grilli, S. T., 2011b, "FUNWAVE-TVD, Version 1.0. Fully nonlinear Boussinesq wave model with TVD solver. Documentation and user's manual," Research Report No. CACR-11-04, Center for Applied Coastal Research, University of Delaware, Newark, June, 2011.

8. Synolakis, C. E., Bernard, E. N., Titov, V. V., Kanoglu, U. and Gonzalez, F. I., 2007, "Standards, criteria, and procedures for NOAA evaluation of tsunami numerical models," NOAA Technical Memorandum OAR PMEL-135, Pacific Marine Environmental Laboratory, Seattle.

9. Tehranirad, B., Shi, F., Kirby, J. T., Harris, J. C. and Grilli, S. T., 2011, "Tsunami benchmark results for fully nonlinear Boussinesq wave model FUNWAVE-TVD, Version 1.0," Research Report No. CACR-11-02, Center for Applied Coastal Research, University of Delaware, Newark, June.

10. Grilli S. T., Loualalen, M., Asavanant, J. Shi, F., Kirby, J. T., and Watts, P., 2007, "Source constraints and model simulation of the December 26, 2004, Indian Ocean Tsunami," Journal of Waterway, Port, Coastal, and Ocean Engineering, 133, 414-428.

11. Web site http://www.earthpoint.us, Web Page State Plane (Tab). (Attachment E)

12. National Oceanic and Atmospheric Administration (NOAA), Web site for Tides and Currents. Cedar Key, Florida, Station ID 8727520, Link: http://tidesandcurrents.noaa.gov/data_menu.shtml?stn=8727520%20Cedar%20Key,%20FL&type=Datums (Attachment E),

13. ten Brink, U., Twichell, D., Lynett, P., Geist, E., Chaytor, J., Lee, H., Buczkowski, B. and Flores, C., 2009, "Regional assessment of tsunami potential in the Gulf of Mexico," U. S. Geological Survey Administrative Report.